12-2015

DEVELOPING EFFECTIVE GROUND AND SPACE-BASED SOIL MOISTURE SENSING TECHNIQUES FOR IRRIGATING COTTON IN COASTAL PLAIN SOILS

XIN QIAO
Clemson University, xqiao@clemson.edu

DEVELOPING EFFECTIVE GROUND AND SPACE-BASED SOIL MOISTURE SENSING TECHNIQUES FOR IRRIGATING COTTON IN COASTAL PLAIN SOILS

A Dissertation
Presented to
the Graduate School of
Clemson University

In Partial Fulfillment
of the Requirements for the Degree
Doctor of Philosophy
Plant and Environmental Sciences

---

by
Xin Qiao
December 2015

Accepted by:
Dr. Ahmad Khalilian, Committee Co-Chair
Dr. Young Han, Committee Co-Chair
Dr. Charles Privette, III
Dr. Jose Payero

DEDICATION

I would like to dedicate this dissertation to my parents, Junhua Chai and Yansheng Qiao for their endless love and support. I would also like to dedicate this dissertation to my grandparents Quanyun Chai, Xiujiao Pang, Wanyun Qiao, and Xianwa Lv, for supporting me throughout my life.

ACKNOWLEDGMENTS

First and foremost I would like to thank my research advisor, Dr. Ahmad Khalilian for his constant support and advice towards the completion of this project. Many thanks to my academic advisor, Dr. Young Han for his support and guidance during my graduate study. And thanks to Dr. Jose Payero and Dr. Charles Privette for all of their endless help and support on this project.

I would like to acknowledge Dr. Hamid Farahani at USDA NRCS for his help and effort on revising my paper. I would also like to thank Dr. Stephen Katzberg, Omar Torres, George Ganoe, and Dr. Michael Grant for their help on the NASA project.

Thanks to Tammy Morton, Christi Leard, Rebecca Ulmer, and Susan Williams for their excellence in handling all of my administrative needs.

I would like to thank fellow graduate students Philip Williams, Nick Rogers, and Reid Miller for their help on this project along with Mr. Richard Hallman for his help at the Edisto REC completing the research. The research work would not have been possible without the endless summer help of Chris Harvey, Jacob Oswald, and Paul Thomas. My appreciation also goes to the faculty and staff at the Edisto Research and Education Center for their help and support with the everyday challenges that occurred throughout the research.

I would like to thank Rebecca Davis, for being a true friend over the years since I started my graduate study in Blackville. My appreciation also goes to my neighbors, Ruben Torres and, soon to be Mrs. Torres, Rosario Curiel-Cervantes, for treating me like family and making me feel at home in a foreign country.

I would like to specially thank Ms. Weizhen Liang, for keeping me company when writing my dissertation, and helping me see the beauty in things.

Last but not least, my sincere thank goes to Cotton Incorporated of Cary, NC along with NASA Langley Research Center for their funding and support of this research project.

TABLE OF CONTENTS

Page

Table of Contents (Continued)

Page

LIST OF TABLES

LIST OF FIGURES

Page

List of Figures (Continued)

Page

List of Figures (Continued)

Page

List of Figures (Continued)

Page

List of Figures (Continued)

Page

List of Figures (Continued)

Page

CHAPTER 1

DEVELOPING AN EFFECTIVE SENSORS-BASED IRRIGATION SCHEDULING TECHNIQUE FOR COTTON PRODUCTION IN COASTAL PLAIN SOILS

1.1 ABSTRACT

Irrigation scheduling based on soil moisture sensor readings has gained popularity in the past few decades since it can enhance crop yield while saving water. Such method is limited since the representativeness of an individual soil moisture sensor measurement is questionable in a large field with variable soil type and texture. The optimum location of soil moisture sensors needs to be determined within such a production field for effective sensor-based irrigation scheduling. Therefore, the first object of this study was to investigate the optimum sensor location and the number of moisture sensors required for irrigating cotton in coastal plain soils. Replicated tests were conducted during 2012, 2013, and 2014 growing seasons in a cotton field located at the Edisto Research and Education Center of Clemson University, on a typical coastal plain soil. The test field was divided into different management zones based on soil electrical conductivity (EC) measurements. Soil moisture sensors including AquaSpy, Sentek EasyAg-50, Decagon EC-5, Watermark 200SS, and 503 DR Hydroprobe neutron probe access tubes were installed side by side in plots of each management zone. Irrigation treatments were based on sensor readings from various management zones. Results showed that irrigation based on sensor readings from higher electrical conductivity zones, can stabilize or even enhance yield while increasing water use efficiency (WUE) significantly. The second

objective of this study was to evaluate the performance of soil moisture sensors mentioned above to determine the most accurate and affordable sensor technology for irrigation scheduling. Season long soil moisture readings of AquaSpy, Sentek EasyAg-50, Decagon EC-5, and Watermark 200SS sensors were collected and compared to neutron probe readings. The results showed that Sentek EasyAg-50 sensor performed the best among tested sensors compared to neutron probe readings with coefficient of determination, R^2 = 0.847 and root mean square error, RMSE= 4.2% for soil profiles up to 50 cm. The performance of Decagon EC-5 sensor was acceptable with R^2 of 0.6 to 0.7 and RMSE ranged from 4.9% to 6.7% during the three growing seasons. Further field and lab calibration of Decagon EC-5, reduced RMSE from 4.4% to 3.3% at topsoil (10-30 cm). Compared to Sentek EasyAg and Decagon EC-5 sensors, AquaSpy and Watermark 200SS sensors performances in measuring soil moisture contents, were not satisfactory, as indicated by low R^2 of less than 0.45 and high RMSE of 9.5% to 14%. The results of this study suggested that in a field with variable soil type, it would be beneficial to install moisture sensors in management zones with higher EC readings (heavier soil textures) to obtain maximum yield and WUE. The results also indicated that, although the Sentek EasyAg-50 sensor had the highest accuracy among the sensor types tested, Decagon sensor offered more promise for irrigation scheduling than the rest of the sensors tested, since it offered good accuracy and is affordable.

1.2 INTRODUCTION

Irrigation management in the coming decades will emphasize maximizing crop production per unit water consumed. From 2002 to 2007, irrigated acreage in the western states declined significantly, while in the southeastern states, irrigated acreage increased by 70% (USDA, National Agricultural Statistics Serves, 2007). Recent drought periods (1998-2002, 2007, & 2011) in the Southeastern U.S. and trans-boundary water conflicts between neighboring states have elevated the importance of water resources conservation. Competition for limited water resources has become a critical issue in some parts of the southeastern states.

Irrigation scheduling based on soil moisture sensors has provided an opportunity to conserve water. However, high variability in soil types within production fields in the Southeastern Coastal Plain region make this task challenging, since these soils have different water holding capacities. Therefore, efficient irrigation in these fields is best achieved using a sensors-based variable rate irrigation (VRI) system which takes all of these variations into consideration. Although variable-rate water application technology is commercially available and over 100 units has already been installed on growers' pivots in South Carolina and Georgia, many cotton growers either don't have access to this technology or don't have the time or comfort level with higher-tech gadgets. Therefore, until VRI systems become simpler for grower use, an efficient and affordable sensor-based irrigation scheduling technique for cotton needs to be developed to account for field variability in the Southeastern Coastal Plain soils. Optimum locations of

moisture sensors in a field in this region become very critical and can significantly affect irrigation scheduling when amount of sensors is limited.

Accurate soil moisture sensors can be an important component of precision irrigation water management. Previous work has shown that irrigation management using soil moisture sensors can significantly reduce water use while maintaining or increasing yields and profits (Irmak et al., 2012; Khalilian et al., 2008; Miller et al., 2012). There is a large variety of commercial sensors that relate electrical output to soil water content. However, sensor electrical output is also affected by soil characteristics other than water content, such as texture, salinity, temperature, organic matter, etc. This makes it difficult to accurately measure soil moisture with most sensors without prior on-site calibration. The wide variety of commercial soil moisture monitoring systems currently available makes it very complex for farmers to make a good educated decision on which of them to use. These systems range from single moisture sensing probes to multiple depth probes, utilizing a variety of sensing technologies, such as electrical resistance, neutron scattering, capacitance, time domain reflectometry, etc. In addition, these systems can vary significantly in cost depending on things like the number of sensors, data logging options and data transmission capabilities. Therefore, there is a need to develop guidelines on how to interpret the output of soil moisture sensors for different soil types, and on how to use this information to make irrigation scheduling decisions.

1.3 OBJECTIVES

The overall objective of this study was to determine and improve the feasibility of utilizing sensor-based soil water monitoring techniques in southeastern Coastal Plain soils to more effectively manage agricultural water resources.

The specific objectives were to:

- Determine the most accurate and affordable sensor technology for irrigation scheduling in cotton production by calibration, verification, and soil water management; and
- Determine the optimum sensor location in a production field with variable soil type and texture in Southeastern Coastal Plain region.

1.4 LITERATURE REIVEW

1.4.1 Soil Moisture Sensors

Accurate measurement of soil water content is an important component of the irrigation management. Thermogravimetric method is the most accurate way to measure soil water content by taking known volume of soil from field and comparing the weight before and after drying in oven. However, such method is labor and time consuming, especially for large area applications. Sensors which measure soil water content or soil water potential have been widely used to assist irrigation management. These sensors utilize different technologies such as electromagnetic (EM), gypsum blocks, and neutron scattering sensors. The EM sensors measure soil permittivity (ε) since various permittivity values were found for water ($\varepsilon_w \approx 80$), mineral soil solids ($\varepsilon_s \approx 2\text{-}9$), and air ($\varepsilon_a \approx 1$). After soil permittivity value is obtained, the EM sensors, such as time domain reflectometry (TDR) and capacitance devices, usually use empirical (Topp et al. 1980) or dielectric mixing models to convert soil permittivity to volumetric water content expressed in m^3m^{-3}.

The TDR sensor was originally designed to detect line break in a cable system, since the signal propagation velocity is governed by the cable dielectric constant. Later this concept was employed to measure soil moisture by inserting a known length of probe to soil medium. By measuring the time duration of EM signal traverse the probe, bulk permittivity of soil medium around the probe is determined (Jones et al. 2002). TDR sensor has the advantage of high accuracy and companion electrical conductivity

measurements (Jones et al. 2002, Walker et al. 2004), yet such sensor is expensive and temperature can affect sensor readings.

Capacitance soil moisture sensors measure capacitance of soil medium around sensors since the soil around sensors is incorporated as part of the dielectric of a capacitor (Dean et al. 1987). Such sensor usually comes in parallel pronged probes or parallel pairs of rings installed in a plastic access pipe (Topp 2003). The parallel prong shaped sensor usually measure soil volumetric water content (VMC) at one depth while the other type of sensor can measure multiple depths since it has multiple pairs of rings. The range of capacitance probe measurement is usually limited and only responds to a small volume of soil (Topp 2003, Dean et al. 1987). Capacitance sensors vary in shapes, prices, and accuracies. The low cost capacitance soil moisture sensor Decagon EC-5 (Decagon Devices Inc., Pullman, WA, U.S.A.) has been proved to be a suitable sensor for soil moisture monitoring (Bogena et al., 2007; Ritsema et al. 2007; Parsons and Bandaranayake, 2009). The Decagon EC-5 sensor operates at a frequency of 70 MHz and the sensor error was reported to be 0.02 m^3m^{-3} in a lab calibration experiment (Kizito et al. 2008). Drawbacks of EC-5 sensor are small sample volume (~0.2L) and tendency to be affected by temperature (Bogena et al., 2007). Meanwhile, Decagon EC-5 sensor can only measure VMC at one depth. Multiple Decagon EC-5 sensors have to be installed if multiple VMC readings are desired. AquaSpy probe (AquaSpy Inc., Adelaide, South Australia) is a multi-sensor capacitance probe (MCP) which can measure soil water content at depths of 10, 20, 30, 40, 50, and 60 cm. Bellamy (2009) utilized the AquaSpy probe readings for irrigation management. He also calibrated this probe for both topsoil

(10 – 30 cm) and subsoil (30 – 50 cm) at a coastal plain soil and the standard error was 1.8% and 2.16%, respectively. Miller et al. (2013) utilized MCP Sentek EasyAg-50 probe (Sentek, Pty., Ltd., Stepny, South Australia) to automate high frequency drip irrigation for watermelons on sandy coastal plain soils. In his study, it was reported that the Sentek EasyAg-50 manufacturer's calibration equation was as good as on-site calibration and sufficient for irrigation scheduling. However, Polyakov et al. (2005) reported that, the Sentek EasyAg-50 probe underestimated VMC severely at range of 0.2-0.35 cm^3cm^{-3} and on-site calibration was needed.

Beside EM sensors, gypsum blocks have also been used for measuring soil moisture content. One such sensor, the Watermark 200SS sensor (Irrometer Co. Inc., Riverside, CA) measures electrical resistance between a pair of coiled wire electrodes and then calculates soil matrix potential in centibars (Shock et al., 1998). Such sensor has been utilized for irrigating vegetable crops (Thompson et al., 2006) under drip irrigation settings. Their results showed that, this sensor responded more slowly in rapidly drying soil compared to continual drying soil, otherwise, this sensor was able to accurately measure soil water potential. Intrigliolo and Castel (2004) suggested Watermark 200SS is useful only when relative wetness of soil is needed due to high variability of Watermark 200SS readings found in their study. Thus the Watermark 200SS is not suitable for accurate measurement of soil moisture contents.

Neutron probe have been used for soil water content measurements for many years. Neutron probe consists of a radioactive probe and an electronic counting scaler which are connected by an electric cable. The neutron probe emits high energy neutrons

which are slowed by moisture content of soils. Then the fast neutrons are counted by the electronic scaler. Soil water content can be determined based on the ratio of fast neutrons to slow neutrons (Bell 1987). However, increasing regulatory restrictions and need for automation of measurement limit the usefulness of the method. Additionally, accurate measurements of surface soil moisture cannot be made since neutron probe has a sphere influence sampling shape (Chanasyk and Naeth, 1996).

There were no published data in the literature related to performances of these soil moisture sensors, compared side by side, in a production field in the Atlantic Coastal Plain region, with varying soil type and texture. Therefore, there is a need to determine the most accurate and affordable sensor technology for irrigation scheduling by calibration and verification to develop guidelines for growers how to use these sensors on local soils.

1.4.2 Irrigation Scheduling Techniques

The increasing worldwide shortages of water are leading to an emphasis on developing methods of irrigation that minimize water use. Development of precision irrigation method such as variable irrigation system is able to deliver proper rates of water to different soil types and hence improve water and energy use (Han et al., 2009). Such system also requires proper irrigation scheduling techniques to maximize its capability. The purpose of irrigation scheduling is to determine the amount of water to apply to the field and the timing for application. Irrigation scheduling methods are either based on soil moisture content soil water balance or checkbook method or plants response to water deficit.

Irrigation based on soil moisture content normally utilizes soil moisture sensors which are easy to use, more accurate, and readily automated (Jones 2004). Burnett and Van Iersel et al. (2008) used a capacitance sensor-automated irrigation system to irrigate Gaura at greenhouse, and results showing that such system had higher water use efficiency and minimized or eliminated leachate. Vellidis et al. (2008) developed a smart irrigation sensor array which measures soil water tension to schedule irrigation for cotton at an open production field, and utilized a variable-rate irrigation (VRI) system to apply water at based on sensor readings. However, as stated in Jones (2004), spatial variation of a larger production field makes the soil moisture sensor-based irrigation scheduling difficult, since the optimum locations of moisture sensors in these fields become very critical and can significantly affect irrigation scheduling when amount of sensors is limited. There were no published data in the literature for sensors-based irrigation of

cotton, in fields of coastal plain region with varying soil types, using limited number of soil moisture sensors.

The soil water balance or checkbook method computes the change in moisture by comparing the difference of input (rainfall and irrigation) and output (evapotranspiration, runoff, and drainage). Such method is able to indicate the amount of water needed but it is not as accurate as irrigation scheduling based on soil moisture sensor readings. The soil water balance method requires calibration (actual soil moisture measurement) from time to time, due to cumulative error may occur over time (Jones 2004).

In order to use plant-based method for irrigation management, it is important to determine which measure would be appropriate for irrigation scheduling. Choices of plant-based measurements include direct plant water status (stem water potential, psychrometer, tissue water content, etc.) and indirect crop responses (stomatal conductance and sap flow) which are known to be affected by irrigation deficit (Jones 2014). Direct plant water status seems to be useful to reflect irrigation requirement of plants. However, as argued by Jones (2004), plants tend to maintain their leaf or shoot water status in both short and long terms under different soil water conditions and evaporation demands. Also, the relationship of leaf water potential to stomata aperture is misleading as described in Hsiao (1973), since root shoot signaling plays a major role of controlling stomata aperture (Davies and Zhang, 1991). Hence, plant water status is not ideal for irrigation scheduling. Generally speaking, plant-based irrigation scheduling techniques do not indicate the amount of water to apply and require calibrations to determine control thresholds.

1.5 MATERIAL AND METHODS

1.5.1 Site Condition

Field experiments were conducted at the Edisto Research and Education Center (EREC) of Clemson University near Blackville, South Carolina during 2012, 2013, and 2014 growing seasons. The climate at the experimental site is subtropical with hot and humid summer with maximum temperature about 30℃ and mild to chilly winter with minimum temperature about 3℃. Annual precipitation is abundant, ranging from 1000 to 1700 mm, with intermittent occurrence of summer drought and excess rainfall events. Rainfall distribution in the Southeast U.S.A. is very uneven. The on-site NOAA weather station (Figure 1.1) recorded climate data such as maximum temperature (T_{max}), minimum temperature (T_{min}), solar radiation (SR), wind speed, maximum relative humidity (RH_{max}), and minimum relative humidity (RH_{min}) at five minutes interval. Average values of T_{max}, T_{min}, SR, wind speed, RH_{max}, and RH_{min} were calculated on daily basis. Total solar radiation received per day was summed to get daily solar radiation. Daily reference evapotranspiration (ET_o) was computed using the Penman-Monteith approach (Allen et al., 1998).

Figure 1.1 Weather station located at Edisto R.E.C.

The soil type at the experimental site, as reported by Bellamy (2009), is characterized to be Varina loamy sand. This typical coastal plain soil is comprised of three often distinct layers: a sandy topsoil (A horizon), a sandy clay subsoil (Bt horizon), and a sand to sandy clay layer in between (E horizon) (Figure 1.2). The E horizon is most often referred to as the hardpan layer and is a very hard mix of clay and sand. Field capacity (FC) of soil at experimental field was obtained from previous study (Nayazi 2006), i.e. 0.158 cm^3/cm^3 (15.8%) and 0.245 cm^3/cm^3 (24.5%) for topsoil (sand layer) and subsoil (clay layer), respectively.

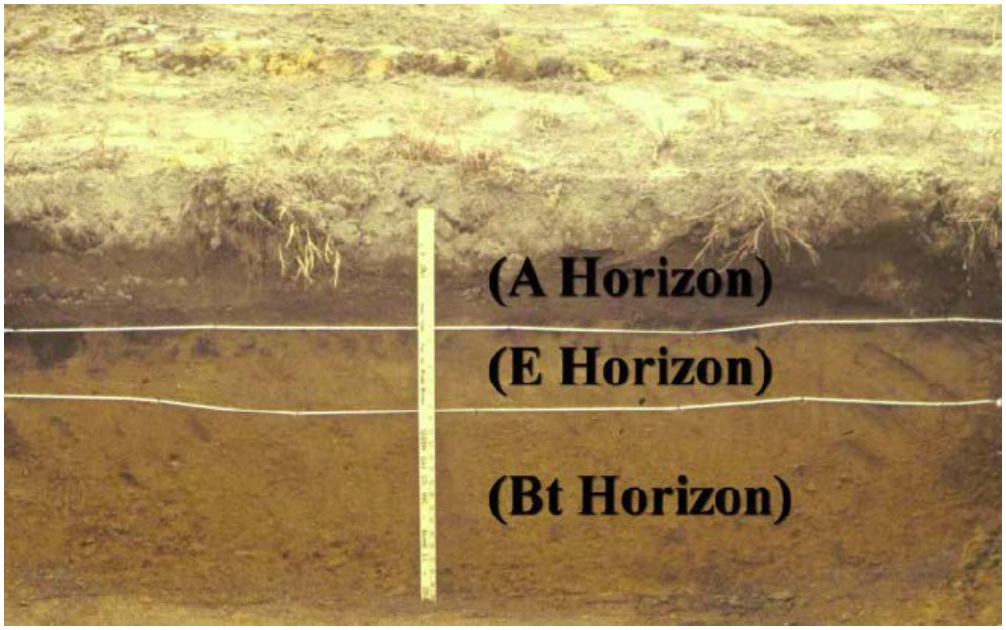

Figure 1.2 Typical Southeastern Coastal Plain soil profile (Bellamy 2009).

1.5.2 Calibration of sensors

Sensors used in this study included AquaSpy probe (AquaSpy Inc., Adelaide, Australia), Decagon EC-5 (Decagon Inc., Pullman, WA, USA), Watermark 200SS (Irrometer Co. Inc., Riverside, CA, USA), Sentek EasyAg-50 (Sentek Sensor Technologies, Stepney SA, Australia), and 503DR Hydroprobe (CPN International Inc., Martinez, CA, USA) (Figure 1.3). Specifications of sensor are listed in Table 1.1.

Table 1.1 Specifications of soil moisture sensors used in this study.

Brand	Model	Measured parameter	Communication protocol	Accuracy (%)	Resolution (%)	Excitation voltage (V)
Decagon	EC-5	VMC, %[1]	Analog	3	0.25	2.5-3.6
Sentek	EasyAg 50	VMC, %	SDI_12	0.10	0.008	12
Water Mark	200SS	SWP, cb[2]	Analog	N/A	N/A	9
CPN	503DR					
International	Hydroprobe	VMC, %	Analog	0.40	0.20	9
AquaSpy	-	VMC, %	N/A	N/A	N/A	N/A

[1]VMC is volumetric water content in the unit of percentage (%)

[2]SWP is soil water potential in the unit of cb (centibar)

AquaSpy probe has been calibrated in previous studies for topsoil (sand) and subsoil (clay) at same experimental field. As reported by Bellamy (2009), sensor readings of AquaSpy were highly correlated with actual soil moisture content with R^2 of 0.73 and 0.76 for topsoil (10 – 30 cm) and subsoil (40 – 60 cm), respectively. The two calibration equations were employed in this study are:

$$Sand \quad VMC = \mathrm{SR} * 0.3205 - 6.4753 \qquad 1.1$$

$$Clay \quad VMC = \mathrm{SR} * 0.4623 - 7.5982 \qquad 1.2$$

where VMC is volumetric water content of soil and SR is sensor readings of AquaSpy. Watermark 200SS measures soil water potential which requires soil tension curves to be able to convert to volumetric water content (VMC). Nayazi (2006) developed soil tension curves for topsoil (sand) and subsoil (clay) at the same experimental field which can be used to convert soil matrix potential to VMC. The two soil tension curve equations are:

$$Sand \quad VMC = -0.054Ln(x) + 0.263 \qquad 1.3$$

$$Clay \quad VMC = -0.0305Ln(x) + 0.3049 \qquad 1.4$$

Where x is sensor reading of Watermark 200SS in centibar (cb). The 503DR Hydroprobe has also been calibrated at a field located at Edisto R.E.C with similar soil type by scientists at the EREC (Farahani, 2015). However, since neutron probe was going to be used as baseline of evaluating other sensors in this study, calibration was conducted at the experimental field. Hence, calibration in this study mainly refers to Decagon EC-5, Sentek EasyAg-50 sensors, and 503DR Hydroprobe (neutron probe).

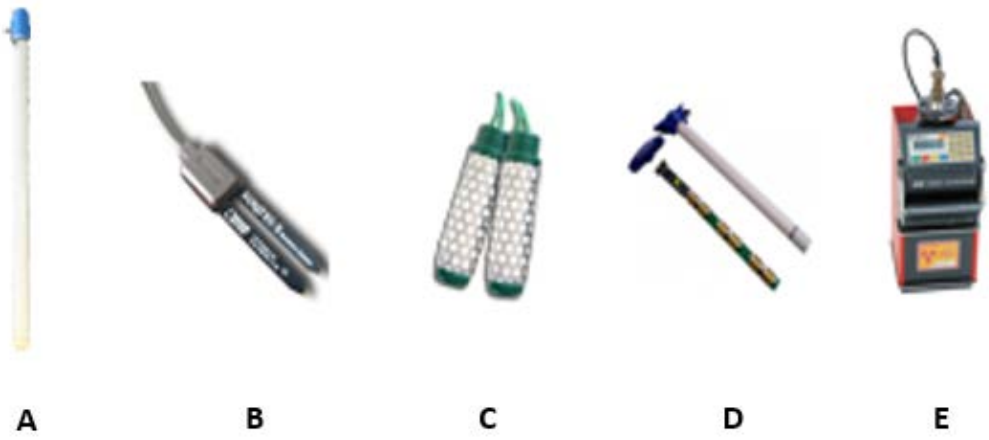

Figure 1.3 Soil moisture sensor used in this study were AquaSpy (A), Decagon EC-5 (B), Watermark 200SS (C), Sentek EasyAg50 (D), and 503DR Hydroprobe (E).

Before calibrating Sentek EasyAg-50 probe, a normalization procedure was required. The sensor's output is frequency value (raw count), which later was converted to VMC using normalization equation and default or user-defined calibration equation. The effective range of raw count needs to be set between a high and low value (TriSCAN Agronomic User Manual Version 1.2a). The high value refers to air count and low value refers to water count. To normalize sensor in air, sensor was held in air without interference of any other object. Sensor counts of air were taken using Probe

Configuration Utility program (Sentek Sensor Technologies, Stepney SA, Australia). To normalize sensor in water, a special cylindrical case with a hole at the top, was constructed using a 15-cm PVC pipe, and filled with reverse osmosis water (EC < 300 µs/cm). The hole at top of the case, which is same diameter of Sentek EasyAg-50 sensor, allows sensor body to be inserted and centered in the case (Figure 1.4). Sensor raw counts of water were also taken using Probe Configuration Utility. All Sentek EasyAg-50 probes used in this study were normalized following this procedure.

Figure 1.4 Normalization of Sentek EasyAg-50 probe in water.

Calibrations of Decagon EC-5, Sentek EasyAg-50, and neutron probe were performed both under lab and field conditions. For field calibration of sensors, a trench was dug and three groups of sensors were installed 3 meters apart from each other and approximately 40 to 50 cm away from the trench (Figure 1.5). Thus soil samples can be

reached from the side, minimizing disturbing effects of taking soil samples (Sentek calibration manual) (Figure 1.6). Each group of sensors was comprised of two Sentek EasyAg-50 probes, two Decagon EC-5 sensors installed at sandy layer (10 cm) and clay layer (40 cm), and one 60 cm long neutron probe access tube. The three sites were determined to be dry, normal, and wet sites. Water was added to the wet and normal sites until sensors readings at various depths reached to field capacity. No water was added to the dry site. Sensors at wet, normal, and dry site were read two, seven, and fourteen days after applying water, respectively. All sites were covered with a plastic tarp during the whole process to prevent effect of precipitation.

Figure 1.5 Digging trench for sensor calibration.

Figure 1.6 Taking soil samples near two Sentek EasyAg-50 probes.

Decagon EC-5 sensor was read using a handheld reader named Procheck sensor read-out and storage system (Decagon Inc., Pullman, WA). Sentek EasyAg-50 probe readings were taken using the Probe Configuration Utility program (Sentek Sensor Technologies, Stepney SA, Australia). When sensor readings were taken at various depths, gravimetric soil samples were taken at the same time using a soil core sampler (Soil Moisture Corp., Santa Barbara, CA), shown in Figure 1.7. The sampler is consisted of a hammer, a metal cylinder, a 6 cm by 5.4 cm brass ring, and three 1 cm by 5.4 cm brass rings. Before digging around individual sensors, two sensor readings were taken a minute apart and recorded. Soils were removed layer by layer, and soil around sensors was carefully dug to desired depths for collecting samples from sensing depths of 10, 20, 30, 40, and 50 cm. For the 10-cm depth, the soil around the sensor was carefully dug to a depth of 7cm. This would center the 6-cm long brass ring at the sensing depth of 10 cm.

Soil core samples were then removed from the brass rings and were placed in an aluminum can. Three soil samples were taken at each sensing depth. Similar procedure was used for the remaining sensing depths.

Figure 1.7 Soil coring tool used in this study.

Wet soil samples with can were weighed immediately after samples were taken and recorded as Wt_{wet} (g). Then wet soil sample with can were dried under 105℃ for 24 hours. After drying, soil sample with can were weighed and recorded as Wt_{dry} (g). Soil volumetric water content (VMC, %) was calculated using equation:

$$\mathrm{VMC} = \frac{(Wt_{wet} - Wt_{dry})/\rho_{water}}{V_{core}} \qquad 1.5$$

where ρ_{water} is density of water equal to 1 g/cm^3 and V_{core} is volume of soil sample equal to 137 cm^3. Soil volumetric water contents of three soil samples at each sensing

depth were averaged and compared to corresponding sensor readings. Bulk density was also calculated using equation:

$$\rho_{bulk} = \frac{Wt_{dry} - Wt_{can}}{V_{core}} \qquad 1.6$$

Where ρ_{bulk} is bulk density of soil in g/cm^3 and Wt_{can} is weight of aluminum can in gram.

Sensor calibration was performed also in laboratory using sandy and clay soils, corresponding to the soil texture of topsoil and subsoil in the experimental field (Figure 1.8). Forty litters of soil samples were extracted from 10 cm depth (sandy soil) and 40 cm depth (clay soil), respectively. Soil samples were then air dried, grinded, and sifted through a 500 μm sieve, and were divided into four 20-L buckets, resulting in two replicates for each soil type. For sandy soil, the first soil moisture level was achieved by mixing soils in each bucket with 500 ml of water in a wheel barrel separately until moisture was uniformly distributed. After mixing, soil was carefully packed to field measured bulk density. One Sentek EasyAg-50 and two Decagon EC-5 soil moisture sensors were installed in each bucket. Same soil core sampler shown in Figure 1.7 was used to extract two soil samples in each bucket. Soil samples were weighted before and after drying in the oven. Soil volumetric water content was calculated using equation 5 and compared to sensor readings. After first calibration point was obtained, sensors were removed and soils from the two buckets were mixed with another 500 ml of water. Sensors were installed and similar procedure was repeated. This process was repeated several times until soil reached to field capacity. Calibration of clay soil followed the

same procedure, except that 1000 ml of water was added each time to each bucket due to higher field capacity of clay soil.

Figure 1.8 Laboratory calibration of sensors for sand (left) and clay (right).

1.5.3 Crop management and experiment design

1.5.3.1 Soil Electrical Conductivity Measurements

At the initiation of the tests, a commercially available soil electrical conductivity (EC) meter (Veris-3100) (Figure 1.9) was used to identify variations in soil texture across the experimental field. The Veris 3100 soil EC meter can collect geo-referenced soil electrical conductivity measurements as it is pulled across field by a tractor. This EC meter has 3 pairs of rolling electrode coulter disks (lung et al. 1999). One pair of the coulters emits electric current into soil while the second and third pair of disks measure drop in voltage which is proportional to the electrical conductivity of soil medium at

shallow (0 – 30 cm) and deep (0 – 91 cm) depths. Data was stored in CF card in the Veris data logger and a DGPS unit (AgGPS, Tremble Navigation Limited, Sunnydale, CA) was used for geo-referencing measured points (Figure 1.9).

Figure 1.9 Veris 3100 EC meter (left) and Veris data logger accompanied with Trimble DGPS (right).

Based on soil EC data, the 2.5 ha experimental field was divided into four management zones in 2012, and three management zones in 2013 and 2014 (Figure 1.10). Beside EC readings, soil samples were also taken during the three growing seasons to identify soil variation in test field in terms of depths of sand (A horizon), hardpan (E horizon), and clay (Bt Horizon), respectively. Prior to planting, 890 kg/ha Potash and 2.4 L/ha Treflan were incorporated by disking. The test field then was sub-soiled/bedded and 28 L/ha Telone II was injected for nematode and thrip control. Cotton variety DP 1133 was planted on June 5th, 2012. Cotton variety DP 1050 was planted on May 22nd, 2013 and May 7th, 2014, respectively. Cotton was harvested on October 17th, 2012, October 31st, 2013, and October 10th, 2014, respectively. A spindle picker equipped with an AgLeader yield monitor and a GPS unit was employed to map changes in cotton lint

yield within and among treatments. Water use efficiency (WUE) was calculated by dividing cotton lint yield by total water applied in each treatment.

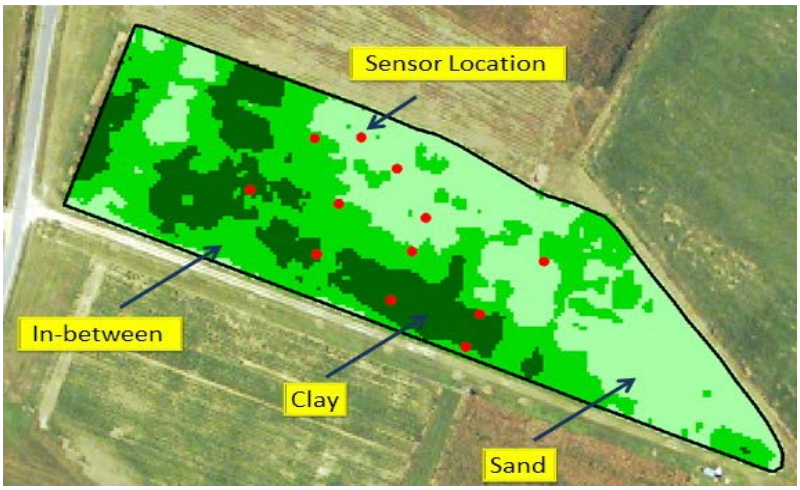

Figure 1.10 Soil electrical conductivity map of experimental field in 2013 growing season

1.5.3.2 Sensor installation and instrumentation

In each management zone, at least 4 plots were used to install all of the moisture sensors. Sensors were installed side by side in these plots with appropriate data loggers for continuous soil moisture monitoring, as shown in Figure 1.11. It was desired to use same types of sensor throughout the three growing seasons. However, due to the availability of sensors, AquaSpy probe, Decagon EC-5, and Watermark 200SS sensors were installed in 2012 growing season. The Decagon EC-5 and watermark 200SS sensor were installed at 20, 35, and 50 cm from soil surface. In 2013 and 2014 growing seasons, AquaSpy probe was no longer used due to high cost of data transmission service. During 2014 growing season, Sentek EasyAg-50 probe was employed, together with Decagon EC-5 and Watermark 200SS sensors. Neutron probe was utilized throughout the three

growing seasons. A 60 cm long neutron probe (503DR Hydroprobe) access tubes were installed adjacent to other sensors in the same plot and used as a reference. Neutron probe readings were taken at weekly basis and used as references. Daily average of sensor readings (AquaSpy, Decagon EC-5, Watermark 200SS, and Sentek EasyAg 50) were then fitted against neutron probe readings to calculate coefficients of determination. Root mean square errors of sensor readings versus neutron probe readings were also calculated. Detailed information of data loggers used for each sensor type is described in the following section.

Figure 1.11 Decagon EC-5, Watermark 200SS data loggers, and 503DR Hydroprobe in the field in 2014 growing season.

AquaSpy probe

As shown in Figure 1.12, each AquaSpy probe at each sensing plot was connected to a T20 cellular telemetry (AquaSpy Inc.), which delivered real time data of the probe to the AgWISE website. Data was logged at 15 min interval and was averaged on daily basis.

Figure 1.12 AquaSpy probe and telemetry (Bellamy 2009).

Watermark 200SS

Data transmission system for Watermark 200SS sensors was equipped with one wireless base receiver (Model 950R) for the whole experimental field and one field transmitter (Model 950T) at each sensing plot. Each field transmitter could read up to four Watermark 200SS sensors while transmitting data to base receiver. According to

manufacturer description (Installation and Operating Instructions of Watermark 950R & 950T), field transmitter has a maximum transmitting range of 457 m line-of-sight. In addition, base receiver and field transmitter should be installed at least 1.2 m above canopy. Hence, the base receiver was installed at center of experimental field. Antennas of field transmitter and base receiver were about 1.2 m above cotton canopy (Figure 1.13).

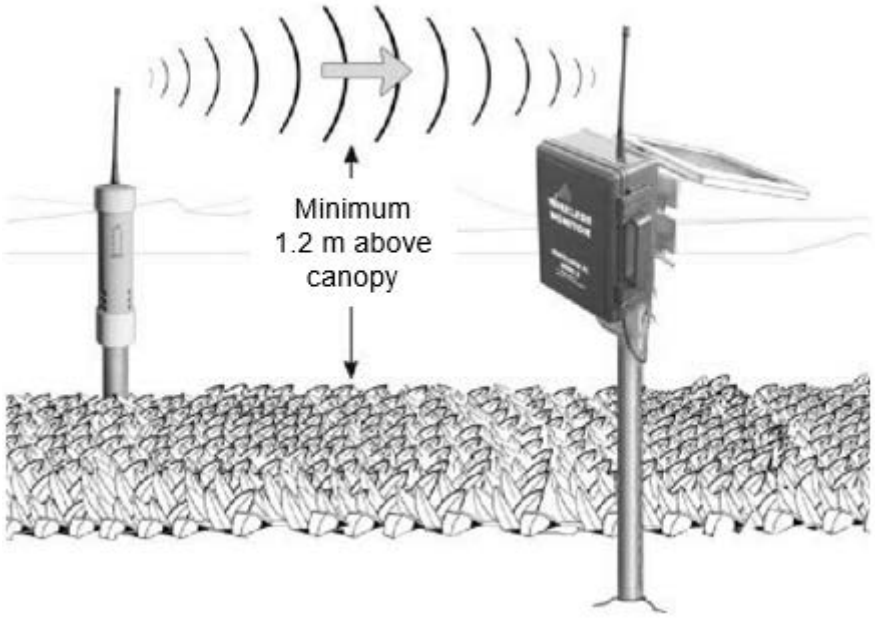

Figure 1.13 Watermark 950T transmitter send data to 950R base receiver (photo from Watermark 950R and 950T manual)

The dip switches on 950T transmitter are used for setting transmitter ID, receiver ID, and sensing mode. With different combinations, transmitter ID can be set from 1 to 16, receiver ID can be set from 1 to 8, and sensing mode can be set to “all four Watermark sensors” or “three Watermark sensors and one temperature sensor”. In this study, the dip switches at bottom of 950T transmitter were set to be all four watermark

sensors (Figure 1.14). One 950R receiver can receive readings from 16 950T field transmitters at maximum.

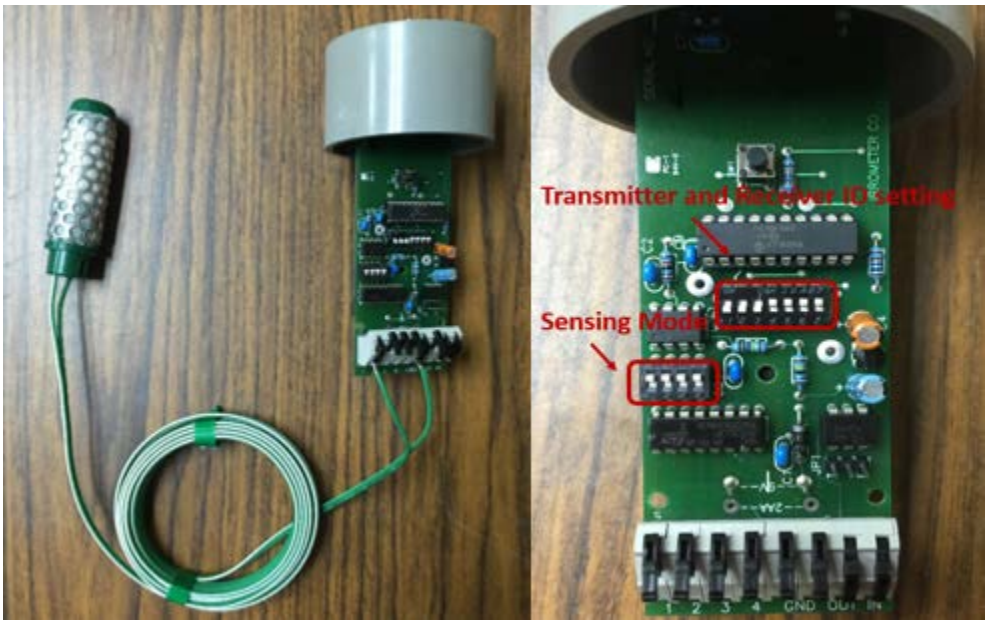

Figure 1.14 Watermark 950T connected with one Watermark 200SS sensor (left), 950T transmitter.

Base receiver 950R was mounted on a metal pole and located in the middle of the test field. A solar panel was connected through a voltage regulator for charging a 12 V battery, which supplied power to the 950R receiver (Figure 1.15). When soil water potential changed and was sensed by the Watermark 200SS sensor, the 950T field transmitter sent readings to the base receiver. The communication between 950R base receiver and 950T field transmitter was tested using the test button on the field transmitter. Once the test button is pressed, “readings’ count” on the base receiver should add one, if communication is successful. The field transmitter doesn’t store any data.

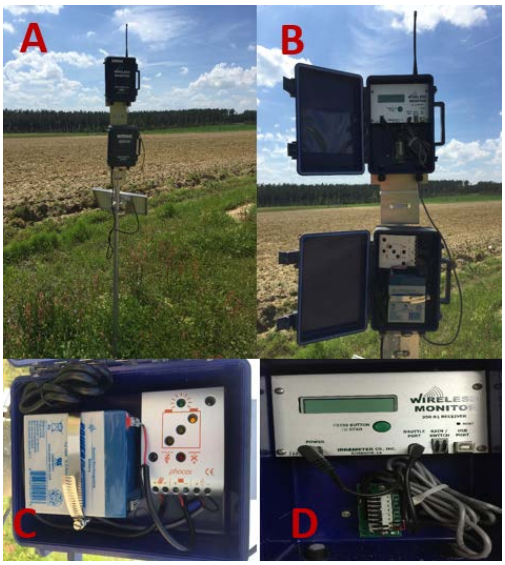

Figure 1.15 Watermark 950R receiver installed in field (A); 950R receiver and battery component (B); solar panel charging regulator (C); Power is supplied through the bottom two terminals in 950R receiver (D).

Decagon EC-5

The Em50R Wireless Data logger (Decagon Inc.) was employed to log Decagon EC-5 sensor's data. The EM50R data logger utilizes five AA batteries and is capable of connecting up to five Decagon EC-5 sensors. Figure 1.16 shows the Em50R data logger connected with one Decagon EC-5 sensor. In this study, Port P1 to port P3 were programmed to receive EC-5 sensor readings installed at depth 20, 35, and 50 cm, respectively. An Omni antenna was installed at a telephone pole in front of the office building to receive sensor readings form EM50R data loggers installed at the field. The Omni antenna was connected to a base receiver DataStation (Decagon Inc.) located inside office building through cable. The DataStation was programmed and set to the same channel of field data loggers. In the same time, to ensure data was successfully received,

the transmitting mode “Confirmed Delivery Transmit” was used. This mode ensures base station (DataStation) receiving data correctly by requesting field data logger (Em50R) to send data up to 25 attempts if data transmission fails initially. Data was stored in the Em50R even when transmitting data to the DataStation was failed (after 25 attempts). Data was logged at hourly frequency and averaged on daily basis.

Figure 1.16 Decagon EC-5 sensor connected to Em50R data logger (left) and DataStation (right)

Sentek EasyAg-50

The Sentek EasyAg-50 probe utilizes a SDI-12 digital communication protocol. To obtain this data, an embedded computing device named MoteStack developed at Clemson University was employed. This sensing platform has advantages of: 1) low cost; 2) low power consumption; 3) capability of connecting to multiple SDI-12 sensors; and 4) wireless data transmission (White et al., 2010). The MoteStack and a 12 volt battery were fitted into a weather proof enclosure (Figure 1.17). Each enclosure was designed with three connectors. Two connectors were used for connecting two EasyAg-50 probes to the

MoteStack and one connector was used for the antenna (Figure 1.17). Each probe was assigned with unique SDI-12 address and each enclosure was assigned with a unique identifier. Data was logged at hourly frequency and sent to a gateway installed nearby the test field (Figure 1.18). The gateway then sent data to an online website at Clemson University and data was downloaded weekly.

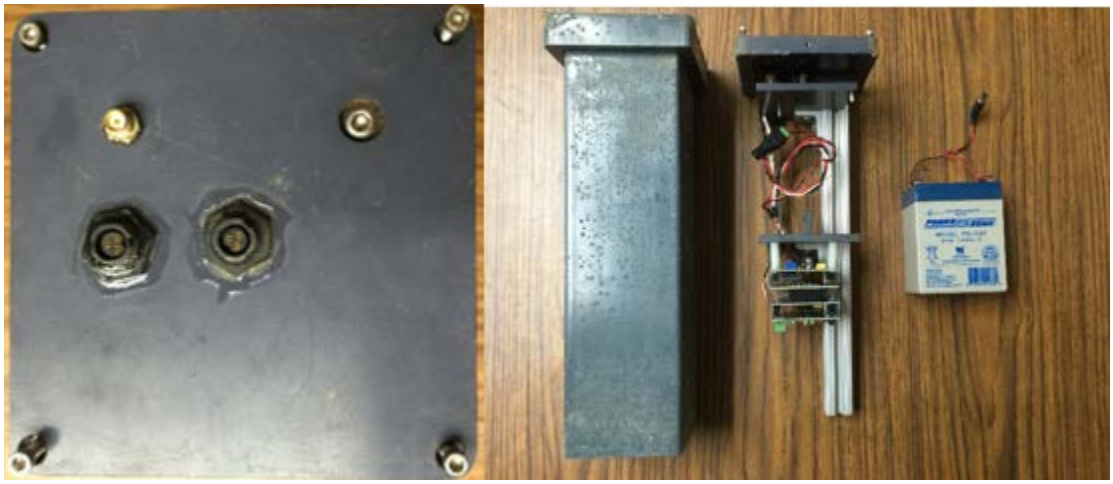

Figure 1.17 Top view of enclosure (left), MoteStack, and battery (right)

Figure 1.18 Gateway antennas nearby the test field.

1.5.3.3 Irrigation treatments

During the three growing seasons, irrigation was performed on weekly basis using a variable rate irrigation system (VRI) with Low Energy Precision Application (LEPA) nozzles (Han et al., 2009). In 2012 growing season, twenty plots (8-row by 18 m) were established in each management zone. Irrigation treatments were replicated four times per management zone using a randomized complete block arrangement (RCBD). The irrigation treatments in 2012 growing season were:

- Treatments 1 to 4: irrigation rates calculated based on average sensor readings (neutron probe) from zone 1 to 4, i.e.:

$$I_{trt1} = \left(FC_{sand} - VMC_{avg\_zone1\_sand}\right) \times D_{sand\_zone1} + \left(FC_{clay} - VMC_{avg\_zone1\_clay}\right) \times D_{clay\_zone1}$$

...

$$I_{trt4} = \left(FC_{sand} - VMC_{avg\_zone4\_sand}\right) \times D_{sand\_zone4} + \left(FC_{clay} - VMC_{avg\_zone4\_clay}\right) \times D_{clay\_zone4}$$

$$D_{sand\_zone} + D_{clay\_zone} = 60\ cm$$

Where I_{trtn} is irrigation rate in zone *n* (cm).

FC_{sand} is field capacity of sand which equal to 15.8%.

FC_{clay} is field capacity of clay which equal to 24.5%.

D_{sand_n} is depth of sand layer in zone *n* (cm).

D_{clay_n} is depth of clay layer in zone *n* (cm).

$VMC_{avg\_zonen\_sand}$ is average soil volumetric water content of sand layer in zone n measured by neutron probe in percentage.

$VMC_{avg\_zonen\_clay}$ is average soil volumetric water content of clay layer in zone n measured by neutron probe in percentage.

- Treatment 5: Irrigation rate was calculated based on single crop coefficient procedure (Allen et al. 1998). Equations are:

$$I_{ET} = \sum_{i}^{n} (ET_i - P_i)$$

$$ET_{a\_i} = K_{c\_i} \times ET_{o\_i}$$

Where I_{ET} is required irrigation amount (cm).

N is number of days since last irrigation event.

ET_{a_i} is crop evapotranspiration on day i.

K_{c_i} is single crop coefficient on day i.

ET_{o_i} is reference evapotranspiration on day i.

In 2013 and 2014 growing seasons, plot size was the same but the following irrigation treatments were replicated five times per management zone using RCBD arrangement as well. Irrigation rates were calculated using the same method of 2012. The treatments in 2013 and 2014 growing seasons were:

- Treatments 1 to 3: irrigation rates calculated based on average sensor readings (neutron probe) from zone 1 to 3,
- Treatment 4: Irrigation rate calculated based on single crop coefficient procedure (Allen et al. 1998).

Detailed information of management zones in the three growing seasons are listed in Table 1.2. Lint yield and water use efficiency (WUE) of cotton for different treatments in the three growing seasons were analyzed using R (2015). Water use efficiency of cotton was calculated using:

$$WUE = \frac{\mathrm{Y}}{I + P} \qquad 1.7$$

Where Y is lint yield of cotton in kg/ha,

I is total irrigation applied of treatment in mm,

P is total precipitation during the growing season in mm.

Table 1.2 Soil EC, depth of sandy layer, and soil composition of management zones in the three growing seasons

Year	Zone	S_EC[1]	D_EC[2]	Depth of sand	Sand %	Silt %	Clay %
			ms/m	cm			
2012	1	1.1	3.0	32	/	/	/
2012	2	1.6	3.8	30	/	/	/
2012	3	2.3	5.0	24	/	/	/
2012	4	2.7	5.8	25	/	/	/
2013	1	1.1	3.2	32	/	/	/
2013	2	1.9	4.5	29	/	/	/
2013	3	2.7	5.6	25	/	/	/
2014	1	1.4	2.5	30	78	3	19
2014	2	2.5	4.0	25	74	4	22
2014	3	3.7	5	22	71	6	23

[1]S_EC is average electrical conductivity of top 30 cm of soil (shallow).

[2]D_EC is average electrical conductivity of 91 cm of soil (deep).

1.6 RESULTS AND DISCUSSION

1.6.1 Weather data in 2012, 2013, & 2014 growing seasons

At the experimental site, the maximum air temperature during the three growing seasons (2012, 2013, and 2014) ranged from 15.9 to 40^{o}C and the minimum from 1.2 to 24.1^{o}C (Figure 1.19). Daily total solar radiation ranged from 3 to 30 MJ/(m^2*day) (Figure 1.20). The average of maximum relative humidity during the growing seasons was 93.9% and the average of minimum relative humidity was 50.5% (Figure 1.21). As shown in Figure 1.22, average of wind speed during the three growing seasons was 1.3 m/s. Reference evapotranspiration ranged from 0.5 to 7.1 mm during the three growing seasons (Figure 1.23). Total rainfall during the growing seasons was 510.6, 574.6, and 508.8 mm for the 2012, 2013 and 2014 growing seasons, respectively (Figure 1.24).

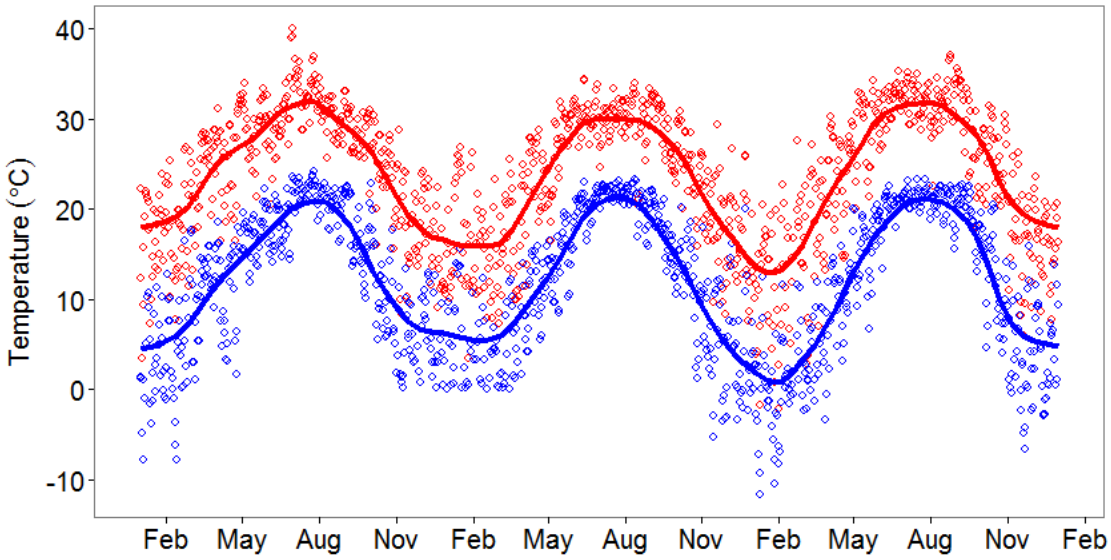

Figure 1.19 Daily maximum temperature (red dots) and minimum temperature (blue dots) in three growing seasons.

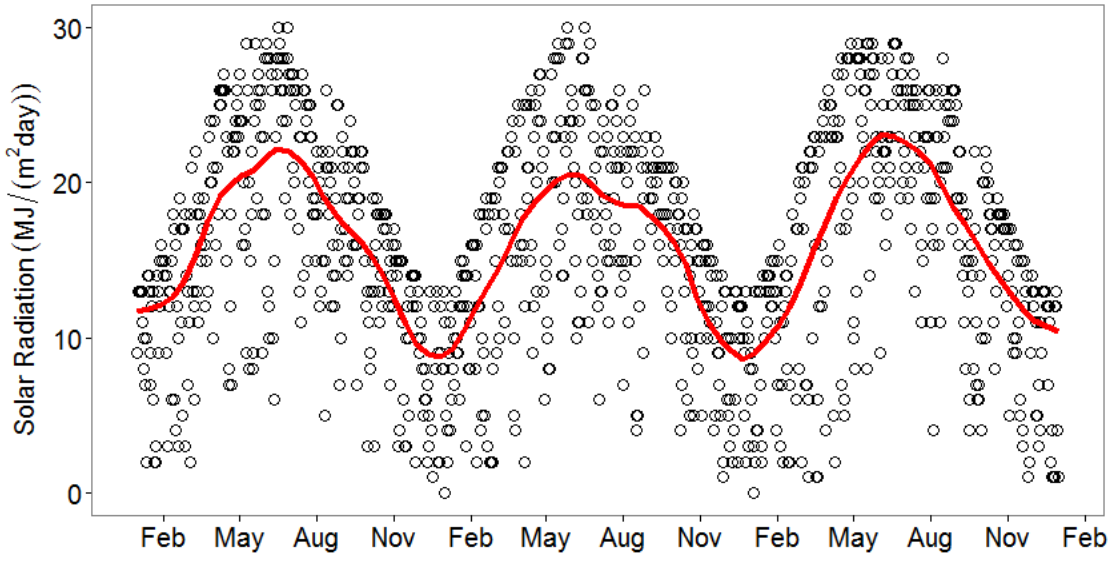

Figure 1.20 Daily solar radiation (black dots) with running average (red line) at experimental field in three growing seasons.

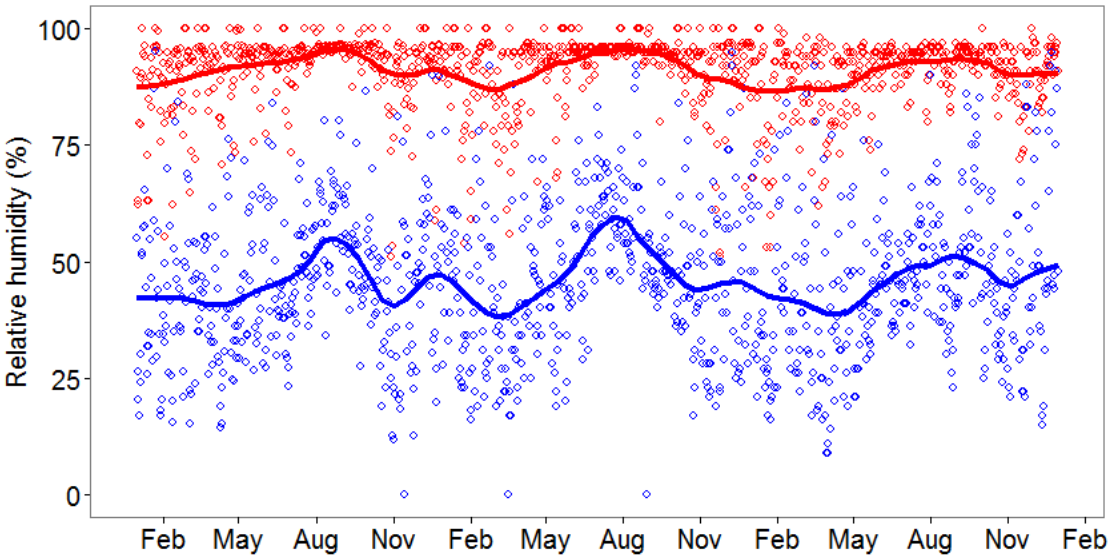

Figure 1.21 Daily maximum relative humidity (red dots) and minimum relative humidity (blue dots) at experimental field in three growing seasons.

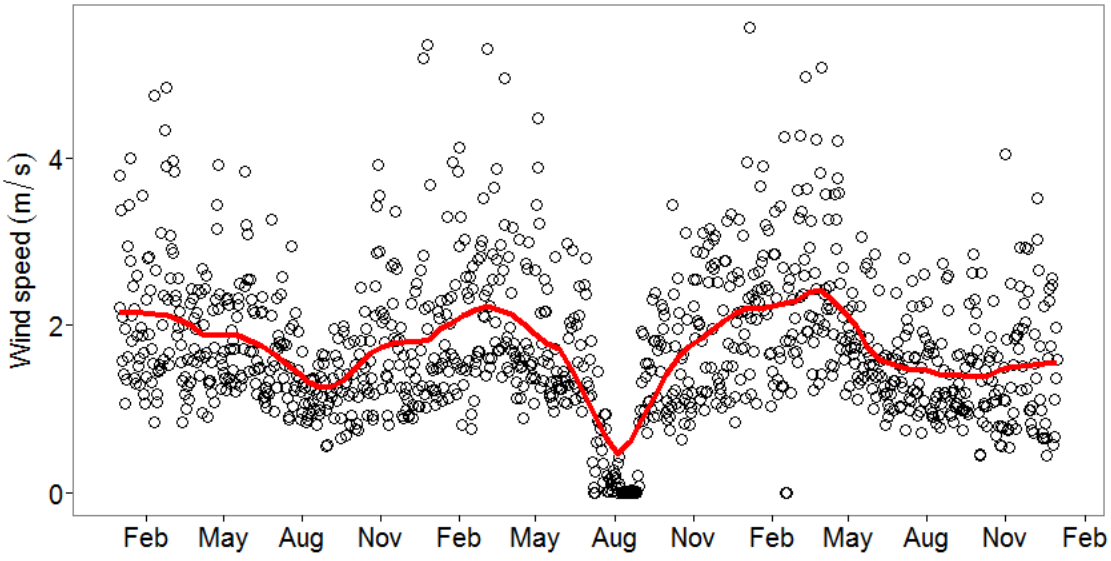

Figure 1.22 Daily average wind speed (black dots) and running average (red line) at experimental field in three growing seasons.

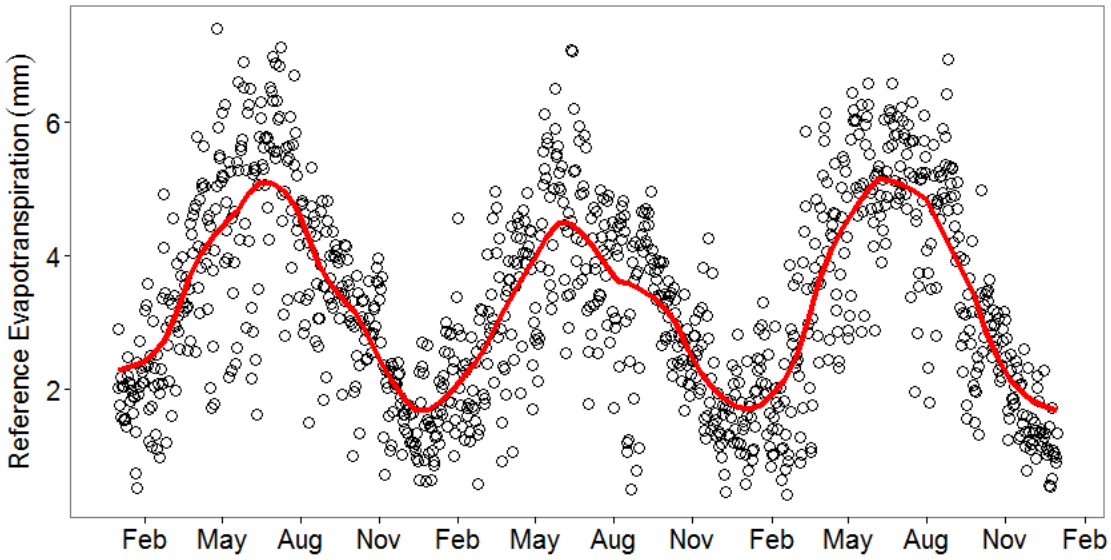

Figure 1.23 Daily reference ET (black dots) and running average (red line) at experimental field in three growing seasons.

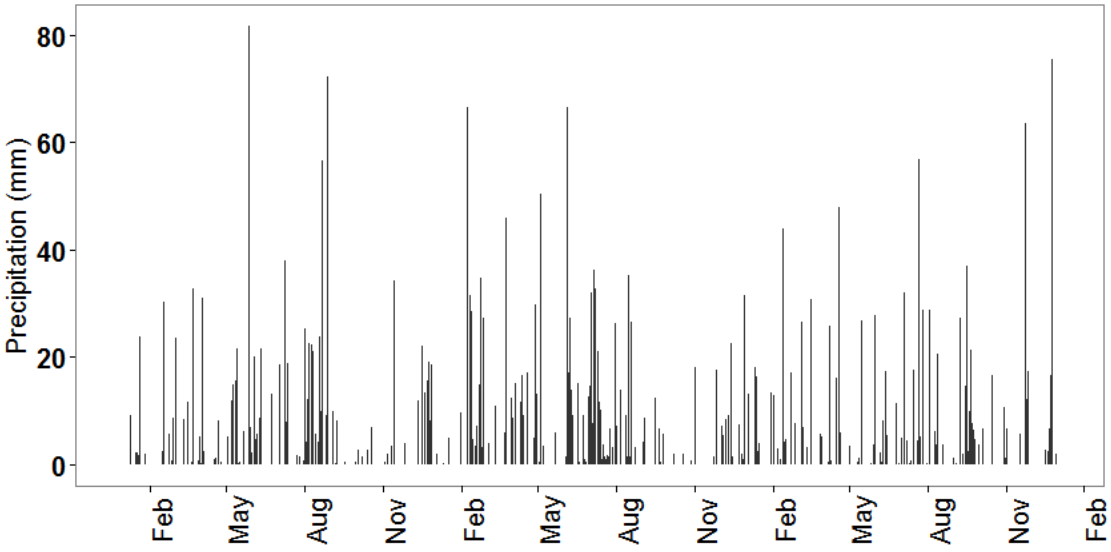

Figure 1.24 Daily precipitation at experimental field in three growing seasons.

1.6.2 Sensor Performance

1.6.2.1 Calibration in lab and field conditions

Field and lab calibration results of Decagon EC-5 sensor, Sentek EasyAg-50 probe, and 503DR Hydroprobe were all satisfactory. Field calibration of Sentek EasyAg-50 showed that sensor readings based on manufacture's calibration, correlated strongly with actual soil moisture content using linear regression method with R^2 of 0.803 for the entire soil profile (Figure 1.25). However, the Sentek EasyAg-50 underestimated VMC at higher range, i.e. when VMC was higher than 15%, and deviated from the slope and intercept. Due to the soil variability at the calibration site, separate calibration equations for the top and bottom soil were developed. As shown in Figure 1.25, sensor readings of Sentek EasyAg-50 correlated with actual soil moisture content with R^2 of 0.74 for topsoil (sand). The calibration for sandy soil didn't improve R^2 but it improves the slope and intercept of calibration equation significantly. Sensor readings of Sentek EasyAg-50 correlated with actual soil moisture content with R^2 of 0.58 for subsoil (clay) (Figure 1.26). Slope and intercept of calibration equation for clay soil were almost the same, as compared to the calibration for the entire soil profile.

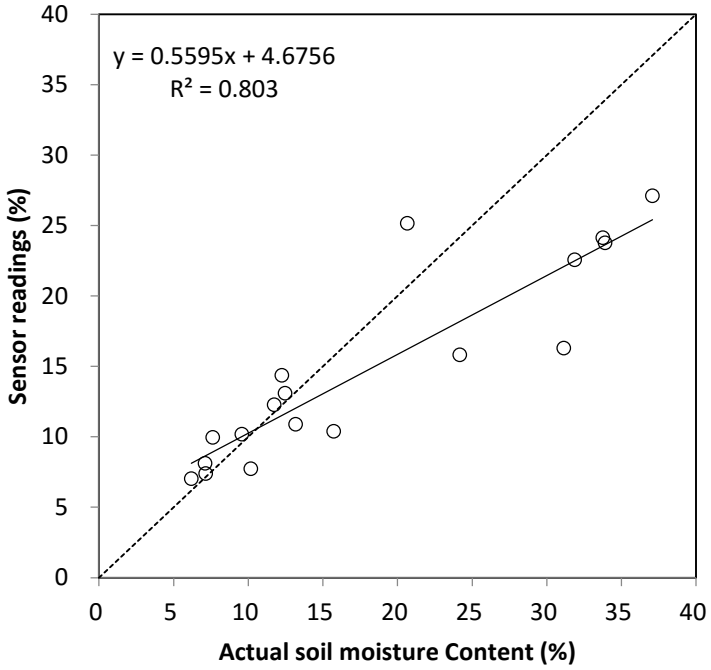

Figure 1.25 Field calibration of Sentek EasyAg-50 for the entire soil profile (0 – 50 cm)

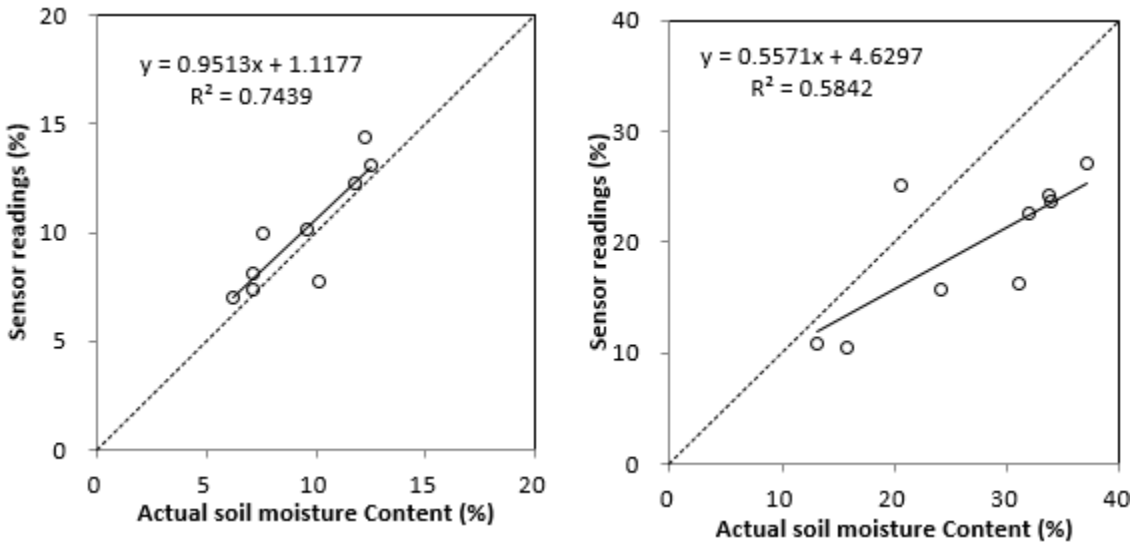

Figure 1.26 Field calibration results of Sentek EasgAg-50 sensor at topsoil (10 – 30 cm) (left) and subsoil (30 – 50 cm) (right).

As shown in Figure 1.27, there was a strong linear correlation between Decagon EC-5 readings and the actual soil moisture contents with R^2 equal to 0.8809 for the entire soil profile. Slope of the linear calibration equation was 0.94 and intercept was 1.12. Separate calibration equations for the top soil and sub soil were also developed. As shown in Figure 1.28, VMC of Decagon EC-5 sensor correlated well with actual soil moisture content with R^2 of 0.89 and 0.76, for topsoil and subsoil, respectively. At topsoil, the Decagon EC-5 sensor slightly over estimated VMC when VMC was higher than 15%. The soil also became saturated at this point, since field capacity of sand layer in this field was 15.8%. For subsoil, the Decagon EC-5 sensor slightly underestimated the actual VMC but still yielded high R^2 (0.76) and good slope (1.09).

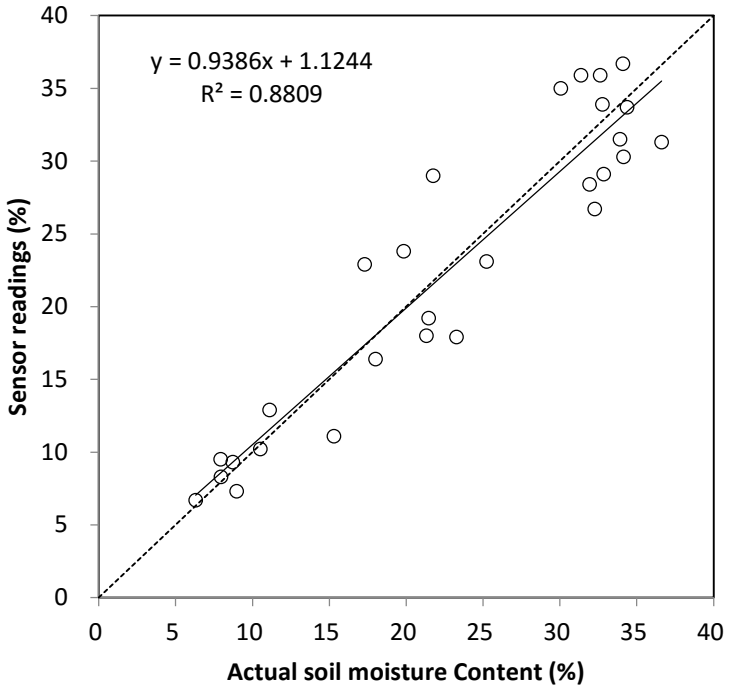

Figure 1.27 Field calibration of Decagon EC-5 for the entire soil profile (0 – 50 cm)

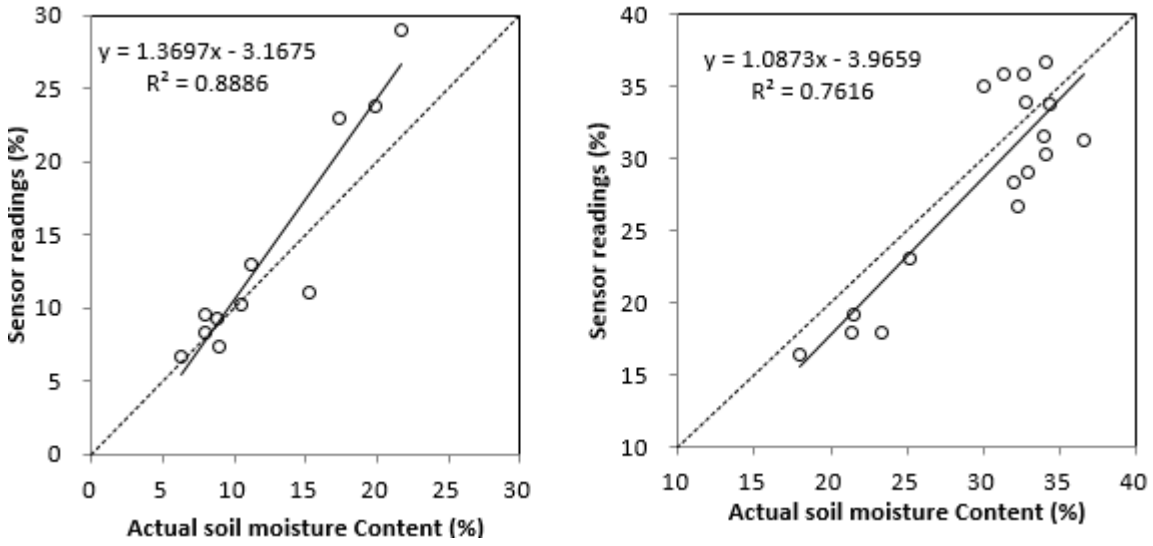

Figure 1.28 Field calibration results of Decagon EC-5 sensor at topsoil (10 – 30 cm) (left) and subsoil (30 – 50 cm) (right).

Neutron probe has been previously calibrated at another field at the Edisto REC by station scientists (Farahani, 2015). Also, the calibration was conducted in a field with similar soil type compared to experimental field of this study. The previous calibration equation yielded high R^2 equal to 0.89 for the entire soil profile. Separate calibration equations for top and sub soils were also developed according to previous dataset, and the results are shown in Figure 1.29. Calibration results from the experimental field of this study are shown in Figure 1.30. In this study, neutron probe readings correlated with actual soil moisture content linearly with R^2 of 0.81 and 0.81 for topsoil and subsoil layers, respectively. It was noted that the actual soil moisture contents of top soil calibration conducted at this study ranged from 8% to 26%, which covered a wider soil moisture range compared to the previous study. Thus, calibration equation for top soil from this study was used throughout the whole study. In terms of calibration equation for

sub soil, equation from this study was used simply due to higher R^2 compared to previous study.

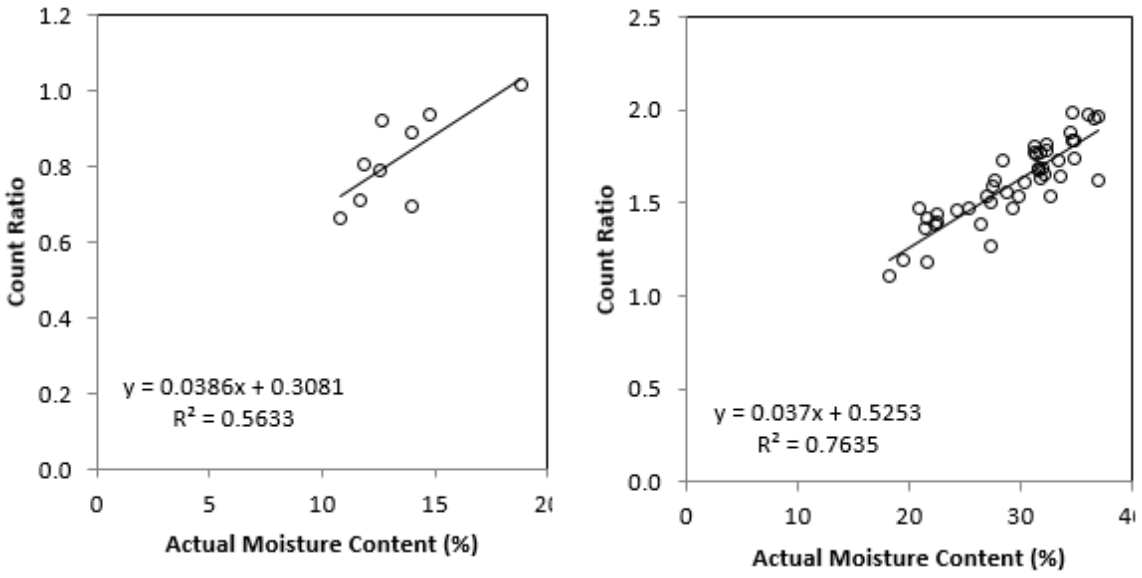

Figure 1.29 Field calibration results of 503DR HydroProbe conducted previously at similar soil type for topsoil (left) and subsoil (right), respectively.

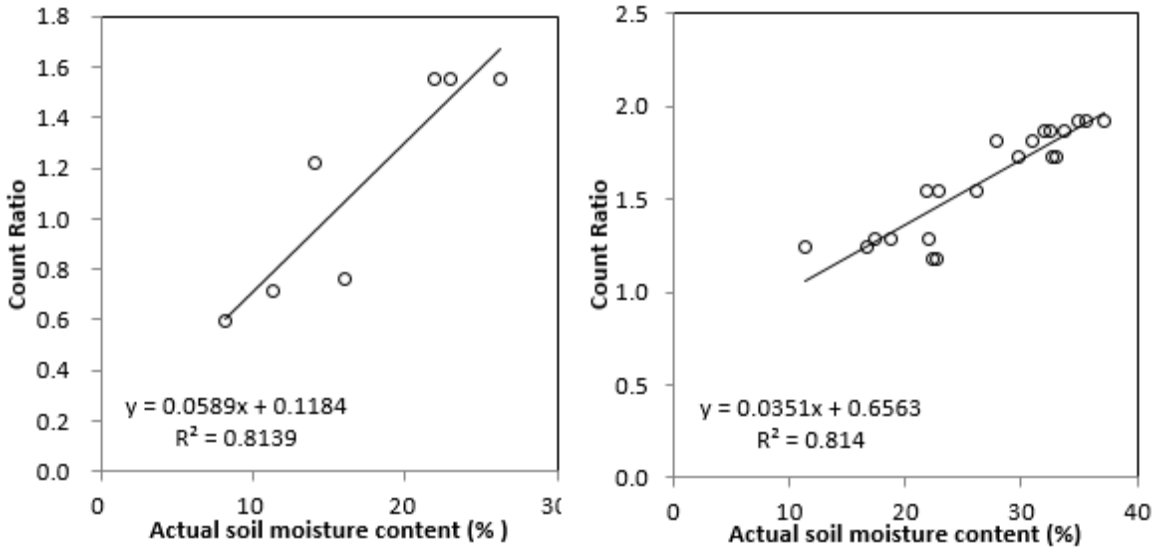

Figure 1.30 Field calibration results of 503DR HydroProbe conducted at experimental field in this study for topsoil (left) and subsoil (right), respectively.

Lab calibration results of Sentek EasyAg-50 and Decagon EC-5 sensor for sandy top soil were also satisfactory. For this layer, sensor readings of Sentek EasyAg-50 and Decagon EC-5 correlated with actual soil moisture content with R^2 of 0.96 and 0.97, respectively (Figure 1.31). In contrast to field calibrations, the Sentek Easy-Ag 50 sensor underestimated VMC rather under lab calibration condition for the topsoil. While the Decagon EC-5 sensor performed similarly under lab and field calibrations for the topsoil, i.e. underestimated VMC at lower range and overestimated VMC at higher range. Lab calibrations of Sentek EasyAg-50 and Decagon EC-5 sensors for subsoil were not successful, due to the difficulty of uniformly mixing soil. Calibration equations developed either under lab or field conditions were compared to manufacturer's calibration equations. Calibration equations are summarized in Table 1.3.

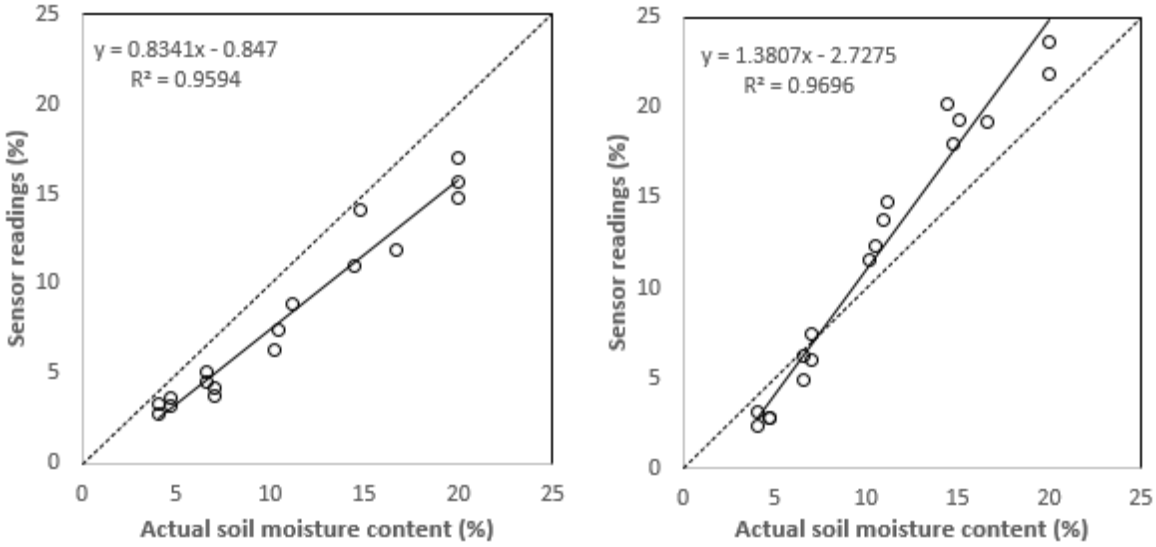

Figure 1.31 Lab calibration results of Sentek EasyAg-50 (left) and Decagon EC-5 (right).

Table 1.3 Calibration results of Sentek EasyAg-50 and Decagon EC-5 sensors

Sensors	Equations
Sentek EasyAg 50 field calibration	
Topsoil	$\mathrm{VMC} = (\mathrm{SR} - 1.1177)/0.9513^{*}$
Subsoil	$\mathrm{VMC} = (\mathrm{SR} - 4.6297)/0.5571$
Sentek EasyAg 50 lab calibration	
Topsoil	$\mathrm{VMC} = (\mathrm{SR} + 0.847)/0.8341$
Subsoil	NA
Decagon EC-5 field calibration	
Topsoil	$\mathrm{VMC} = (\mathrm{SR} + 3.1675)/1.3697$
Subsoil	$\mathrm{VMC} = (\mathrm{SR} + 3.9659)/1.0873$
Decagon EC-5 lab calibration	
Topsoil	$\mathrm{VMC} = (\mathrm{SR} + 2.7275)/1.3807$
Subsoil	NA

*SR is sensor readings.

1.6.2.2 Field performance of sensors compared to neutron probe

During 2012 growing season, even AquaSpy probe which was calibrated in previous study at the same experimental field (Bellamy 2009), did not perform satisfactory. Volumetric water content readings of AquaSpy didn't correlate well with neutron probe readings (R^2 = 0.418 and RMSE = 13.98%). In addition, the AquaSpy probe underestimated volumetric soil moisture severely compared to neutron probe readings (Figure 1.32). Decagon EC-5 sensor performed the best among all three sensors, by correlating with neutron probe readings with R^2 of 0.58 and RMSE of 4.86% (Figure 1.35). However, the sensor tended to overestimate soil moisture at lower VMC range (less than 25%) while underestimating soil moisture at higher VMC range (over 25%). Watermark 200SS sensor performed slightly better than AquaSpy probe, by correlating with neutron probe readings with R^2 of 0.58 and RMSE of 9.47% (Figure 1.35). The Watermark 200SS sensor also underestimated VMC compared to neutron probe readings (Figure 1.34). In addition, compared to AquaSpy (Figure 1.32) and Decagon EC-5 (Figure 1.33) sensors, Watermark 200SS sensor failed to distinguish variation of VMC among treatments (Figure 1.34). The 950R base receiver began to receive data intermittently during the middle of the season and was sent to factory for repair, thus the scattered data points of Watermark 200SS readings in Figure 1.34 was caused by this issue.

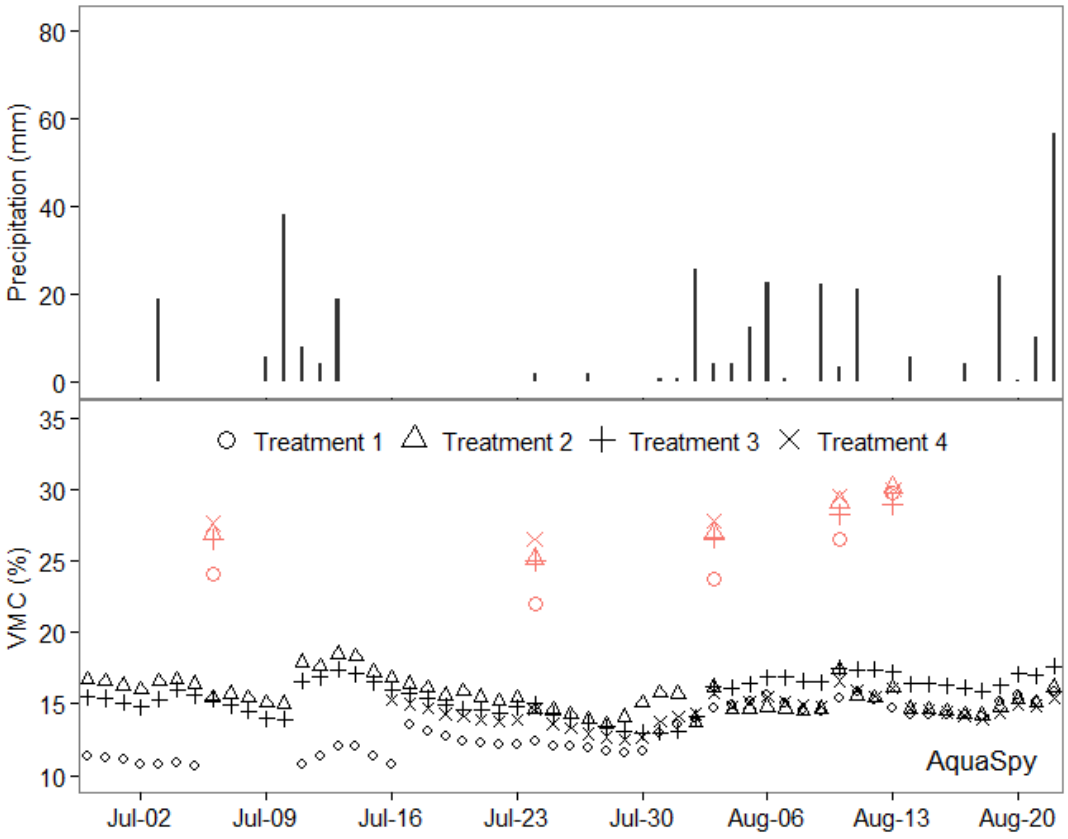

Figure 1.32 Rainfall (top panel) and measured soil volumetric water content in the top 60 cm of soil profile for AquaSpy and neutron probe (red dots) between July 1st and August 20th during the 2012 growing season.

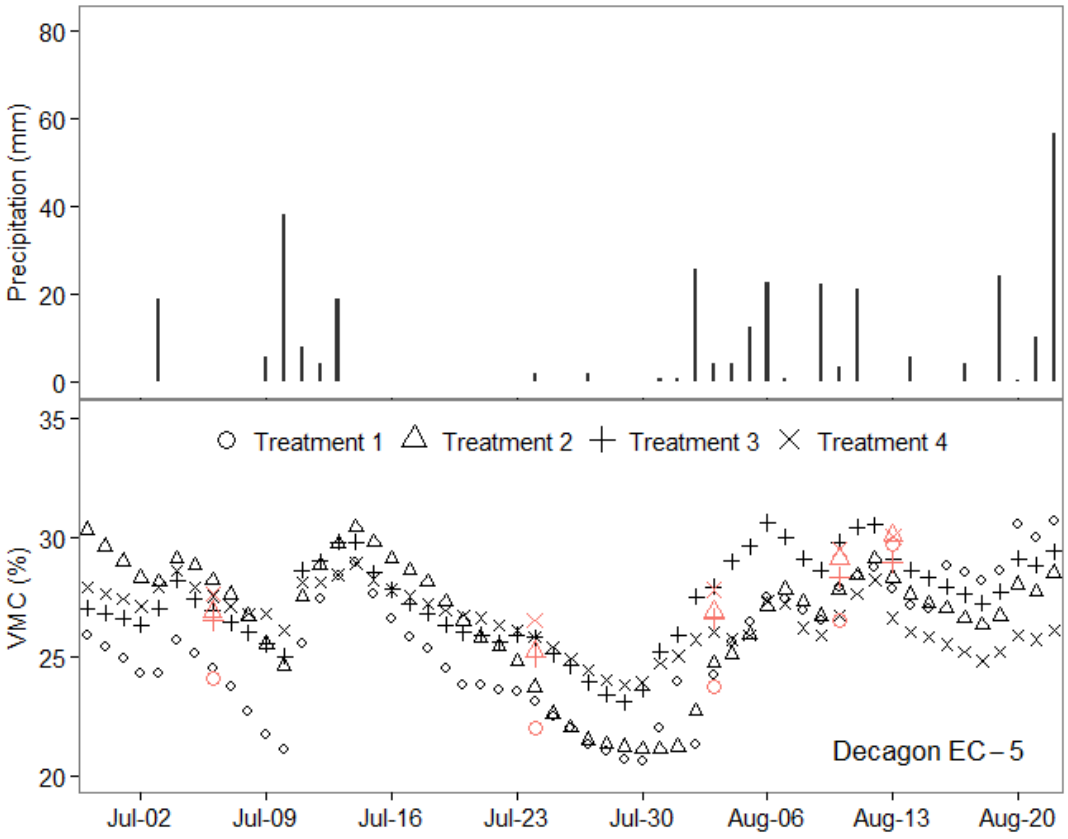

Figure 1.33 Rainfall (top panel) and measured soil volumetric water content in the top 60 cm of soil profile for Decagon EC-5 sensor and neutron probe (red dots) between July 1st and August 20th during the 2012 growing season.

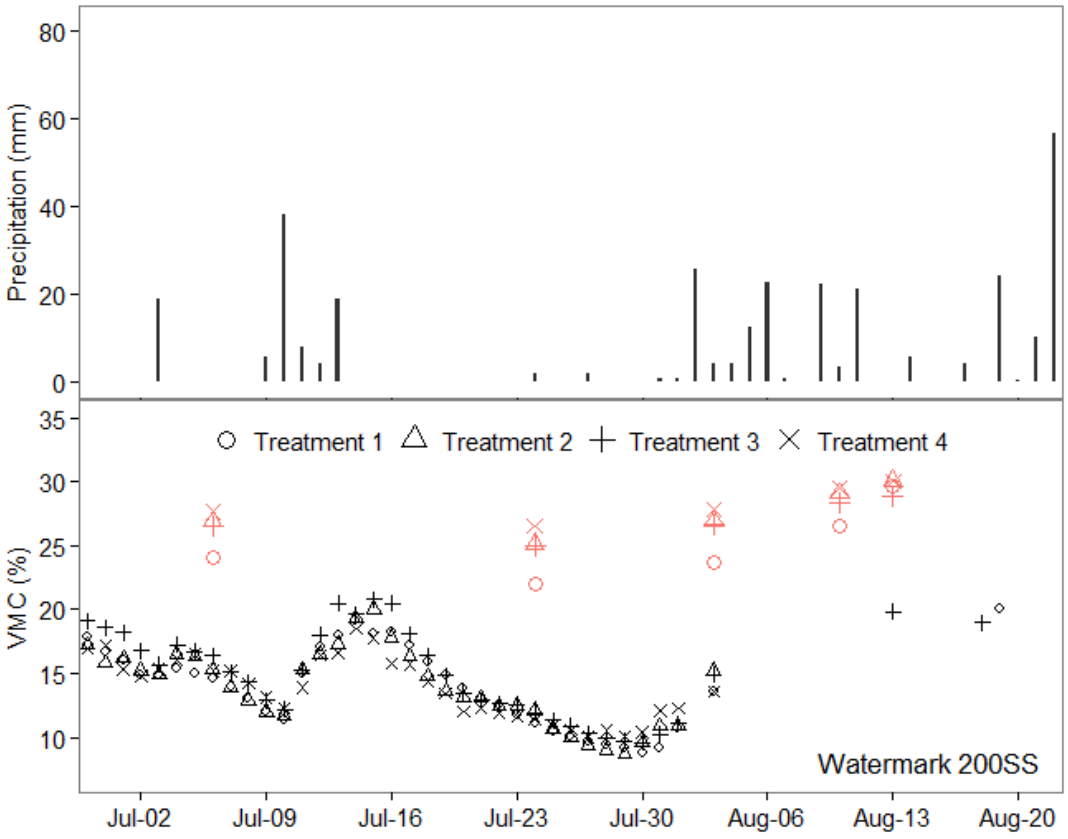

Figure 1.34 Rainfall (top panel) and measured soil volumetric water content in the top 60 cm of soil profile for Watermark 200SS sensor and neutron probe (red dots) between July 1st and August 20th during the 2012 growing season.

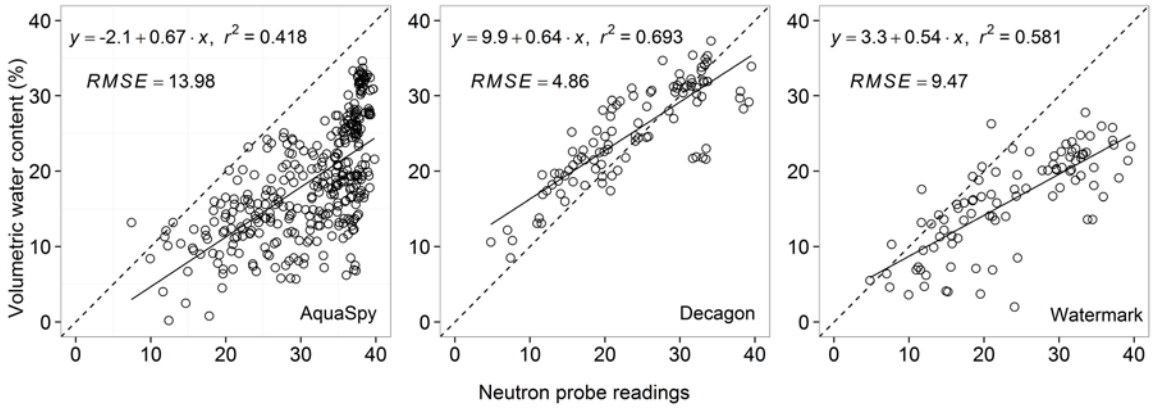

Figure 1.35 Factory calibrated readings of Aquaspy, Decagon EC-5, and Watermark 200SS compared to neutron probe readings in 2012 growing season.

In 2013, due to the high cost of data service, AquaSpy probe was no longer used. The Decagon EC-5 sensors still performed better compared to Watermark 200SS sensors. Volumetric water contents of Decagon EC-5 sensors had a strong correlation with neutron probe readings with R^2 of 0.626 and RMSE was 5.68% (Figure 1.38). Contrary to 2012 growing season, the Decagon EC-5 sensors tended to overestimate soil moisture at higher range in 2013 growing season (Figure 1.36). This alternation of behaving pattern could be a result of human error such as improper installation of sensors and also much wetter soil profile in 2013 growing season. Volumetric water contents of Watermark 200SS sensors correlated with neutron probe readings with R^2 of 0.445 and RMSE was 11.93% (Figure 1.38). Similar to 2012 growing season, Watermark 200SS sensors underestimated soil moisture compared to neutron probe readings, however, followed the same trend of soil moisture changes (Figure 1.37).

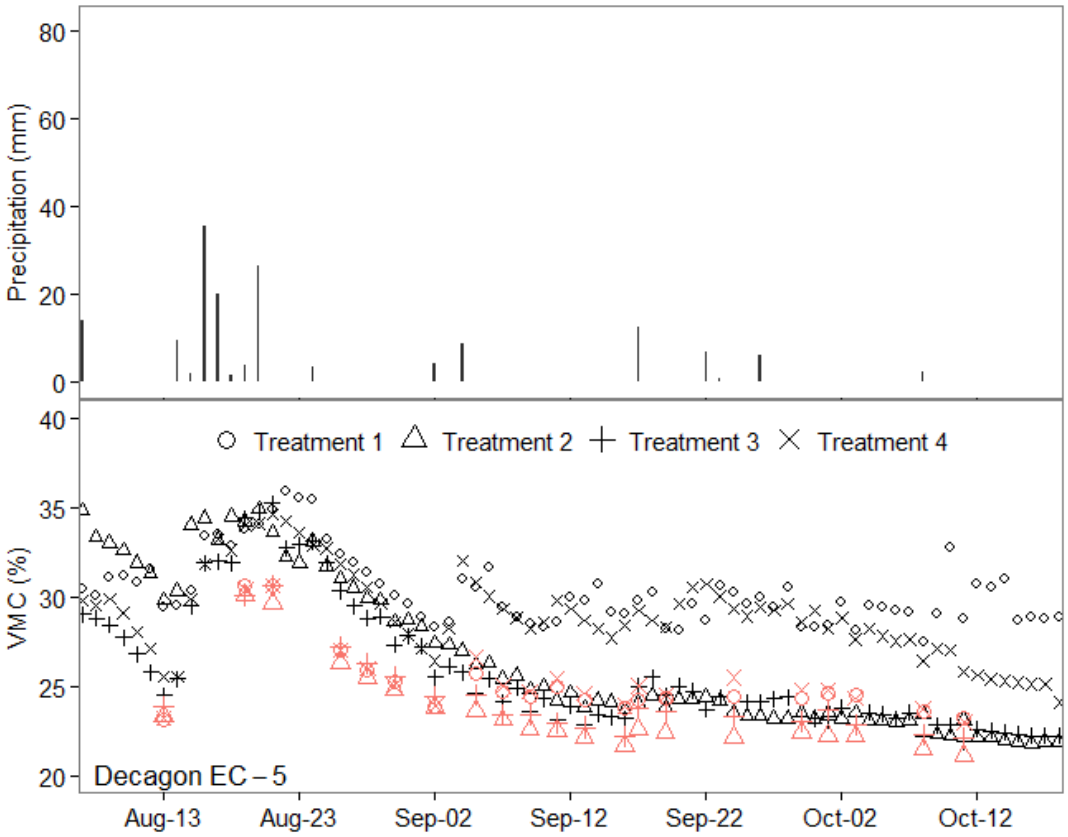

Figure 1.36 Rainfall (top panel) and measured soil volumetric water content in the top 60 cm of soil profile for Decagon EC-5 sensor and neutron probe (red dots) between August 10th and October 15th during the 2013 growing season.

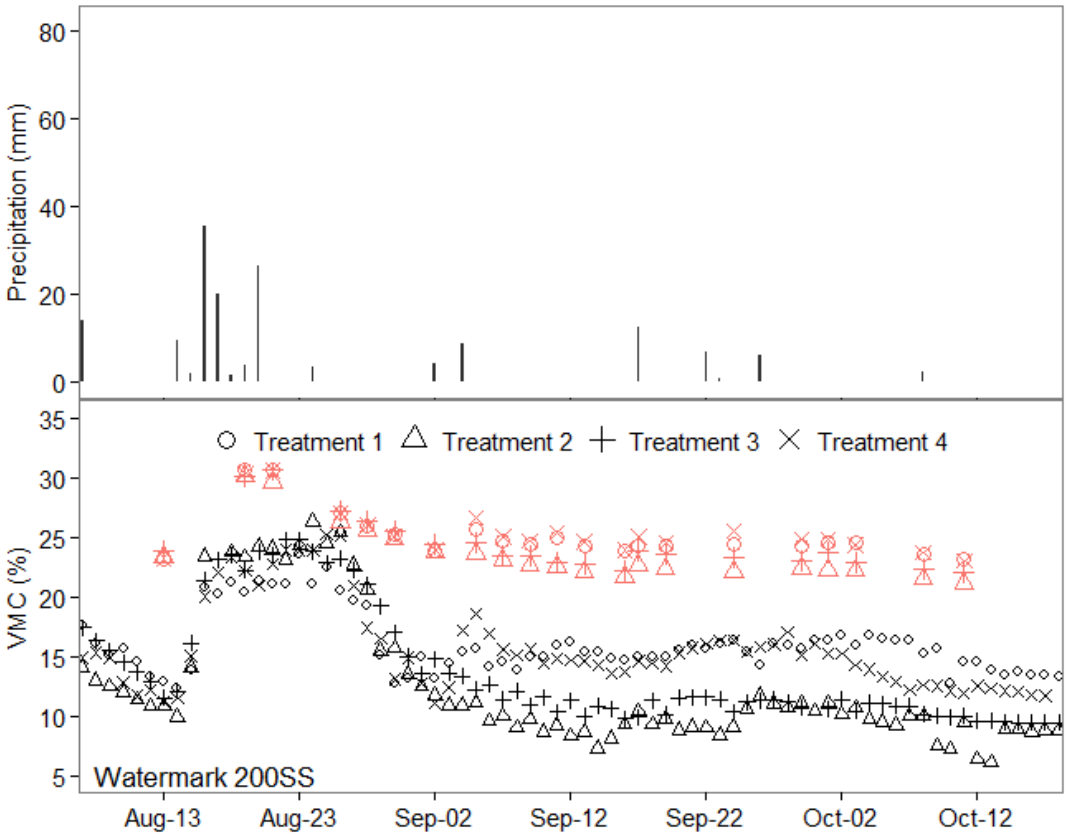

Figure 1.37 Rainfall (top panel) and measured soil volumetric water content in the top 60 cm of soil profile for watermark 200SS sensor and neutron probe (red dots) between August 10th and October 15th during the 2013 growing season.

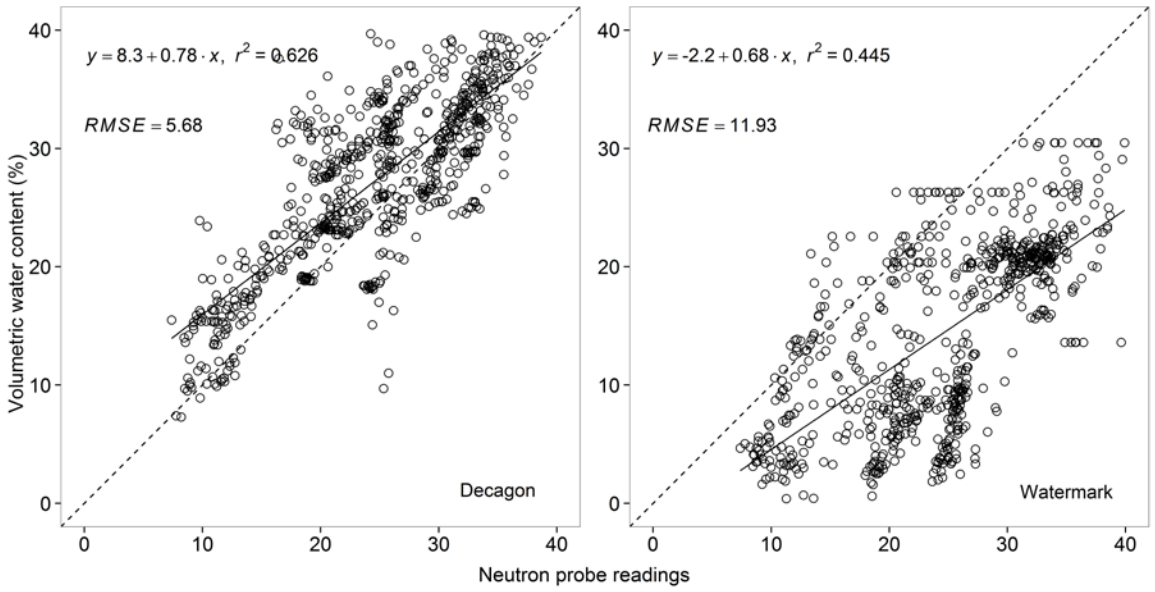

Figure 1.38 Factory calibrated readings of Decagon EC-5 and Watermark 200SS compared to neutron probe readings in 2013 growing season.

During 2014 growing season, Sentek EasyAg-50 readings (based on manufacturer's calibration) had a strong correlation with VMC readings of neutron probe (R^2 = 0.837 and RMSE = 4.21) (Figure 1.42). Volumetric soil water content measured by Sentek EasyAg-50 followed VMC of neutron probe and rainfall events seamlessly throughout the entire growing season (Figure 1.39). The correlation between Decagon EC-5 sensor readings and neutron probe readings was not satisfactory but acceptable (R^2 = 0.602 and RMSE = 6.7%) (Figure 1.42). Also, Decagon EC-5 sensor performed in the same pattern as it did in 2012 growing season, i.e., overestimated VMC at lower range (VMC < 25%) and underestimate VMC at higher range (VMC > 25%) (Figure 1.42). Volumetric water content readings of Watermark 200SS sensor correlated with neutron probe readings with R^2 of 0.505 and RMSE was 9.51% (Figure 1.42). Yet again, the

Watermark 200SS sensor underestimated VMC compared to neutron probe readings (Figure 1.41).

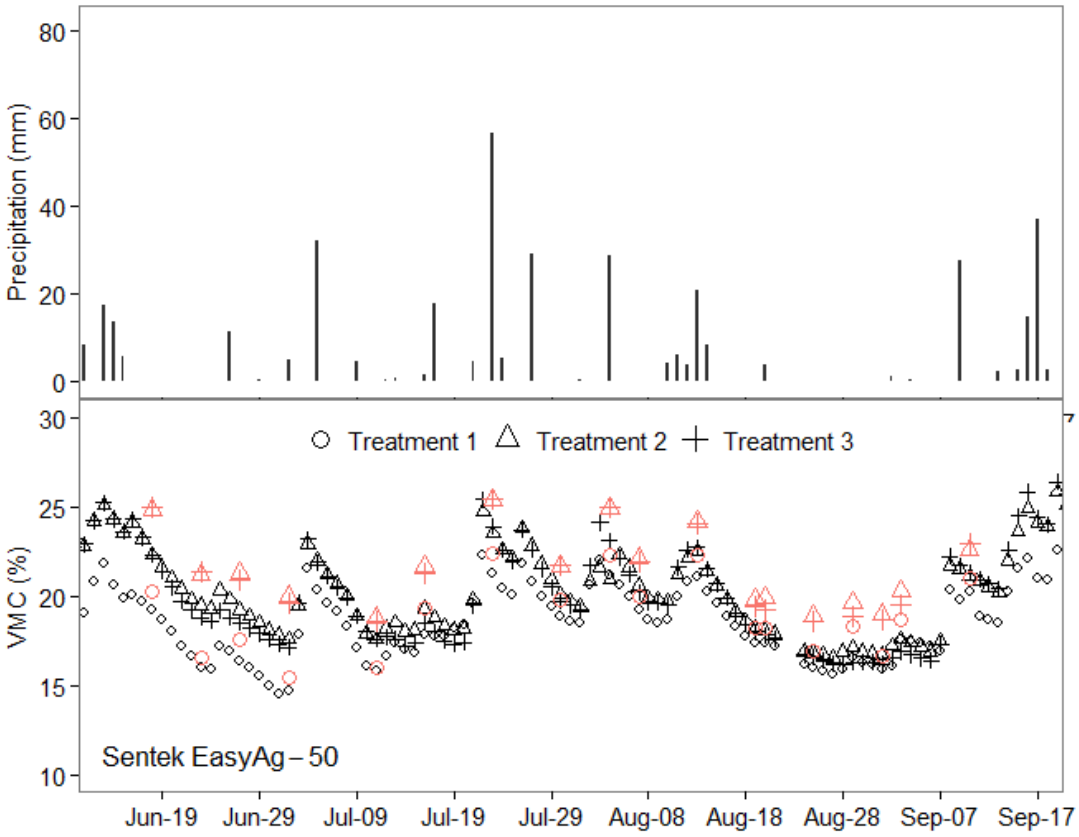

Figure 1.39 Rainfall (top panel) and measured soil volumetric water content in the top 60 cm of soil profile for Sentek EasyAg-50 and neutron probe (red dots) during the 2014 growing season.

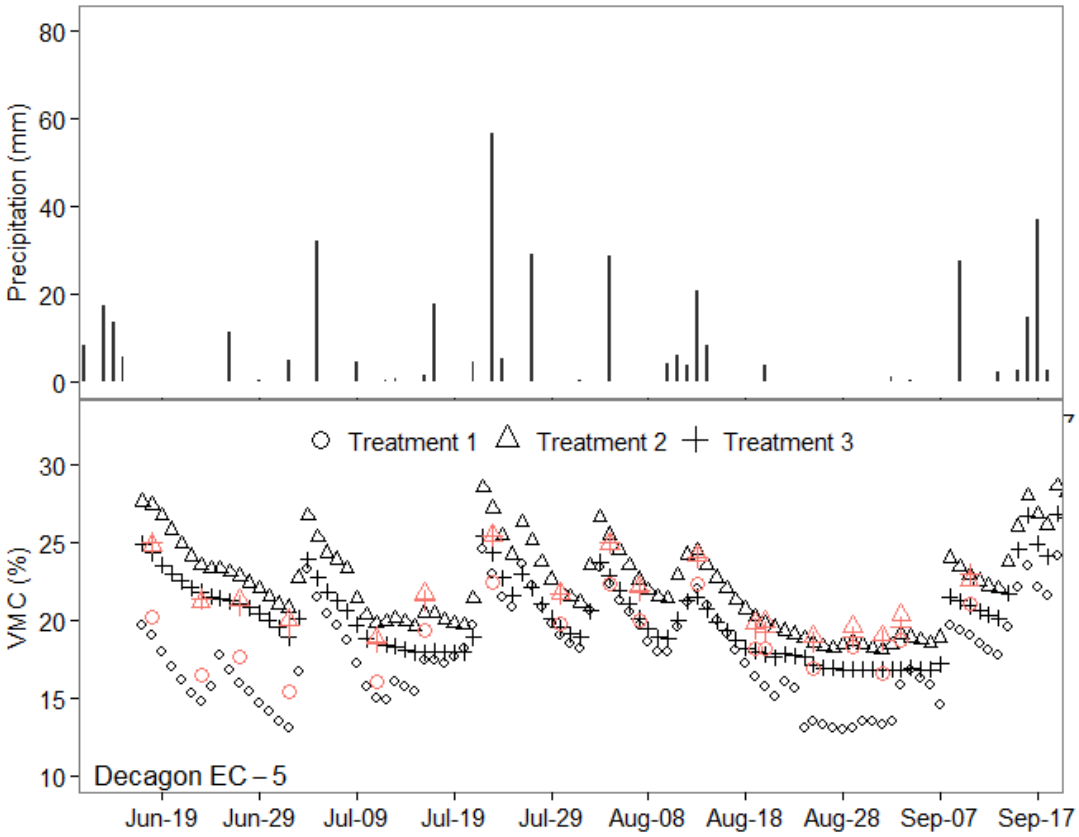

Figure 1.40 Rainfall (top panel) and measured soil volumetric water content in the top 60 cm of soil profile for Decagon EC-5 and neutron probe (red dots) during the 2014 growing season.

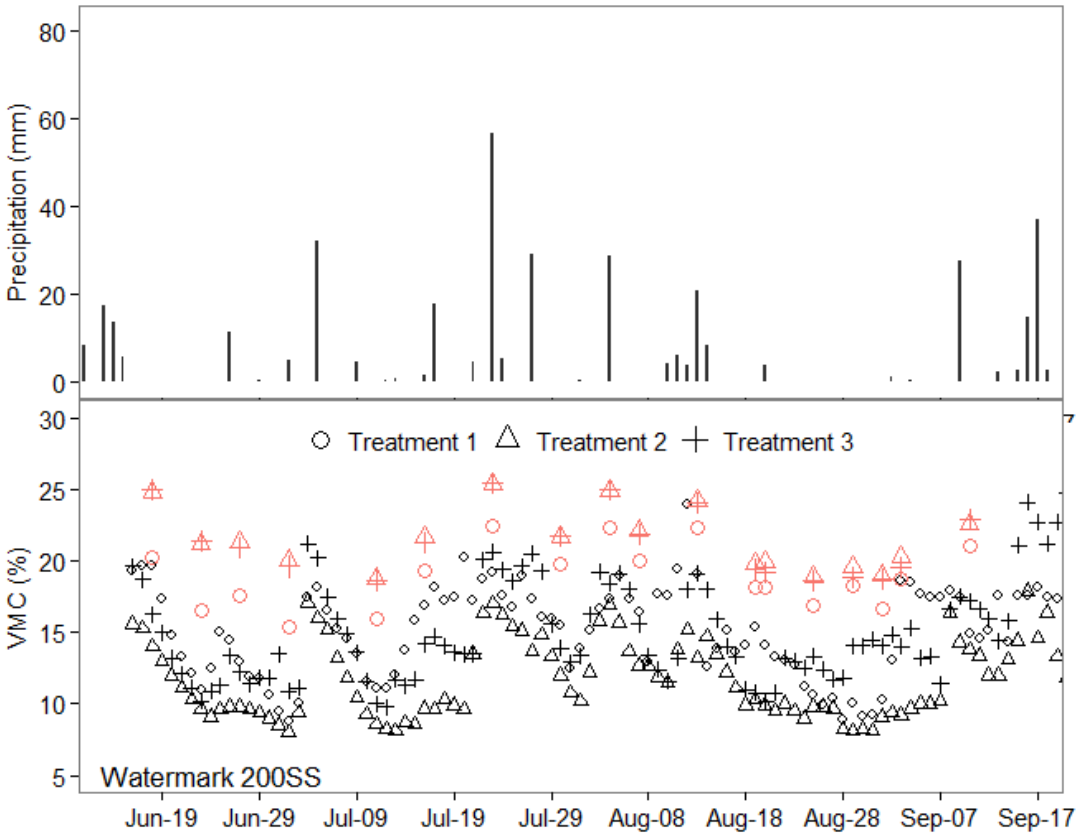

Figure 1.41 Rainfall (top panel) and measured soil volumetric water content in the top 60 cm of soil profile for Watermark 200SS and neutron probe (red dots) during the 2014 growing season.

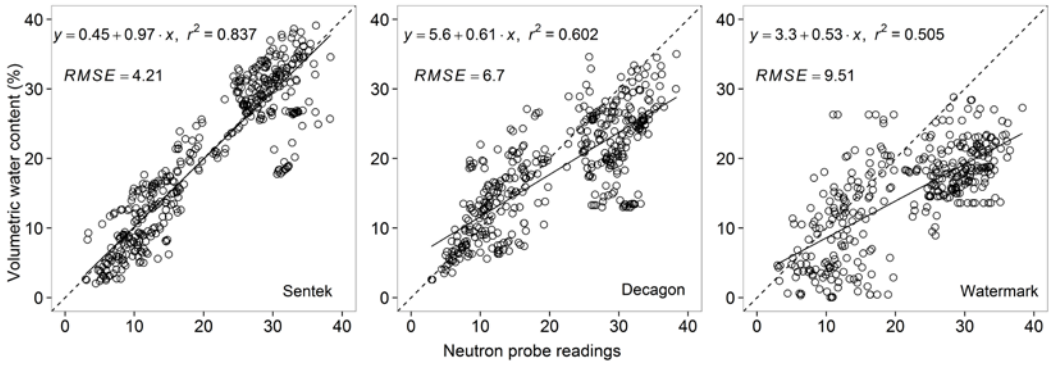

Figure 1.42 Factory calibrated readings of Sentek, Decagon EC-5, and Watermark 200SS compared to neutron probe readings in 2014 growing season.

Data from 2014 growing season was used to evaluate lab and field calibration equations for Sentek EasyAg-50 and Decagon EC-5 sensors. The field and lab calibrations of top soil (sand, 10 – 30 cm) for Sentek EasyAg-50 sensor didn't improve the linear calibration equation in terms of slope and intercept. Also, using field and lab calibration equations, RMSE of Sentek EasyAG-50 readings versus neutron probe readings increased, to 3.48 and 5.17, respectively (Figure 1.43), compared to factory calibrated Sentek EasyAg-50 RMSE (3.21). Similarly, field calibration of subsoil (clay, 30 – 50 cm) didn't improve the linear relationship between Sentek EasyAg-50 and neutron probe readings. Root mean square error of field calibrated Sentek EasyAg-50 readings versus neutron probe increased significantly to 17% compared to factory calibrated RMSE which was 5% (Figure 1.44).

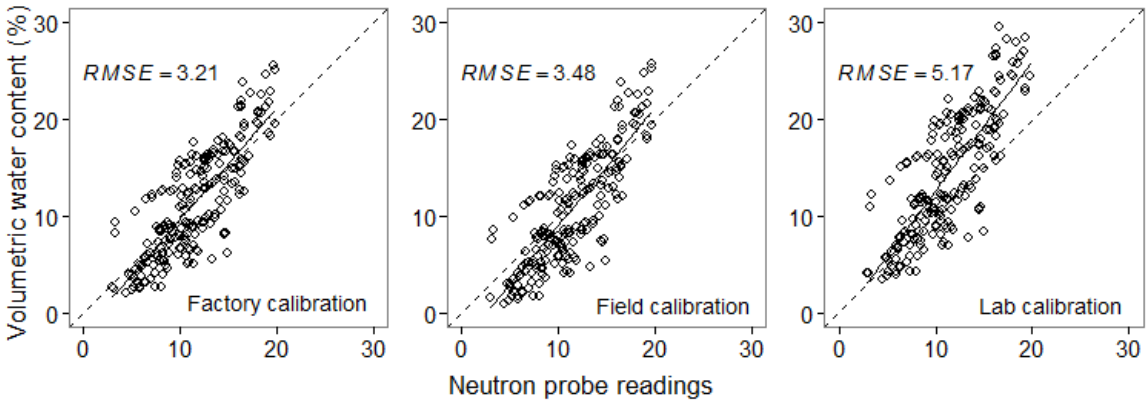

Figure 1.43 Factory, field calibrated, and lab calibrated readings of Sentek EasyAg-50 probe versus neutron probe at topsoil (10 – 30 cm)

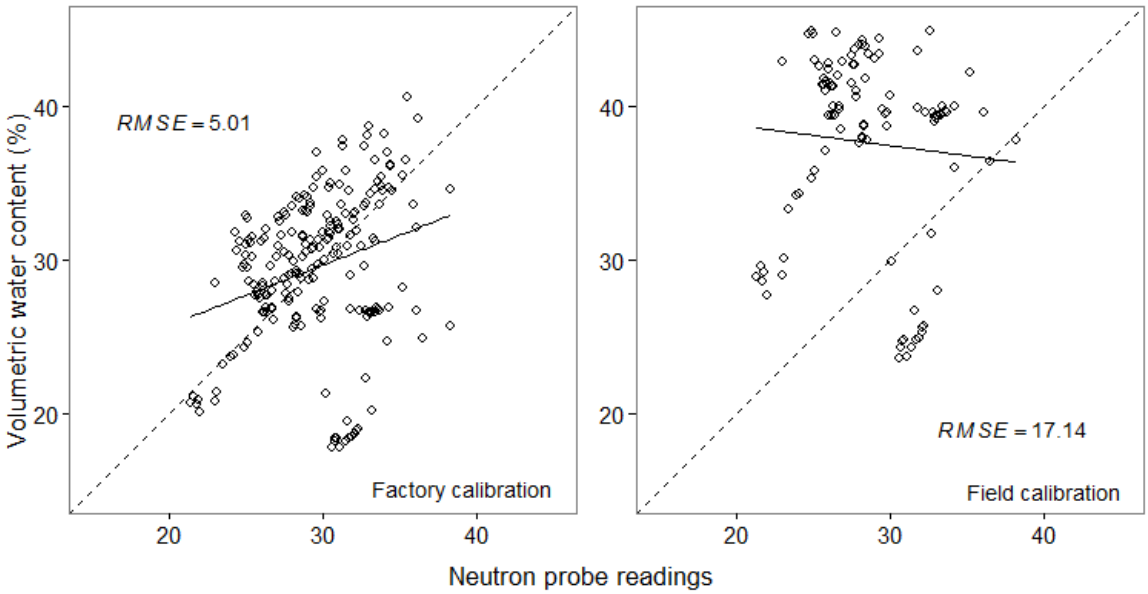

Figure 1.44 Factory and field calibrated readings of Sentek EasyAg-50 probe versus neutron probe at subsoil (30 – 50 cm)

Field calibrated and lab calibrated Decagon EC-5 readings at topsoil decreased the RMSE from 4.36% to 3.32% and 3.33, respectively (Figure 1.45). The field calibrated and lab calibrated Decagon EC-5 readings resulted similar linear relationship with

neutron probe readings in terms of slope and intercept. Calibrated readings of Decagon EC-5 were preferred since they produced smaller RMSE compare to neutron probe readings. At subsoil, field calibrated Decagon EC-5 readings produced larger RMSE (6.6) compared to RMSE of factory calibrated readings (5.93) (Figure 1.46). Thus factory calibrated Decagon EC-5 readings at subsoil were preferred.

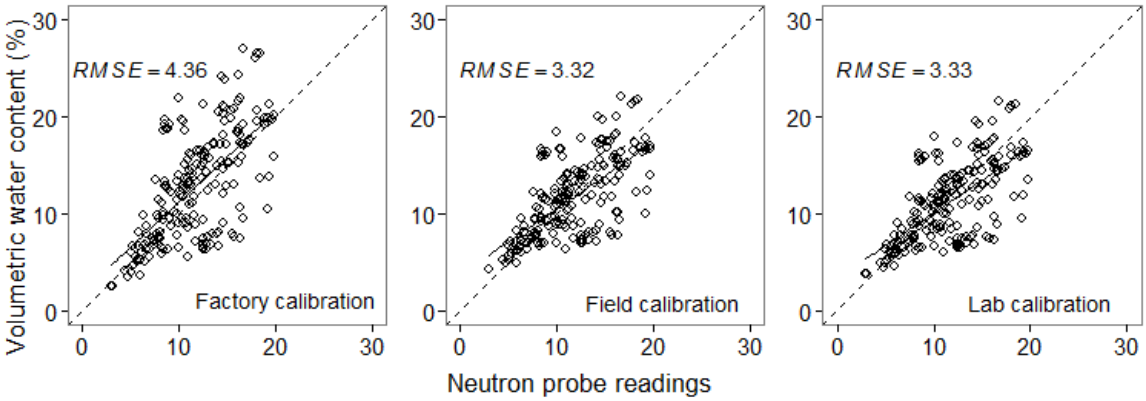

Figure 1.45 Factory, field, and lab calibrated readings of Decagon EC-5 sensor versus neutron probe at topsoil (10 – 30 cm)

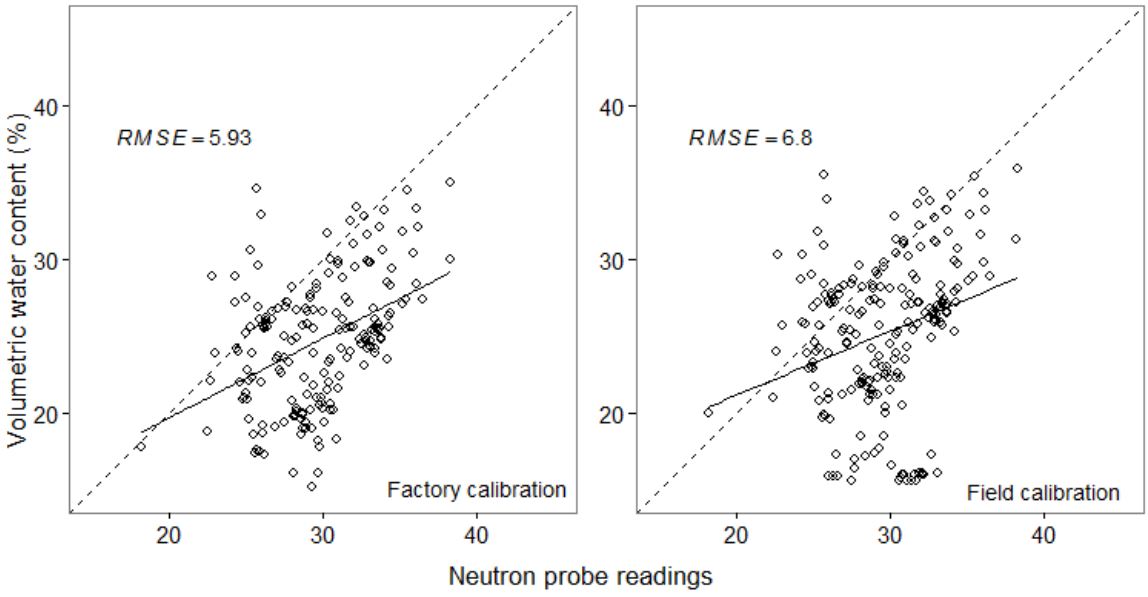

Figure 1.46 Factory and field calibrated readings of Decagon EC-5 sensor versus neutron probe at subsoil (30 – 50 cm)

As summarized in Table 1.3, results from the three growing seasons showed that Sentek EasyAg-50 performed the best among all of the sensors tested, with highest coefficient of determination of 0.837 and lowest RMSE of 4.21% for the entire soil profile. Furthermore, the slope (0.97) and intercept (0.45) of regression line of Sentek EasyAg-50 readings versus neutron readings also indicated better performance of Sentek EasyAg-50 probe. Similar to finding of Miller et al. (2014), factory calibration of Sentek EasyAg-50 was sufficient for coastal plain soils. The performance of Decagon EC-5 sensor was acceptable. Therefore, it was suggested to use Decagon EC-5 sensor when budget is limited, considering the lower cost of this sensor. The field calibration of Decagon EC-5 sensor at subsoil didn't improve the linear relationship between sensor readings and neutron probe readings. However, either field or lab developed calibration

equation for topsoil for Decagon EC-5 sensor was recommended since it lowered RMSE from 4.36 to 3.3. It was interesting that, in 2014 growing season, the RMSE of Sentek EasyAg-50 probe and Decagon EC-5 sensor at subsoil (5% and 5.9%, respectively) were higher compared to RMSE of the two sensors at topsoil (3.2% and 4.4%, respectively). The relative poor performance of Sentek EasyAg-50 and Decagon EC-5 sensors at subsoil might be attributed to the special characteristic of clay soil. As concluded by Jones et al. (2002), clay soils have larger porosity and thus are easier to bind more water compared to sandy soils. He also pointed out the presence of bound water at soil surface would change dielectric signature of soil. It was also possible that sensors (Sentek EasyAg-50 and Decagon EC-5) at deeper depth didn't have good contact with soils. When sensors were initially installed, air gaps at topsoil were minimized by carefully packing sandy soil around the sensor, which would fill those air gaps if there were any at top layer of the soil. However, it was problematic whether air gaps at sub layer of the soil could be filled using this method.

The Watermark 200SS sensor underestimated VMC throughout the three growing seasons. Yet Watermark 200SS readings were able to trace the trend of soil moisture change (Figure 1.34, 1.37, and 1.41). However, the lower R^2 and higher RMSE of Watermark 200SS sensor indicated it was not suitable for accurate measurement of volumetric water content of soil. Furthermore, as concluded by Thompson (2006), the slow response of Watermark 200SS sensor to quick drying or wetting events also limit its application in precision irrigation management. Similar to Intrigliolo and Castel's

conclusion (2004), the Watermark 200SS sensor was recommended to use only when information of relative wetness or dryness of soil was desired.

Table 1.4 Summary of factory calibrated sensor performances in terms of RMSE, slope, intercept, and R^2 versus neuron probe readings

Type of Sensors	RMSE	Slope	Intercept	R^2
2012 growing season				
AquaSpy	13.98	0.67	-2.1	0.418
Decagon EC-5	4.86	0.64	9.9	0.693
Watermark 200SS	9.47	0.54	3.3	0.581
Sentek EasyAg-50	/	/	/	/
2013 growing season				
AquaSpy	/	/	/	/
Decagon EC-5	5.68	0.78	8.3	0.626
Watermark 200SS	11.93	0.68	-2.2	0.445
Sentek EasyAg-50	/	/	/	/
2014 growing season				
AquaSpy	/	/	/	/
Decagon EC-5	6.70	0.61	5.6	0.602
Watermark 200SS	9.51	0.53	3.3	0.505
Sentek EasyAg-50	4.21	0.97	0.45	0.837

1.6.3 Effect of Irrigation Treatments

Average cotton lint yield were 2082, 1257, and 1824 kg/ha for 2012, 2013, and 2014 growing seasons, respectively. Water use efficiency of cotton lint yield ranged from 0.18 kg/m^3 to 0.36 kg/m^3 across the three experimental years. Though total rainfall in 2013 growing season (574.6 mm) was only 64 mm more than 2012 growing season (510.6 mm), total rainfall between planting and first square in the 2013 growing season was 218.4 mm more than during the 2012 growing season. These rainfall events caused intermittent waterlogging in the field and inhibited plant development. As a result, average cotton lint yield in 2013 was significantly lower than average cotton lint yield in 2012. Bange et al. (2004) conducted experiments on effect of waterlogging and found that early water logging events during early squaring showed marked impact on reduction of yield compared to late water logging events. Hocking et al. (1987) also pointed out that early flooding impaired uptake of most nutrients by young cotton plants. He also showed that concentrations of P and K were continuously reduced by waterlogging events, which are crucial for cotton development.

Table 1.5 Summary of irrigation treatments, precipitation, cotton lint yield, water use efficiency (WUE) for 2012, 2013, and 2014 growing seasons.

Year	TRT[1]	I	P	I+P	Lint	Lint_sd[2]	WUE	WUE_sd[3]
		mm	mm	mm	Kg/ha	Kg/ha	Kg/m^3	Kg/m^3
2012	1	102	511	613	2096 ab	88	0.34 a	0
2012	2	80	511	591	2055 ac	46	0.35 a	0.01
2012	3	106	511	617	2122 ab	97	0.34 a	0
2012	4	111	511	622	2146 b	106	0.35 a	0
2012	5	61	511	572	1990 c	68	0.35 a	0
2013	1	67	575	642	1255 a	60	0.2 a	0
2013	2	11	575	586	1276 a	82	0.22 b	0.01
2013	3	0	575	575	1250 a	118	0.22 b	0.01
2013	4	91	575	666	1249 a	59	0.19 b	0.01
2014	1	211	509	720	1855 a	129	0.26 a	0.01
2014	2	139	509	648	1810 a	67	0.28 a	0
2014	3	108	509	617	1802 a	67	0.29 b	0.01
2014	4	150	509	658	1838 a	73	0.28 a	0.01

[1]TRT represents treatment.

[2]Lint_sd is standard deviation of cotton lint yield among replicates of each treatment

[3]WUE_sd is standard deviation of water use efficiency among replicates of each treatment

1.6.3.1 Experiment in 2012

As summarized in Table 1.4, total irrigation applied for the five treatments in 2012 growing season were 102, 80, 106, 111, and 61 mm, respectively. At the initiation of 2012 growing season, daily VMC in the top 60 cm of all treatments measured by Decagon EC-5 started from a high value due to frequent rainfall events during June (Figure 1.47). Statistical analysis showed that means of cotton lint yield among the five treatments were significantly different (Figure 1.48). In addition, Tukey's 'Honest Significant Difference' test was employed to examine the difference of cotton lint yield between pairs of irrigation treatments. As shown in Figure 1.48, cotton lint yield of

treatment 5 (ET-based irrigation scheduling) was significantly lower than lint yield of treatment 1, 3, and 4. There were no significant difference for means of cotton lint yield among treatment 1, 3, and 4. Cotton lint yield of treatment 2 was significantly smaller than cotton lint yield of treatment 4, where treatment 4 is based on senor readings from heavier soil. This suggests that, in a production field with soil variability, it would be beneficial to install moisture sensors in management zones with higher EC readings to obtain maximum yield. The means of water use efficiency (WUE) were not significantly different among treatments, as shown in Figure 1.49.

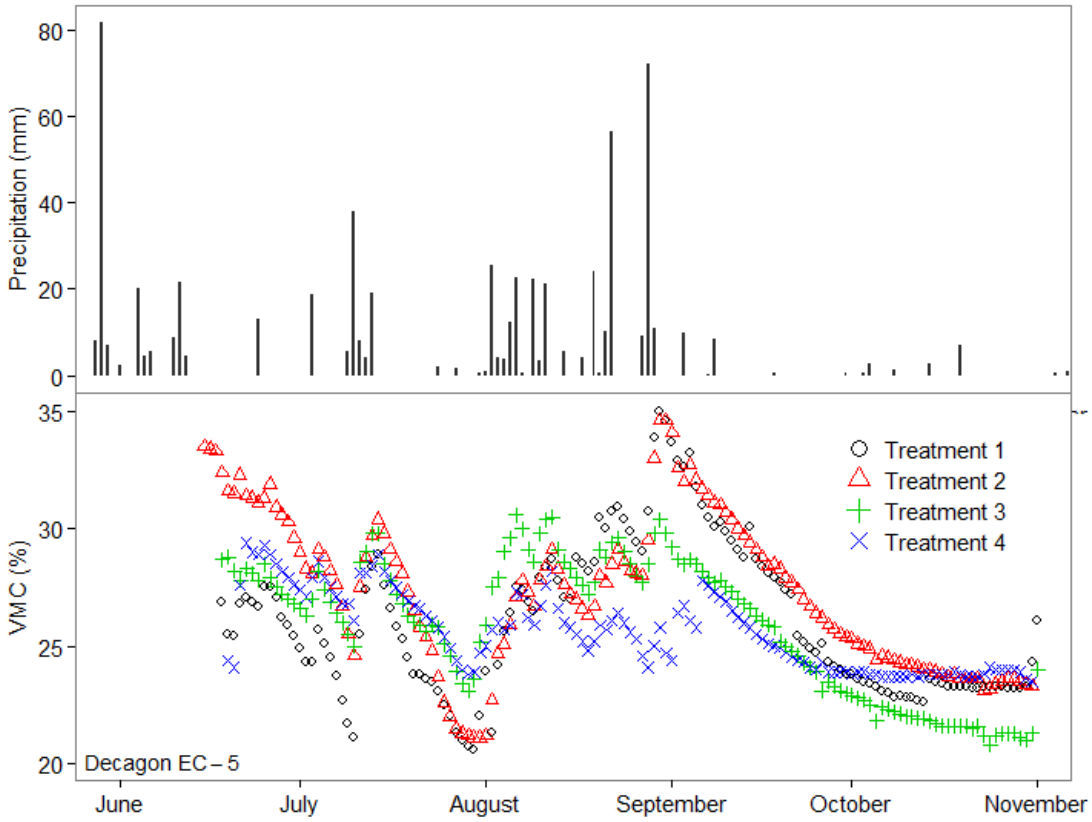

Figure 1.47 Rainfall (top panel) and measured soil volumetric water content in the top 60 cm soil profile of different treatments measured by Decagon EC-5 sensor during the 2012 growing season.

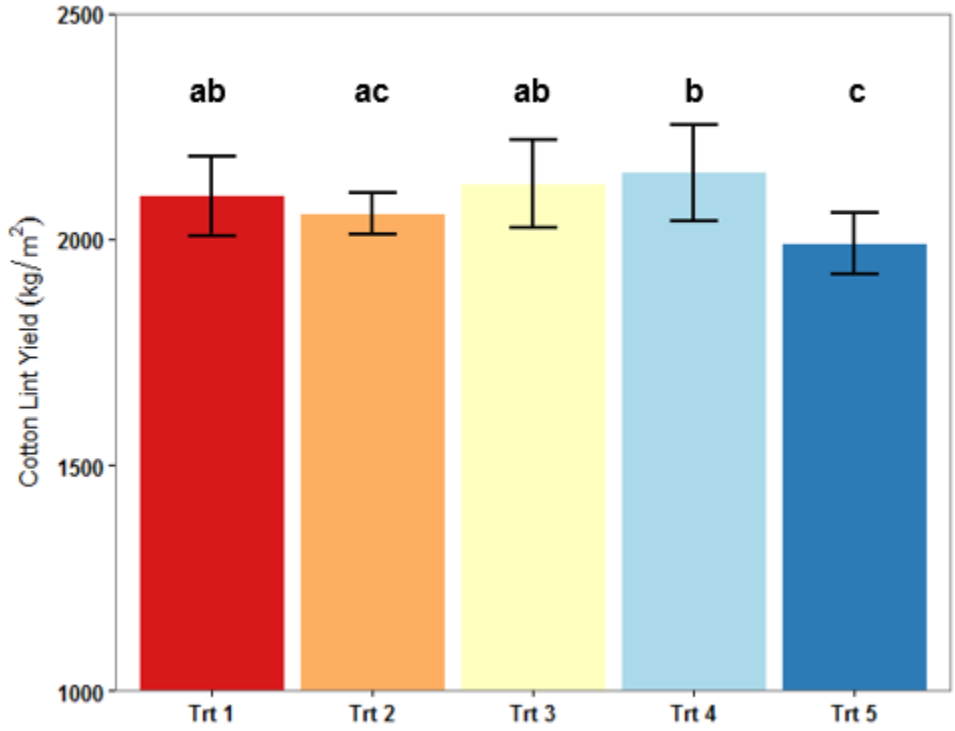

Figure 1.48 Effect of irrigation treatments on cotton lint yield in 2012 growing season

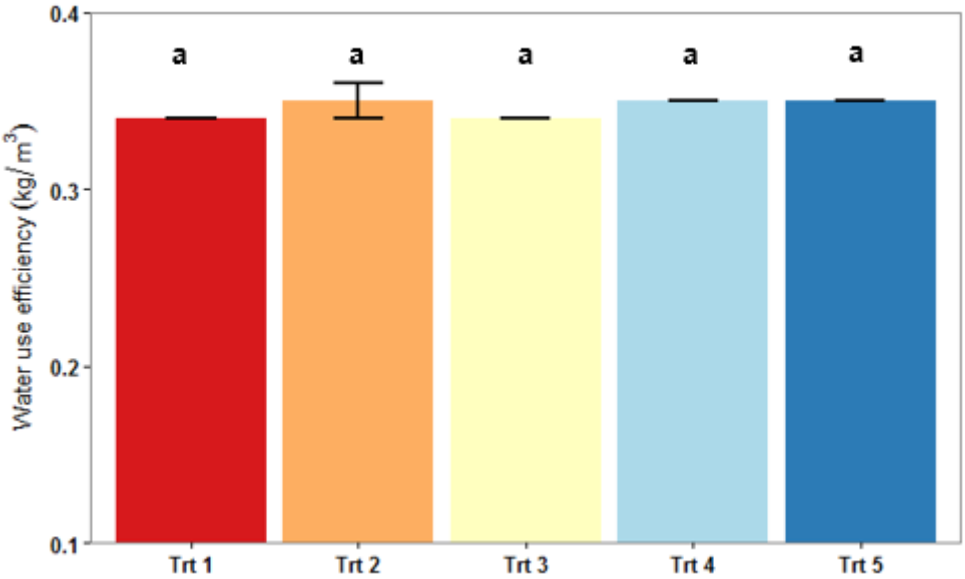

Figure 1.49 Effect of irrigation treatments on water use efficiency of cotton in 2012 growing season

1.6.3.2 Experiment in 2013

Total irrigation applied for the four treatments in 2013 growing season were 67, 11, 0, and 91 mm, respectively. During 2013 growing season, means of cotton lint yield among treatments were not significantly different (Figure 1.51). However, as shown in Figure 1.52, average WUE of treatment 2 and treatment 3 were significantly higher than average WUE of treatment 1 and treatment 4. Average WUE of treatment 2 was not significantly different with average WUE of treatment 3, neither between treatment 1 and 4. Therefore, even cotton lint yield were not significantly different, irrigation based on higher soil EC zones resulted in significantly higher WUE.

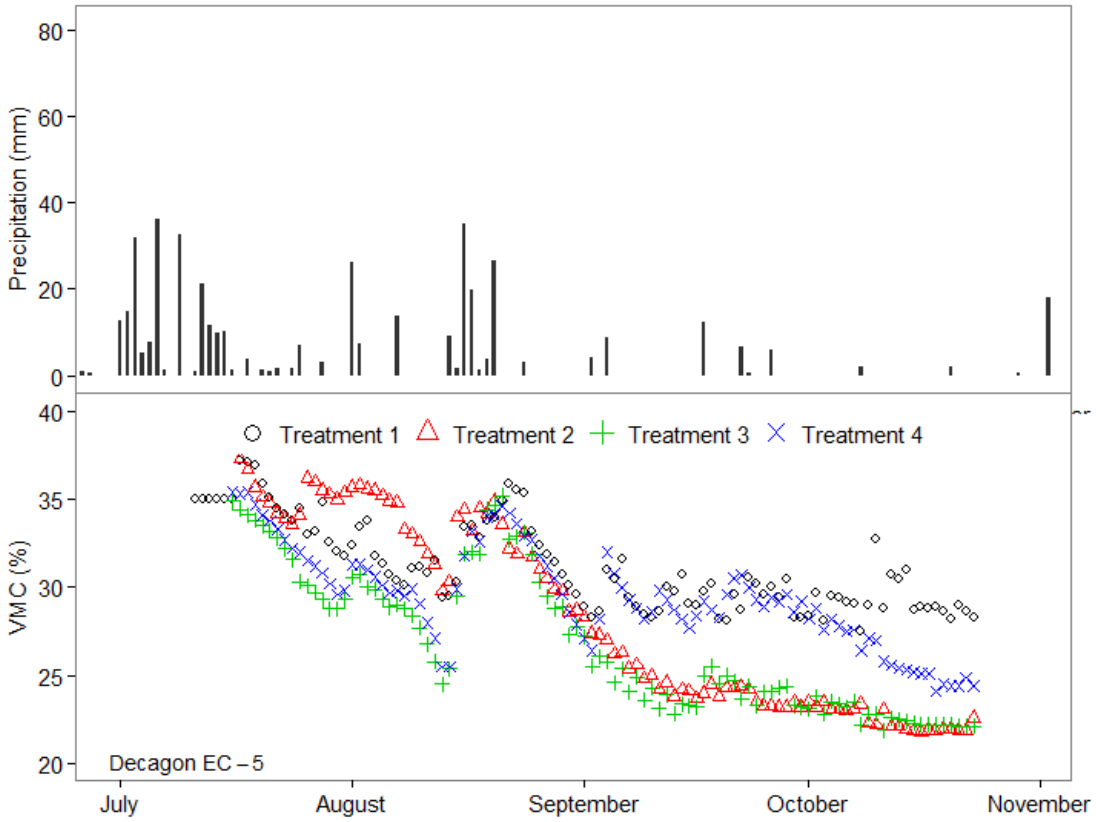

Figure 1.50 Rainfall (top panel) and measured soil volumetric water content in the top 60 cm soil profile of different treatments measured by Decagon EC-5 sensor during the 2013 growing season.

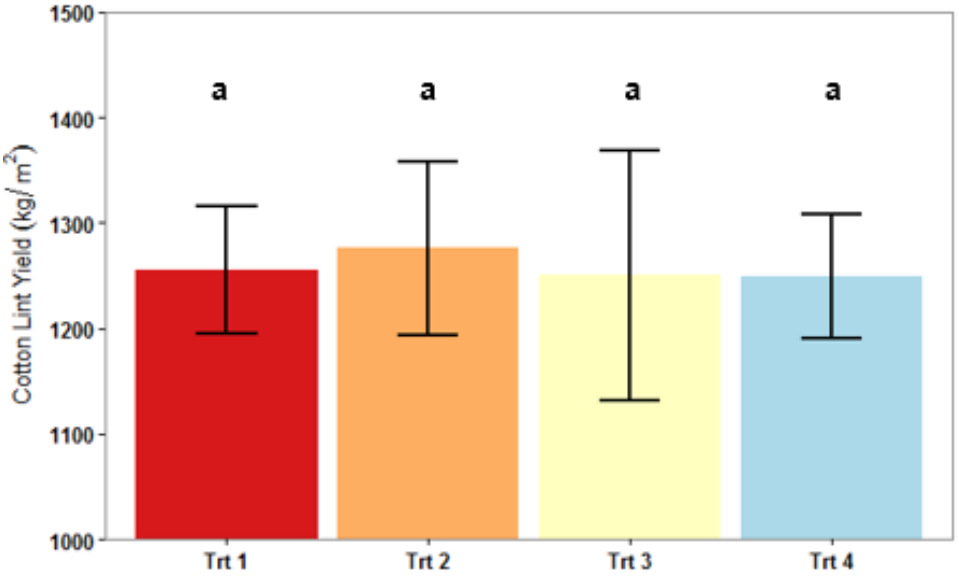

Figure 1.51 Effect of irrigation treatments on cotton lint yield during 2013 growing season

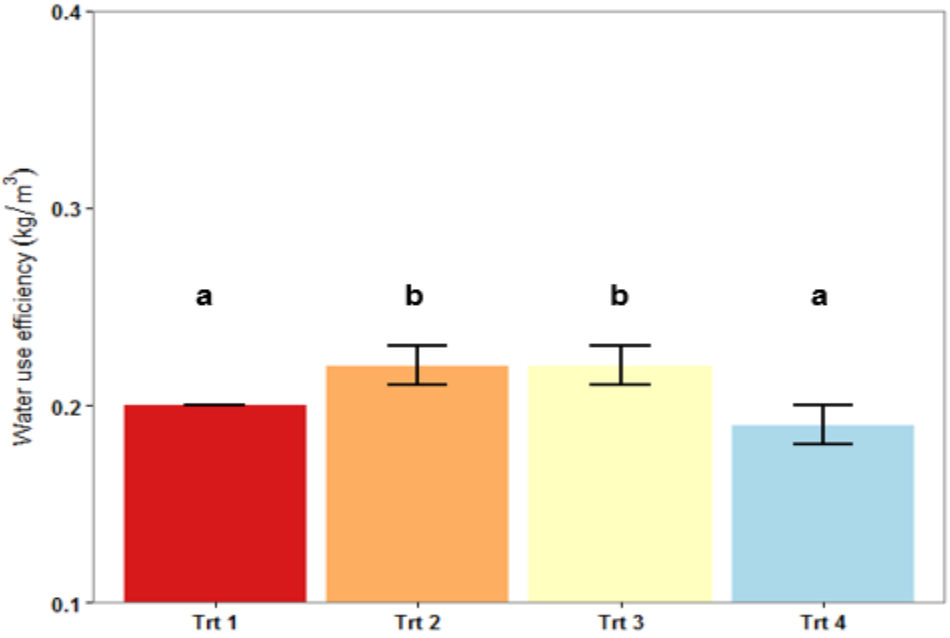

Figure 1.52 Effect of irrigation treatments on water use efficiency during 2013 growing season

At the initial of 2013 growing season, average VMC in the top 60 cm of different treatments measured by Decagon EC-5 were at high level due to frequent rainfall events during July and beginning of August (Figure 1.50). After mid-August, irrigation effects start to show as rainfall become less frequent. The amounts of irrigation of the four treatments (67, 11, 0, and 91 mm for treatment 1, 2, 3, and 4, respectively) definitely resulted in different levels of soil water profile. It can be seen that VMC of treatment 2 and treatment 3 measured by Decagon EC-5 remains at lower level compared to VMC of treatment 1 and treatment 4 (Figure 1.50). Similarly, VMC at 20 cm measured by neutron probe at zone 2 also indicates higher VMC level of treatment 1 and 4, as compared to treatment 2 and 3 (Figure 1.53). It was also noted that VMC at 20 cm of treatment 1 and 4 were nearly constantly over 15.8%, which is the field capacity of the soil type at that depth. In addition, it was noted the fact that cotton lint yield of treatment 1 and 4 were not significantly but numerically lower than treatment 2 and 3 (Figure 1.51).The results implied that at higher EC zone (Zone 2 and Zone 3 in 2013 growing season) where soil is heavier, irrigation based on sandy soil (treatment 1) or ET (treatment 4) could produce water saturation and may reduce yield and WUE.

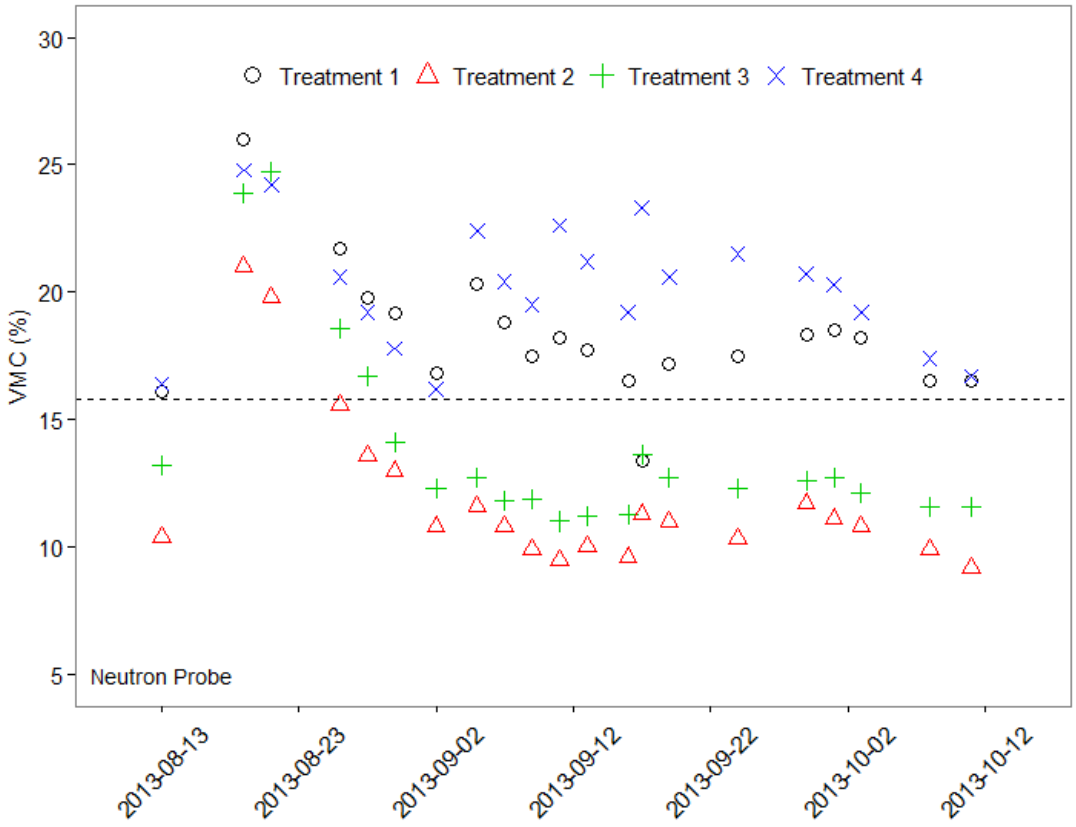

Figure 1.53 Volumetric soil moisture content of 20 cm of treatments measured by neutron probe at zone 2 in 2013 growing season. Dotted line indicate field capacity of soil at 20 cm (15.8%).

1.6.3.3 Experiment in 2014

Total irrigation applied in 2014 growing season was 211, 139, 108, and 150 mm for treatment 1, treatment 2, treatment 3, and treatment 4, respectively. During 2014 growing season, means of cotton lint yield among treatments were not significantly different (Figure 1.55). However, as shown in Figure 1.56, average WUE of treatment 3 were significantly higher than average WUE of treatment 1, treatment 2, and treatment 4. Means of WUE were not significantly different among treatment 1, treatment 2, and

treatment 3. Rainfall events in 2014 growing season were more evenly distributed. However, the extra irrigation applied at treatment 1 didn't produce higher VMC, as compared to treatment 2 and 3 (Figure 1.54). Therefore, similar to 2013 growing season, irrigation based on higher soil EC zones resulted in significantly higher WUE even cotton lint yield were not significantly different.

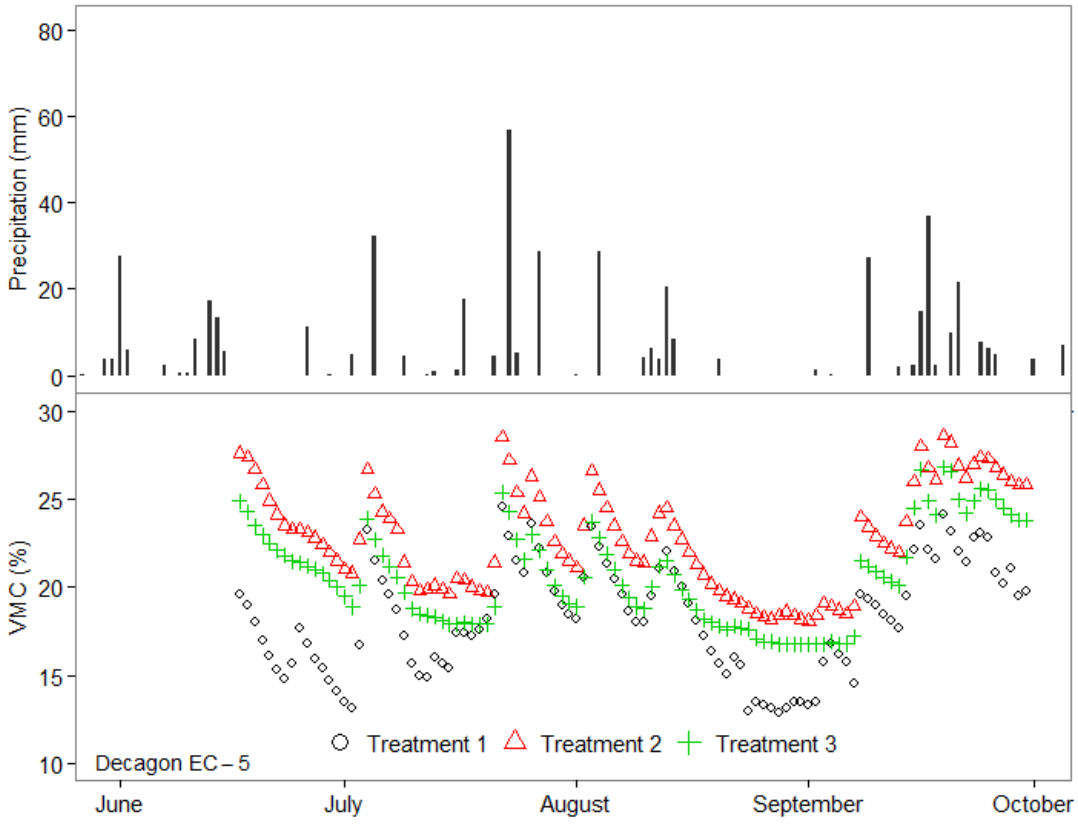

Figure 1.54 Rainfall (top panel) and measured soil volumetric water content in the top 60 cm soil profile of different treatments measured by Decagon EC-5 sensor during the 2014 growing season.

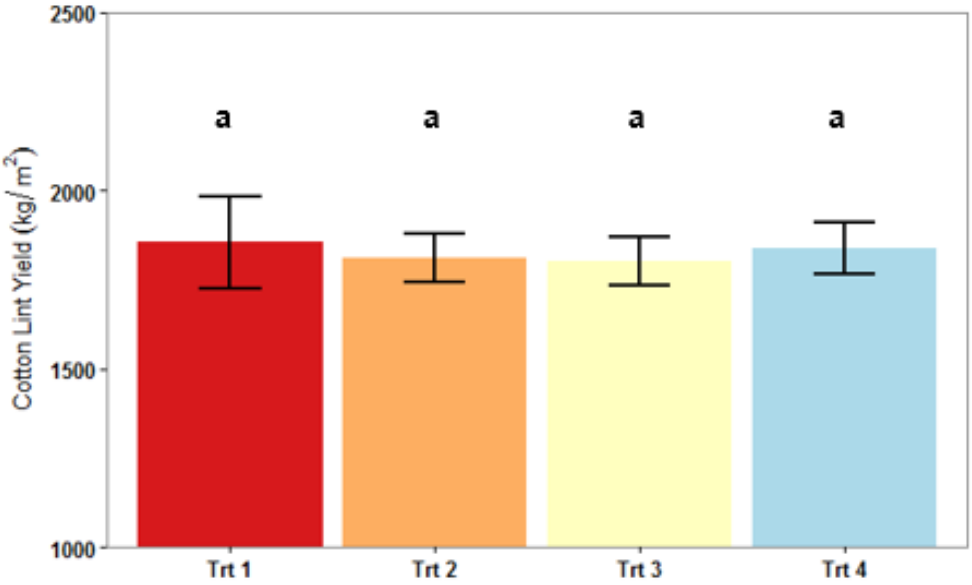

Figure 1.55 Effect of irrigation treatments on cotton lint yield in 2014 growing season.

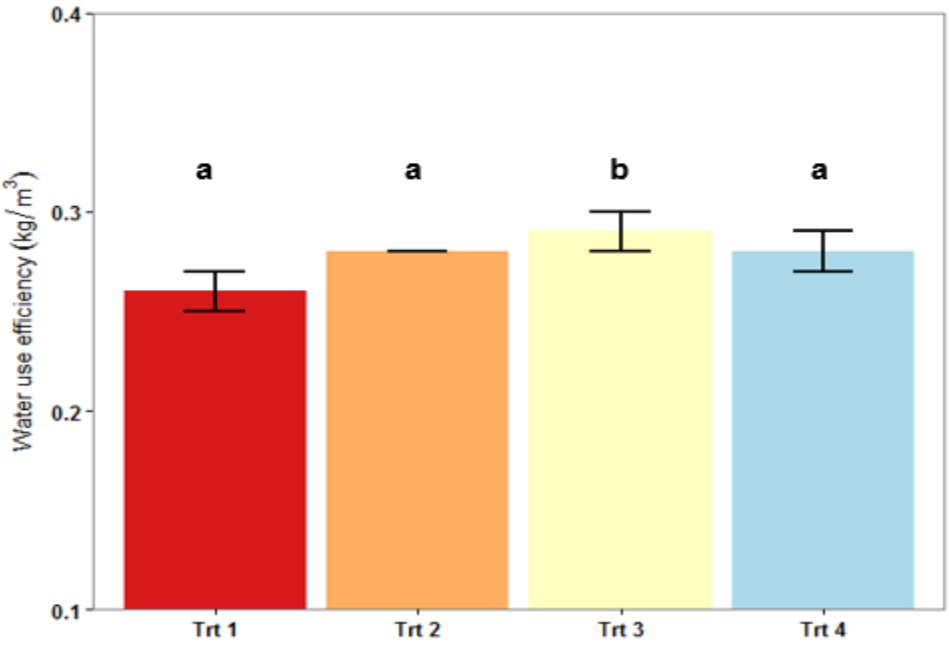

Figure 1.56 Effect of irrigation treatments on water use efficiency in 2014 growing season.

1.7 CONCLUSION

Based on the three years study in a field with typical coastal plain soil, it can be concluded that factory calibrated Sentek EasyAg-50 sensor was sufficient to accurately measure volumetric water content with RMSE of 3.2% and 5% for topsoil and subsoil, respectively. The performance of Decagon EC-5 was acceptable with larger RMSE as compared to Sentek EasyAg-50 sensors. In addition, on-site or lab calibrations, increased accuracy of the Decagon EC-5 sensor. The Watermark 200SS sensor was able to trace the variation of soil water change, yet not able to measure volumetric water content precisely. Readings of AquaSpy probe correlated poorly with neutron probe readings. This was not expected since the AquaSpy probe was calibrated at the same experimental field.

In a cotton production field with coastal plain soils, results indicated that irrigation should be applied based on sensor readings from higher electrical conductivity (EC) management zones, i.e. zones with more clay content. Such management practice could produce higher yield (treatment 4 in 2012 growing season) or result in significantly higher water use efficiency (treatment 2 and 3 in 2013 growing season; treatment 3 in 2014 growing season). In addition, in a growing season with frequent rainfall events (i.e., 2013 growing season), irrigation based on higher EC zones (treatment 2 and 3) are likely to keep root zone from saturation thus preventing loss of yield. Irrigation scheduling using reference evapotranspiration and crop coefficient (treatment 5 in 2012, treatment 4 in 2013 and 2014) didn't produce higher yield or water use efficiency compared to other treatments, but it can be used when soil moisture sensors are not available.

1.8 REFERENCES

Allen, R. G., Pereira, L. S., Raes, D., & Smith, M. (1998). Crop evapotranspiration-Guidelines for computing crop water requirements-FAO Irrigation and drainage paper 56. FAO, Rome, 300(9), D05109.

Bange, M. P., Milroy, S. P., & Thongbai, P. (2004). Growth and yield of cotton in response to waterlogging. Field Crops Research, 88(2), 129-142.

Bell, J. P. (1987). Neutron probe practice.

Bellamy, C.A. (2009). Sensor-based soil water monitoring to more efectively manage agricultural water resources in coastal plain soils. Master Thesis. Clemson, SC: Clemson University, Department of Biosystems Engineering.

Burnett, S. E., & van Iersel, M. W. (2008). Morphology and irrigation efficiency of Gaura lindheimeri grown with capacitance sensor-controlled irrigation.HortScience, 43(5), 1555-1560.

Chanasyk, D. S., & Naeth, M. A. (1996). Field measurement of soil moisture using neutron probes. Canadian Journal of Soil Science, 76(3), 317-323.

Davies, W. J., & Zhang, J. (1991). Root signals and the regulation of growth and development of plants in drying soil. Annual review of plant biology, 42(1), 55-76.

Dean, T. J., Bell, J. P., & Baty, A. J. B. (1987). Soil moisture measurement by an improved capacitance technique, Part I. Sensor design and performance.Journal of Hydrology, 93(1), 67-78.

Doorenbos, J. and Kassam, A.H. (1979). Yield Response to Water, FAO Irrigation and Drainage Paper 33.

Farahani, H.J. (2015). Personal communication. USDA_NRCS East National Technology Support Center. hamid.farahani@gnb.usda.gov

Linvill, D.E. (2002). Personal communication. Agricultural & Biological Engineering Dept., Clemson University..

Han, Y. J., Khalilian, A., Owino, T. O., Farahani, H. J., & Moore, S. (2009). Development of Clemson variable-rate lateral irrigation system. Computers and electronics in agriculture, 68(1), 108-113.

Hocking, P. J., Reicosky, D. C., & Meyer, W. S. (1987). Effects of intermittent waterlogging on the mineral nutrition of cotton. Plant and Soil, 101(2), 211-221.

Hsiao, T. C. (1973). Plant responses to water stress. Annual review of plant physiology, 24(1), 519-570.

Intrigliolo, D. S., & Castel, J. R. (2004). Continuous measurement of plant and soil water status for irrigation scheduling in plum. Irrigation Science, 23(2), 93-102.

Irmak, S., Burgert, M.J., Yang, H.S., Cassman, K.G., Walters, D.T., Rathje, W.R., Payero, J.O., Grassini, P., Kuzila, M.S., Brunkhorst, K.J., et al. (2012). Large-scale on-farm implementation of soil moisture-based irrigation management strategies for increasing maize water productivity. Transactions of the ASABE 55, 881-894.

Jones, H. G. (2004). Irrigation scheduling: advantages and pitfalls of plant-based methods.Journal of experimental botany, 55(407), 2427-2436.

Jones, S. B., Wraith, J. M., & Or, D. (2002). Time domain reflectometry measurement principles and applications. Hydrological processes, 16(1), 141-153.

Kizito, F., Campbell, C. S., Campbell, G. S., Cobos, D. R., Teare, B. L., Carter, B., & Hopmans, J. W. (2008). Frequency, electrical conductivity and temperature analysis of a low-cost capacitance soil moisture sensor. Journal of Hydrology, 352(3), 367-378.

Khalilian, A., Y.J. Han and H.J. Farahani. 2008. "Site-specific irrigation management". In Eidson and Sawyer (ed.), Proceedings of the 2008 Water Resources Conference, ISBN: 978-0-615-39866-2.

Miller, G.A. 2012. Sensor based irrigation effects on root distribution and growth of grafted and non-grafted watermelons. Doctoral Dissertation. Clemson University.

Miller, G. A., Farahani, H. J., Hassell, R. L., Khalilian, A., Adelberg, J. W., & Wells, C. E. (2014). Field evaluation and performance of capacitance probes for automated drip irrigation of watermelons. Agricultural Water Management, 131, 124-134.

Niyazi, B. (2006). Scheduling site-specific irrigation for cotton in the southeastern coastal plain soils using linear-move irrigation system. PhD diss. Clemson, SC: Clemson University,

Polyakov, V., Fares, A., & Ryder, M. H. (2005). Calibration of a capacitance system for measuring water content of tropical soil. Vadose Zone Journal, 4(4), 1004-1010.

R Core Team (2015). R: A language and environment for statistical computing. R Foundation for Statistical Computing, Vienna, Austria. URL http://www.R-project.org/.

Shock, C. C., Barnum, J. M., & Seddigh, M. (1998). Calibration of Watermark Soil Moisture Sensors for Irrigation Management.

Thompson, R. B., Gallardo, M., Agüera, T., Valdez, L. C., & Fernández, M. D. (2006). Evaluation of the Watermark sensor for use with drip irrigated vegetable crops. Irrigation Science, 24(3), 185-202.

Topp, G. C., Davis, J. L., & Annan, A. P. (1980). Electromagnetic determination of soil water content: Measurements in coaxial transmission lines. Water resources research, 16(3), 574-582.

Topp, G. C. (2003). State of the art of measuring soil water content.Hydrological Processes, 17(14), 2993-2996.

TriSCAN Agronomic User Manual Version 1.2a. (2003). Sentek Pty Ltd.

Installation and Operating Instructions of Watermark 950R & 950T. Irrometer Co. Inc.

Vellidis, G., Tucker, M., Perry, C., Kvien, C., & Bednarz, C. (2008). A real-time wireless smart sensor array for scheduling irrigation. Computers and electronics in agriculture, 61(1), 44-50.

Walker, J. P., Willgoose, G. R., & Kalma, J. D. (2004). In situ measurement of soil moisture: a comparison of techniques. Journal of Hydrology, 293(1), 85-99.

White, D. L., Esswein, S., Hallstrom, J. O., Ali, F., Parab, S., Eidson, G., ... & Post, C. (2010, May). The intelligent river©: Implementation of sensor web enablement technologies across three tiers of system architecture: Fabric, middleware, and application. In Collaborative Technologies and Systems (CTS), 2010 International Symposium on (pp. 340-348). IEEE.

CHAPTER 2

UTILIZING SPACE-BASED TECHNOLOGY FOR COTTON IRRIGATION SCHEDULING

2.1 ABSTRACT

The growing shortage of water resources has led to precision irrigation management which requires accurate soil moisture measurements. Remote sensing of soil moisture content using microwave signals has provided a different angle compared to ground-based soil moisture sensors such as capacitance and TDR probes. Since 2008, experiments have been conducted at the Edisto Research and Education Center of Clemson University (EREC) located at Blackville, South Carolina to determine site-specific information such as the soil moisture condition utilizing a GPS Delay Mapping Receiver (DMR) developed at NASA for bare soil (Privette et al., 2011). The DMR utilizes L1 GPS signal (1.57542 GHz) and calculates the ratio of reflected signal to direct signal, i.e. reflectivity, which is affected by soil moisture content, vegetation water content, and surface roughness. The correlation of reflectivity with soil moisture content at bare soil was high where R^2 ranged from 0.34 to 0.75. However, effect of vegetation needs to be quantified before using such device for irrigation scheduling at real production fields. Therefore, experiments were conducted at the EREC in 2013 and 2014, to investigate the feasibility of using GPS reflected signal to determine soil moisture content in two cotton production fields and to evaluate the actuation effect of vegetation on GPS reflected signal. The results showed that, before the vegetation effect was

accounted for, reflectivity measured by DMR fitted with actual soil moisture content of different depths using second order polynomial equations with R^2 ranging from 0.08 to 0.55. After reflectivity were adjusted by loss factors due to leaves, the correlation between reflectivity and actual soil moisture content at various depths were improved, yet limited. There were no correlation between reflectivity and crop stress parameters such as leaf water potential or stomatal conductance. The results indicated that, until effects of vegetation water content and surface roughness on GPS reflected signals are thoroughly studied; utilizing GPS reflected signals for irrigation scheduling of cotton is not suitable at Southeast Coastal Plain soils.

2.2 INTRODUCTION

Competition for limited water resources is one of the most critical issues being faced by civilization today. The ability to make more water available for domestic, agricultural, industrial and environmental uses will depend on better management of water resources, watersheds, and storm water runoff. Many experiments have shown that quantitative measurements of soil moisture in the surface layer of the soil profile are most successful using remote sensing in the microwave region. Within the microwave band, frequencies in the range of 1–2 GHz (30–15 cm) have been shown to be ideally suited to sensing soil moisture due to reduced atmospheric attenuation and better penetration of vegetation at longer wavelengths (Jackson & Schmugge, 1992). The most common remote sensing instrument used to detect soil moisture is the microwave radiometer. This instrument operates by sensing the change in brightness temperature of the soil, which is, in turn, affected by the soil moisture content. However, the microwave radiometer requires complex calibration and some sort of large antenna to achieve high surface spatial resolution (Jackson & Schmugge, 1992).

Recently NASA scientists (Langley Research Center, Hampton, VA) have developed a new technique (modified GPS Delay Mapping Receiver -- DMR) which operates by recording the GPS signal reflected from the earth's surface. The DMR system is compact in size and only use low-gain antenna, giving advantages compare to radiometers and other remote sensing instruments (Grant 2006). Over land, reflectivity measurements can be used to estimate the surface reflectivity (dielectric properties) for estimating changes in surface soil moisture. Since 2008, experiments have been

conducted at the Edisto Research and Education Center of Clemson University located at Blackville, South Carolina to determine site-specific information such as the soil moisture condition utilizing the DMR for bare soil (Privette et al., 2011). The results showed that the space-based technology had a great potential for determining soil moisture contents. Although the initial results looked promising, additional research was needed to investigate the suitability of using GPS reflected signals for irrigation scheduling of cotton on real production fields, since vegetation water content can scatter or attenuate GPS reflected signals.

2.3 OBJECTIVES

The overall objective of this study was to investigate the feasibility of utilizing space-based technology (reflected GPS satellite signals) for irrigation management of cotton in Southeastern Coastal Plain soils.

The specific objectives were to:

- Investigate the feasibility of using GPS reflected signal to determine soil moisture content in cotton production fields.
- Evaluate the attenuation effect of vegetation (cotton) on GPS reflected signal.

2.4 BACKGROUND

2.4.1 Remote Sensing of Soil Moisture

The large contrast between dielectric constant of water ($\varepsilon_w \approx 80$) and dry soil ($\varepsilon_s \approx$ 3-5) at microwave frequency has provided an opportunity to identify soil moisture contents using microwaves (Engman and Narinder, 1995). The relative dielectric constant of soil medium (ε) is usually complex number and is given as:

$$\varepsilon = \varepsilon' + j\varepsilon'' \qquad 2.1$$

Where ε' is permittivity of soil medium, ε'' is the loss factor, and j is the imaginary unit ($\sqrt{-1}$). "Electromagnetically, a soil medium is, in general, a four-component dielectric mixture consisting of air, bulk soil, bound water, and free water" (Hallikainen et al., 1985). Various models have been used to establish the relationship between the complex dielectric constant of soil-water mixture and soil volumetric water content (θ) (Wang and Schmugge, 1980; Hallikainen et al., 1985; Dobson et al. 1985). The Wang and Schmugge empirical model (1980) predicts the dielectric constant of soil over a soil moisture range between 0 and 0.5 cm^3/cm^3 for different soil textures at two frequencies of 1.4 and 5 GHz. The Dobson model is a semiempirical model which utilizes soil volumetric water content and soil texture as inputs, and predicts the dielectric constant of soil for various soil textures at wider range of microwave frequencies from 1.4 to 18 GHz (Dobson et al., 1985).

Remote sensing of soil moisture using microwave frequencies can be classified into two categories: active and passive remote sensing. Active remote sensing technique

utilizes radar which transmits electromagnetic waves to ground surface and measure the backscattered signals, while passive remote sensing technique utilizes radiometer which measures thermal microwave emission from soil (Njoku and Entekhabi, 1996). Active remote sensing system is classified as monostatic or bistatic radar, depending on whether transmitting and receiving antenna are co-located. Both backscattered signal measured by active system and thermal microwave emission measured by passive system are depending on dielectric constant of soil and thus affected by soil volumetric water content. However, active remote sensing techniques have higher spatial resolution but more sensitive to surface roughness and vegetation cover, as compared to passive remote sensing techniques (Engman and Chauhan, 1995). Such limitation is minimized using a combination of the two methods, i.e. using both radar and radiometer in the Soil Moisture Active Passive (SMAP) mission (Entekhabi et al., 2010).

Up to date, various active or passive systems are mounted on ground carrier, aircraft, or spacecraft for the purpose of soil moisture monitoring with different spatial resolutions. Over ground level, Schwank et al. (2005) mounted a radiometer operating at 1.4 GHz on a tower and compared radiometer readings to time-domain reflectometer (TDR) soil moisture readings at different growth stage of clover grass. An aircraft mounted electronically scanned thinned array radiometer (ESTAR) was used to map soil moisture over the Little Washita watershed in Oklahoma (Jackson et al. 1995). While the Soil Moisture and Ocean Salinity (SMOS) mission (Kerr et al., 2001) and recently launched SMAP satellites (Entekhabi et al., 2010) provided soil moisture data on a global scale.

Recently, utilization of GPS signal for remote sensing of soil moisture has been demonstrated over various systems. Larson et al. (2008) utilized geophysical and geodetic intended GPS receivers for soil moisture retrieval with resolution of 300 m^2. A delay mapping receiver (DMR) using L1 GPS signal developed at NASA Langley Research Center was mounted on aircraft (Masters et al., 2004b; Katzberg et al., 2006) and tractor boom (Privette et al., 2011) for soil moisture measurement. The DMR system is compact in size and only uses low-gain antenna, giving advantages compare to radiometers and other remote sensing instruments (Grant 2006).

2.4.2 Theoretical Background

2.4.2.1 GPS specular reflection

In this section, the theoretical background and model of GPS reflection used in this study are described.

The Global Positioning System is a satellite-based navigation system which utilizes a network of 24 satellites, orbiting around the earth. The 24 satellites are placed in a way that at least four satellites are viewing earth at any time and provide 3D navigation. Each satellite in the system broadcasts a publicly available L-Band, civilian-use carrier signal at 1.57542 GHz named L1 Band. This signal is a pseudonoise (PN) binary sequence code of 1023 chips (Parkinson and Spiker, 1996). The period of the signal is 1 ms and thus one chip is 1/1023 ms.

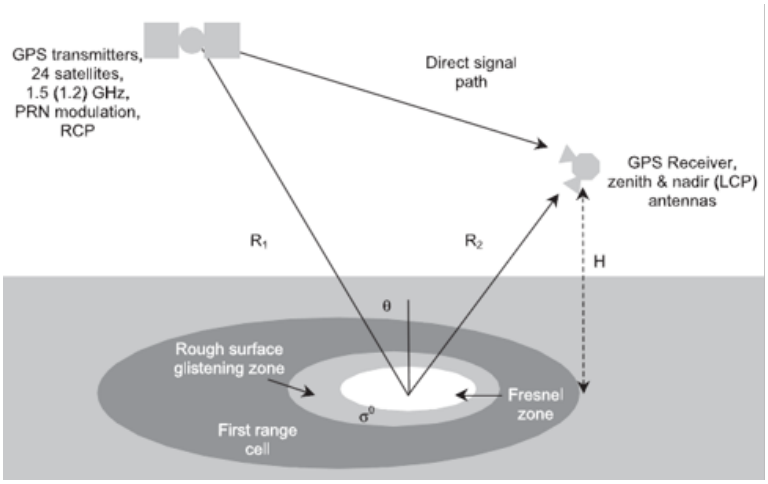

Figure 2.1 Geometry of GPS signal for bistatic set up (Masters et al., 2004b).

When GPS signal strikes a surface, if the surface is electromagnetically smooth, the GPS signal will be reflected back in a mirror-fashion. The mirror-fashion reflection is

thus termed as specular reflection. In this study, surface is considered electromagnetically smooth if as defined by Beckman and Spizzichino (1987) if:

$$h_s \equiv \sigma < \frac{\lambda}{8 \sin \gamma} \qquad 2.2$$

Where h_s is Rayleigh criterion, and it is defined as the height deviations from the mean surface, σ, λ is the incoming signal wavelength and in this study is equal to 19.03 cm, and γ is the elevation angle of satellite signal. Surface is considered electromagnetically specular, when h_s is smaller than the height deviations from the mean surface. An area with equal path delay relative to the path through specular point formed an ellipse and termed as first Fresnel zone (Figure 2.1) (Beckman and Spizzichino, 1987). Signal that passes through the specular point is defined to have zero delay. Reflected signal in this case comes from the energy from First Fresnel zone. When h_s is larger than the height deviations from the mean surface, the surface is considered electromagnetically rough and reflected signal power is contributed from the Glistening zone in addition to the first Fresnel zone. In a study in soybean and corn fields, Grant (2006) showed that the standard deviation of height ranged from 0.005 m to 0.017 m which is below the Rayleigh criterion, hence it was assumed that reflection was specular. Due to limited data and similar field condition compared to Grant (2006) study, reflection in our study is considered to be specular as well. Size of first Fresnel zone is calculated using following equations as defined by Katzberg et al. (2006):

$$A = \pi ab \qquad 2.3$$

$$a = \frac{\sqrt{2hc\tau_s \sin \gamma}}{(\sin \gamma)^2} \qquad 2.4$$

$$b = \frac{\sqrt{2hc\tau_s \sin\gamma}}{\sin\gamma} \quad 2.5$$

Where A is area of first Fresnel zone, a is length of semi major axis, b is length of semi minor axis, h is height of receiver above the surface, c is speed of light, and τ_s is the delay of GPS signal relative to signal pass through specular point. Given that reflection is specular:

$$c\tau_s = \lambda/2 \quad 2.6$$

Combining equations 2.3 to 2.6 results in:

$$A = \pi \times \frac{\sqrt{h\lambda \sin\gamma}}{(\sin\gamma)^2} \times \frac{\sqrt{h\lambda \sin\gamma}}{\sin\gamma} \quad 2.7$$

Equation 2.7 calculates the footprint of GPS reflected signal, A in m^2. The specular reflectivity, Γ_s , is calculated as:

$$\Gamma_s = R_0^2 \quad 2.8$$

Where R_o is Fresnel reflection coefficient, and R_0^2 is given as:

$$R_0^2 = \frac{|R_0^+|^2 + |R_0^-|^2}{2} \quad 2.9$$

Where R_0^+ and R_0^- are the vertical and horizontal polarization reflection coefficients, respectively (Beckman and Spizzichino, 1987):

$$R_0^+ = \frac{Y^2 \sin\gamma - \sqrt{\varepsilon_s - (\cos\gamma)^2}}{Y^2 \sin\gamma + \sqrt{\varepsilon_s - (\cos\gamma)^2}} \quad 2.10$$

$$R_0^- = \frac{\sin\gamma - \sqrt{Y^2 - (\cos\gamma)^2}}{\sin\gamma + \sqrt{Y^2 - (\cos\gamma)^2}} \quad 2.11$$

$$Y = \sqrt{\frac{\varepsilon_s}{\mu_s}} \qquad 2.12$$

Where ε_s is complex dielectric constant of the surface, and μ_s is relative magnetic permeability which is approximately 1. The complex dielectric constant of the surface, ε_s is related to soil volumetric water content, as described in section 2.2.1. Finally, the reflectivity of the surface is given by Grant (2006):

$$\Gamma_s = R_0^2 exp\left[-\left(\frac{4\pi\sigma(\sin\gamma)}{\lambda}\right)^2\right] \qquad 2.13$$

2.4.2.2 Attenuation effect of vegetation

Given description in section 2.4.1, microwave remote sensing has shown promising results. However, the presence of vegetation can attenuate the reflected microwave signal to some extent. Various models have been developed to predict the effect of vegetation (Fung and Ulaby, 1978; Ulaby and Rayes, 1987). Fung and Ulaby (1978) developed a scatter model for leafy vegetation such as soybean, alfalfa, and corn. The model predicts backscattering coefficient and was in agreement with measured data. Yet the model was limited since it only applies to dense vegetation when volume fraction of leaf is in the range of 0.1 – 1.0 out of total volume (leaf and air). Furthermore, Ulaby and Rayes (1987) pointed out that the model of Fung and Ulaby (1978) treated bound water as ice and this led to some shortcomings. Instead, Ulaby and Rayes (1987) treated the bound water as a relaxation component and the predicted real component of dielectric constant of vegetation (ε') was within $\pm$ 20 percent of the measured value, and the imaginary component of dielectric constant of vegetation (ε'') was within $\pm$ 20 percent of measured value when frequencies were above 5 GHz. However, it was also pointed out that by using gravimetric moisture content and density of the vegetation material, the error can be reduced to $\pm$ 5 percent.

The NASA DMR has been tested at various altitudes for bare soil (Master et al., 2004; Privette et al., 2011). However, such system has not been tested over vegetated land. To better understand the relationship of soil moisture content with GPS reflected signal, the vegetation attenuation effect, as often occurred at agriculture lands, needs to be determined.

2.4.2.3 Acquisition of GPS signals using NASA DMR

Hardware of the system was developed by NASA Langley Research Center and several researchers (Katzberg and Garrison, 1996; Garrison et al. 2002; Masters 2004a; Masters 2004b; Grant 2006) were involved in development and refining of the system. However, to better understand the measurement (reflectivity) used in this study, it is necessary to describe the system from ground up.

The system is mainly composed of a DMR (Figure 2.2), a zenith Right-Hand-Circularly Polarized (RHCP) antenna viewing the sky (zenith), a nadir Left-Hand Circularly Polarized (LHCP) antenna viewing the ground (nadir) (Figure 2.3), two GPS inline amplifiers (Figure 2.4) for each antenna (Raven Industry), lengths of coaxial cable, and etc. Detailed components of the system are listed in Table 2.1. The antennas used in this study were all low-gain antennas. The zenith and nadir antennas are common in function except for opposite sense polarization. The DMR is built based on a GEC-Plessey Semiconductors (1995) 12-channel, C/A code receiver. The Zarlink GP2010/2021 chipset (Zarlink Semiconductors) is utilized since this chipset offers two antenna inputs and therefore both the direct and reflected signals can be obtained (Masters 2004a).

Table 2.1 Major components of NASA DMR system.

Parts	**Model**	**Company**	**Quantity**
Active L1 LHCP antenna	3G15L-A-XS-1	Antcom, U.S.A	1
Active L1 RHCP antenna	3G15A-XS-1	Antcom, U.S.A	1
GPS inline amplifier	LA-21-1575-100-S	Raven Industry	2
NASA DMR Receiver	\	\	1

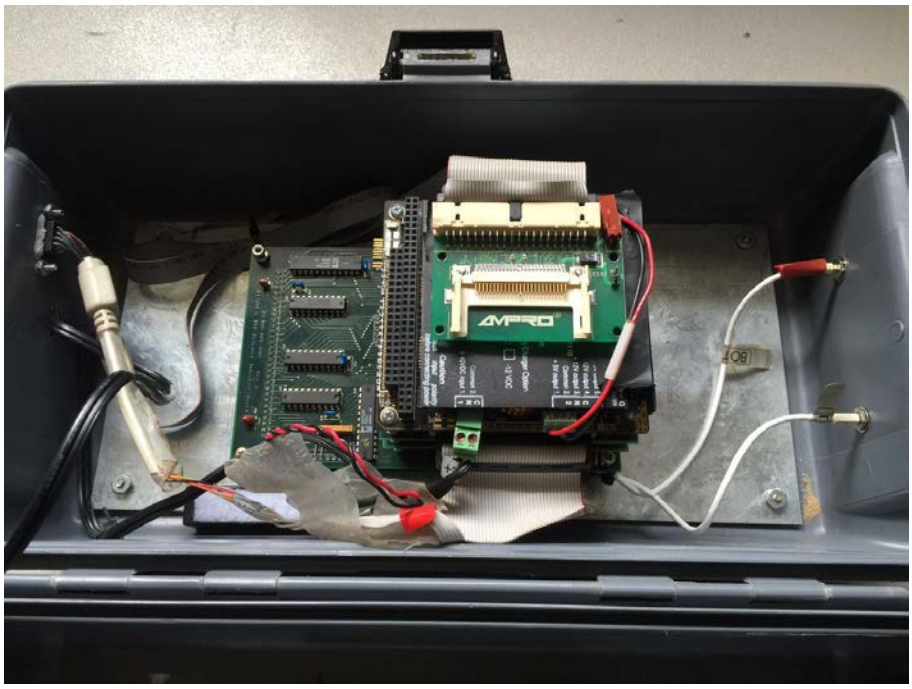

Figure 2.2 NASA GPS Delay Mapping Receiver (DMR)

Figure 2.3 Left hand polarized antenna (left) and right hand polarized antenna (right)

Figure 2.4 GPS inline amplifier

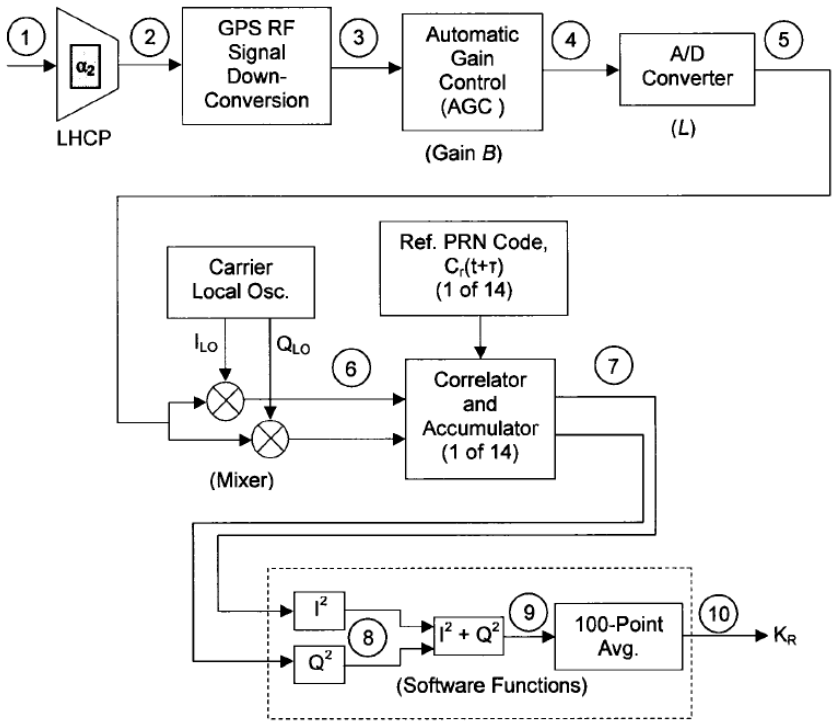

Figure 2.5 Signal processing functional diagram (Reflected channel) (Grant 2006)

The system is unique due to its 1) bistatic setup and 2) utilization of correlation properties of the pseudo-random noise (PRN) signal transmitted by GPS satellites instead of measurement using receiving power (Garrison et al., 2006). Signal processing flowchart of reflected channel is shown in Figure 2.5. The following procedures, equations 2.14 to 2.26 are explained by Grant (2006). At point one (circled number) of Figure 2.5, average power received by the LHCP (bottom) antenna is P_R (W/m^2), and the voltage output at antenna output terminal is:

$$V_{2Pk} = a_2\sqrt{2P_R} \qquad 2.14$$

At point 3, the reflected signal voltage of the RHCP bottom antenna is calculated as:

$$V_3(\mathrm{t}) = a_2\sqrt{2P_R}C(t)D(t)\cos[(\omega_3 + \Delta\omega)t + \psi] + V_n \qquad 2.15$$

Where a_2 is the square root of the antenna load resistance of the reflected signal channel, P_R is time and area averaged power at output terminal of top antenna, C(t) is a binary pseudorandom noise (PRN) code of the specific satellite, D(t) is GPS navigation data, $\cos(\omega_3 t)$ is the 3rd intermediate frequency (IF) waveform, $\Delta\omega$ is the Doppler frequency due to relative motion of the GPS satellite and GPS receiver, ψ is an unknown carrier phase (delay) of reflected signal, and V_n is a zero-mean, Gaussian thermal noise. After the Automatic Gain Control (AGC) block and A/D converter, the voltage of reflected channel at point 5 is:

$$V_5(\mathrm{t}) = \mathrm{BL}(a_2\sqrt{2P_R}C(t)D(t)\cos[(\omega_3 + \Delta\omega)t + \psi] + V_n) \qquad 2.16$$

Where B is a gain factor and L is a scaling factor. They are both influenced by noise of the system including antenna, cable, and amplifier. In-phase ($I_{LO} = \cos\omega t$) and quadrature ($Q_{LO} = \sin\omega t$) local oscillator waveforms are mixed with voltage V_5(t) and resulting in-phase and quadrature voltages:

$$V_{6I}(\mathrm{t}) = V_5(\mathrm{t})I_{LO} \qquad 2.17$$

$$V_{6Q}(\mathrm{t}) = V_5(\mathrm{t})Q_{LO} \qquad 2.18$$

After point 6, instrument generated, 14 replicas of PRN code with 14 delay times (τ_s) were simultaneously correlated with the received signal. The correlation operation $\Lambda(\tau)$ is given as:

$$\Lambda(\tau) = \mathrm{N}\frac{1}{T}\int_0^T C(t)C_r(t+\tau)\mathrm{dt} \qquad 2.19$$

Where N is number of samples, T is period of PRN code (1ms), and $C_r(t+\tau)$ is receiver generated replica PRN code with time delay τ regards to incoming signal. The equation 2.19 generates 14 sets of correlations which are being used for later analysis. It should be noted that τ_s is different than τ, as τ_s refers to the time delay of reflected signal compared to specular reflected back signals. At point 7, the in-phase (V_I) and quadrature voltages (V_Q) become:

$$V_{7I}(\mathrm{t}) = \Lambda(V_{6I}(\mathrm{t})) \qquad 2.20$$

$$V_{7I}(\mathrm{t}) = \Lambda(V_{6Q}(\mathrm{t})) \qquad 2.21$$

Points 1 to 7 are implemented in the DMR hardware while 8-10 are implemented by software. At point 9, the in phase parameter ψ is eliminated by:

$$V_{9I}(\mathrm{t}) = V_{8I} + V_{8Q} \qquad 2.22$$

$$\sin 2 + \cos 2 = 1 \qquad 2.23$$

At point 10, the reflected channel output (K_R) is average of 100 points of $V_9(t)$ in 0.1s, and the digital count value is given as:

$$K_R = (\mathrm{BL})^2(a_2^2 4P_R N^2 + \langle \Lambda_1^2 + \Lambda_2^2 \rangle_t) \qquad 2.24$$

It is assumed that the reflected power P_R remains constant during the 0.1 s averaging period. For direct channel, it is similar except only one PRN code generator and correlator are used. The digital count value of direct channel is:

$$K_D = (\mathrm{B}_D\mathrm{L})^2(a_1^2 4P_D N^2 + \langle \Lambda_{1D}^2 + \Lambda_{2D}^2 \rangle_t) \qquad 2.25$$

Finally, the ratio of reflected signal to direct signal, defined as surface reflectivity, is calculated as:

$$G_c = \frac{K_R - n_{0b}}{K_D} f_c \equiv \Gamma_s \qquad 2.26$$

Where n_{0b} is a running average of the system and f_c is an empirically determined calibration factor that varies with satellite and day of data acquisition.

2.5 MATERIAL AND METHODS

2.5.1 Sites condition

Field experiments were conducted at the Edisto Research and Education Center (EREC) of Clemson University near Blackville, South Carolina during 2013 and 2014 years. During 2013, experiment was conducted at a field equipped with a variable rate irrigation system (VRI), named "Lateral Field (LF)". During 2014, in addition to field LF, a separate field named "Drip Field (DF)" with drip irrigation system was used. Field LF was planted with cotton variety DP 1050 on May 22nd with density of 82145 plants per hectare in 2013. Same cotton variety DP 1050 was planted at same density on May 7th at LF in 2014. Cotton variety PHY333WRF was planted on May 27th at DF in 2014 with density of 82145 plants per hectare. The additional field DF allowed to test the effect of different levels of vegetation on GPS reflectivity since cotton at DF was planted at a later date. The plot size at both fields was 7.6 m by 15.2 m.

Both fields (LF and DF) had the same soil type, Varina loamy sand. This typical coastal plain soil is comprised of three often distinct layers: a sandy topsoil (A horizon), a sandy clay subsoil (Bt horizon), and a sand to sandy clay layer in between (E horizon). Field capacity (FC) of topsoil (A horizon) at the two sites was 0.158 cm^3/cm^3 (15.8%) (Nayazi 2006).

2.5.2 Field installation of system

During 2013 growing season, the RHCP and LHCP GPS antennas were installed on a platform which was mounted on the VRI at LF (Figure 2.6). The platform was made

of two layers of plastic board with one layer of aluminum board in between. In 2014 growing season, the platform was mounted on back of a high-boy sprayer (Figure 2.7) and thus reflectivity readings could be collected at different fields with different levels of vegetation cover. The DMR was connected to the two antennas through two separate coaxial cables. The DMR was located inside the VRI system control box in 2013 and inside the high-boy sprayer cab in 2014.

Figure 2.6 GPS antennas mounted on VRI during 2013 growing season

Figure 2.7 GPS antennas mounted on back of a high-boy sprayer during 2014 growing season

2.5.3 System Calibration

The different gains of channels for top antenna and bottom antenna were evaluated using a balanced RF power divider (Model PE2011, Pasternack Enterprises, Inc. Irvine, CA). To do so, instead of connecting bottom channel to LHCP antenna and connecting top channel to RHCP antenna, the LHCP antenna was connected to one end of the RF power divider and the two splitters of the RF power divider were connected to top and bottom channels of DMR, respectively. Signal noise ratio (SNR) was recorded to see if there was any channel difference.

The system was also calibrated over a circular plastic container (2.4 m diameter and 0.3 m deep) filled with water in 2014. The reflectivity of water body is relatively constant ($\Gamma_s = 0.61$) at temperature range from 20℃ and 30℃ and GPS satellite elevation

angles between 50 and 90 degrees (Grant 2006; Katzberg et al., 2006). The calibration factor f_c, was calculated as described by Grant (2006):

$$f_c = \frac{\Gamma_s}{G_c} \qquad 2.27$$

Where Gc is reflectivity calculated using equation 2.26. This calibration factor accounts for the variation in Satellite power, instrument temperature, cables, and cable connectors (Grant 2006). It should be pointed out that this scale factor was unique to satellite and day of data acquisition.

2.5.4 Field experiments

2.5.4.1 System resolution

Before taking appropriate soil sample in the field, it was necessary to calculate the resolution, i.e. the foot print of the DMR. The resolution of DMR was calculated using equation 2.7, given the assumption of specular reflection that reflectivity comes from First Fresnel Zone. Resolution of DMR changes with elevation angle and height of antennas, as indicated by equation 2.7. As stated by Katzberg (2006), the DMR utilizes highest elevation satellite in view and thus average elevation angle is generally above 65 degrees. Hence, resolution of DMR was calculated for elevation angle from 50 to 90 degrees. During 2013 when antennas (RHCP and LHCP) were mounted on the variable rate irrigation system, the height of antennas was 4.16 m to surface of ground, and this yielded resolution ranging from 4.24 to 2.49 m^2 when elevation angle changed from 50 to 90 degrees (nadir). During 2014, the antennas were mounted on the back of a high-boy sprayer and the height of antennas could be changed from 1.6 to 2.7 m. At height of 2.7

m, the DMR resolution ranged from 2.75 to 1.61 m^2 when elevation angle changed from 50 to 90 degrees. At height of 1.6 m, the DMR resolution ranged from 1.97 to 0.55 m^2 when elevation angle changed from 50 to 90 degrees. The relationship of resolution with elevation angle under different heights is shown in Figure 2.8.

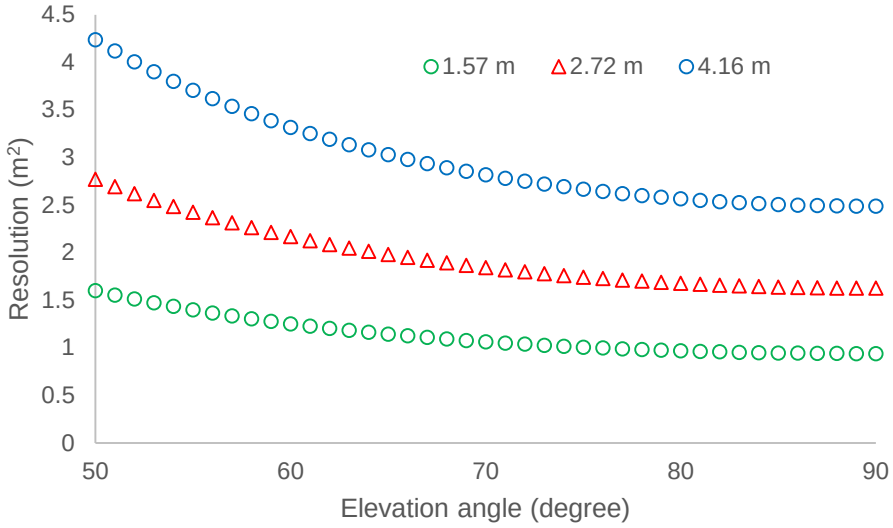

Figure 2.8 Relationship of foot print of DMR with elevation angle for antennas mounted at 1.57, 2.72, and 4.16 m.

2.5.4.2 Sampling strategy

Given the resolution calculated in 2.5.4.1, the largest possible resolution was 4.2 m^2 when antennas were mounted on VRI at LF. Therefore, the plot size at LF and DF (115 m^2) should cover the area where GPS signal was reflected. It was assumed that soil moisture content was uniform within the First Fresnel Zone, i.e. the footprint of DMR. During 2013, when the DMR moved over each plot, the device was powered on and collected data for 20 minutes. Soil samples at 10 and 20 cm were taken immediately

following data collection with the DMR receiver. Soil sampling tool was the same as described in Chapter 1. Soil samples were weighted before and after drying in oven to obtain volumetric water content. Crop stress parameters were also collected at the same time, such as leaf water potential and stomatal conductance. Leaf water potential was measured using a Model 600 Pressure Chamber (PMS Instrument Company, USA) (Figure 2.9). Stomatal conductance samples were collected using a SC-1 Leaf Porometer (Decagon Inc., USA) (Figure 2.10). At each plot, three replicates of leaf water potential and stomatal conductance measurements were taken using randomly selected leaves.

Figure 2.9 Model 600 pressure chamber.

Figure 2.10 SC-1 Leaf Porometer

In 2014, the DMR was calibrated over a circular plastic container (2.4 m diameter and 0.3 m deep) filled with water at beginning of data collection. Then DMR was powered on 10 minutes at each plot. In the meantime, soil samples were taken at 5, 10, and 15 cm, together with leaf water potential measurements. In addition, two randomly selected plant samples were taken and dried in oven at 65℃ for 72 hours to obtain gravimetric water content per plant, M_g:

$$M_g = \frac{(\mathrm{M}_{wet\_plant} - M_{dry\_plant})}{\mathrm{M}_{wet\_plant}} \qquad 2.28$$

Where M_{wet_plant} is average weight of each plant before putting in oven in g,

M_{dry_plant} is average weight of each plant after drying in oven in g.

The volumetric water content per plant, V_l, was calculated using:

$$V_l = \frac{M_g \rho_{dry\_plant}}{\left[1 - M_g\left(1 - \rho_{dry\_plant}\right)\right]} \qquad 2.29$$

Where ρ_{dry_plant} is the bulk density of dry plant in g/cm^3 and calculated as:

$$\rho_{dry\_plant} = \frac{M_{dry\_plant} \times Polulation/10^8}{h_l} \qquad 2.30$$

Where population is plant count per ha equal to 82145,

10^8 is conversion factor of ha to cm^3

h_l is average canopy height of four randomly selected plants in meter.

The attenuation effect of vegetation was calculated as (Ulaby and Rayes, 1987):

$$L'_a(\theta) = \exp\left[\frac{4\pi}{3\lambda_0} V_l \varepsilon_l'' h_l \sec(\theta)\right] \qquad 2.31$$

Where, $L'_a(\theta)$ is leaf loss factor due to canopy cover

V_l is biomass volume moisture content and is dimensionless.

h_l is canopy height in meter.

ε_l'' is loss component of the dielectric constant of water containing leaves and is dimensionless.

λ is wavelength in meter.

Θ is incidence angle and equal to $(90° - \gamma)$ in degrees.

As described in Ulaby and Rayes (1987), dielectric constant of plant has three components including: "1) ε_r, a nondispersive residual component, 2) $v_{fw}\varepsilon_f$, a free-water component, where v_{fw} is the volume fraction of free water and ε_f is its dielectric constant, and 3) $v_b\varepsilon_b$, a bulk vegetation bound water component, where $v_b$is the volume fraction of the bulk vegetation-bound water mixture and ε_b is its dielectric constant." Therefore, the dielectric constant of plant, ε_l was calculated using

$$\varepsilon_l = \varepsilon_r + v_{fw}\varepsilon_f + v_b\varepsilon_b \quad (2.32)$$

The required components in equation 2.32 were calculated using

$$\varepsilon_r = 1.7 - 0.74M_g + 6.16M_g^2 \quad (2.33)$$

$$v_{fw} = M_g(0.55M_g - 0.076) \quad (2.34)$$

$$v_b = \frac{4.64M_g^2}{(1 + 7.36M_g^2)} \quad (2.35)$$

$$\varepsilon_f = 4.9 + \frac{75}{(1 + jf/18)} - j\frac{18\sigma}{f} \quad (2.36)$$

$$\varepsilon_b = 2.9 + \frac{55}{1 + (jf/0.18)^{0.5}} \quad (2.37)$$

Where f is frequency of GPS signal in gigahertz and equal to 1.57542.

σ is ionic conductivity of the free-water solution and found to be constant which equal to 1.27.

$j = \sqrt{-1}$

Then, the reflectivity was adjusted by the leaf loss factor due to canopy cover and calibration factor, given as:

$$G_{c\_adjusted} = G_c \times L'_a \times \mathrm{f}_c \quad (2.38)$$

During a data acquisition event, as satellites traversed an arc in the sky, a series of locus of specular reflection points formed an arc on the ground. Each arc was specific to one satellite and was corresponded to a period of time. The relative position of arcs to location of DMR was constant. However, each arc occurred 4 minutes earlier compared to the same arc occurred one day before. Thus the DMR was set up at a reference point and allowed to collect both direct and reflected GPS signals over time. Then, these arcs

were cut in ArcGIS according to pre-determined time slot. Then the reference point was moved to center of each plot, together with time specific arcs (Figure 2.11). Soil samples and plant samples were taken on the predicted arc at each plot at corresponding time of the arcs. This ensured soil samples and plant samples were taken at places where specular reflection occurred,

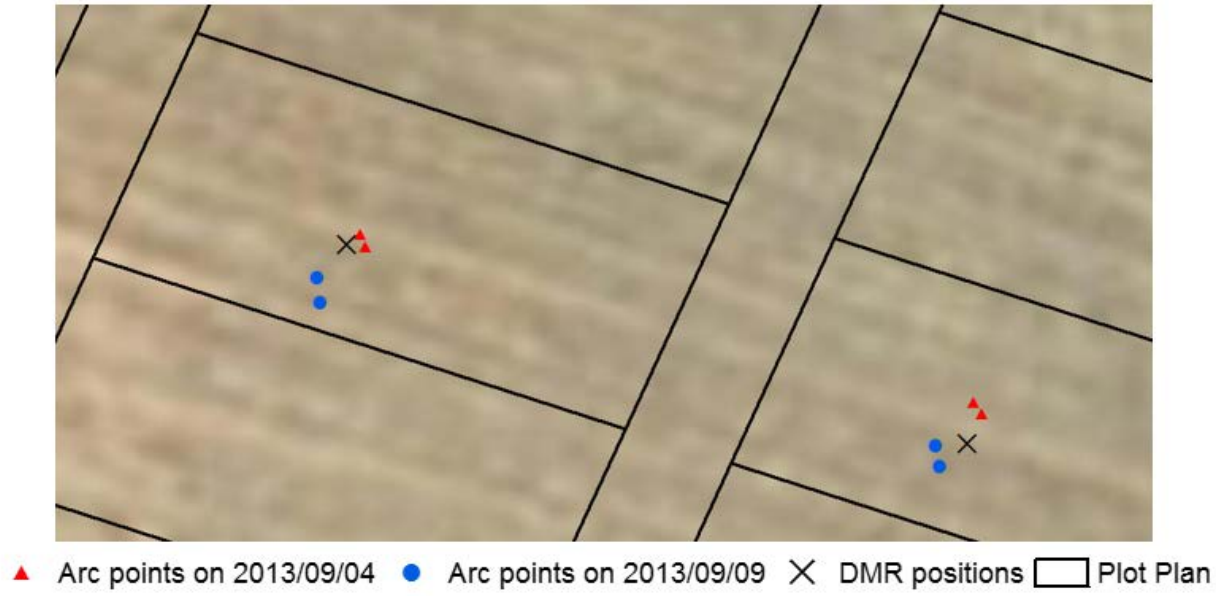

Figure 2.11 An example of predicted GPS reflected arc path with respect to location of the DMR receiver.

2.5.5 Post data processing

For each successful data acquisition event at each plot, the DMR stores a series of txt files, including: DCOERR.txt (delay timing information), DEBUG.txt, DELYSUM.txt, DELYTIC.txt (reflected signal strength), DIRECT.txt (direct signal strength), NAVSTATE.txt (DMR position), RINEX2N.txt, and RINEX2O.txt. Satellite information was stored in the two RINEX files. Data was stored at every 0.1 second, named “tics”. For each series of txt file obtained at each plot, a Matlab program developed by NASA

was used to calculate average reflectivity during sampling cycle in each plot. The program also calculated a series of locus of specular reflection points corresponding to the position of DMR in the plot. Linear regression was used to determine the correlation of reflectivity, either adjusted (in 2014) or not adjusted (in 2013), with actual moisture content and crop stress parameters (stomatal conductance and leaf water potential).

2.6 RESULTS AND DISCUSSION

2.6.1 Calibration results

The RF power divider was utilized to evaluate channel difference of the DMR. As shown in Figure 2.12, there was no difference between the top channel and bottom channel, since signal to noise ratio (SNR) of top channel was correlating with SNR of bottom channel with R^2 of 0.94 and slope of 1.03.

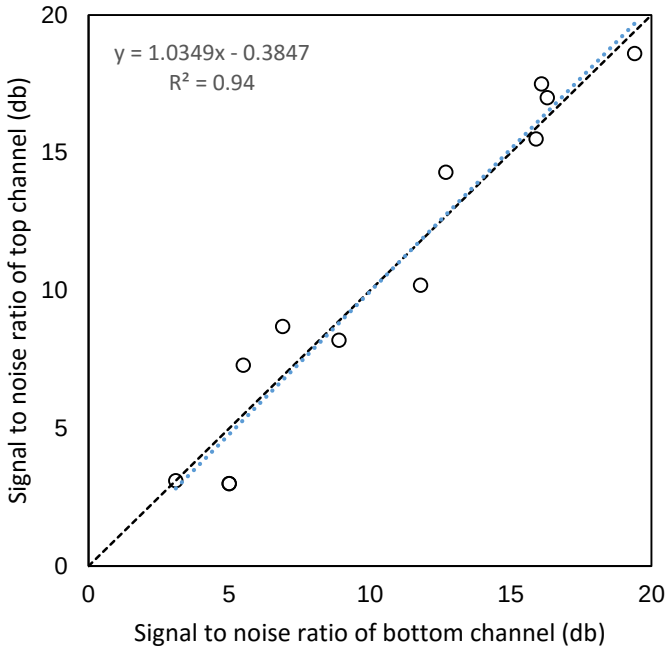

Figure 2.12 Signal to noise ratio of top and bottom channels when DMR was connected to the RF power divider

During 2014, the DMR was calibrated over a circular water body on different days for different satellite. The calibration result is shown in Table 2.2. The calibration

factor (f_c) ranged from 1.03 to 1.21 with standard deviation of 0.06, which is relatively constant. The daily average calibration factor was used to scale reflectivity collected on the corresponding date. Katzberg et al (2006) reported calibration factors of DMR ranged from 1.65 to 1.98, which is larger compared to this study. However, the DMR was installed on an aircraft in study of Katzberg et al. (2006) and resource of noise could be different. The minor difference of the two channels of DMR (Figure 2.12), as well as the slight variation of calibration factor (standard deviation equal to 0.06), indicated the stability of noise in DMR.

Table 2.2 Calibration factors obtained on different dates during 2014

Date	Satellite PRN	Reflectivity	Calibration factor, f_c	Daily Average
8/21/2014	2	0.53	1.15	1.13
	6	0.51	1.19	
	10	0.59	1.04	
8/29/2014	2	0.52	1.18	1.15
	6	0.51	1.20	
	10	0.56	1.08	
9/5/2014	2	0.53	1.16	1.18
	6	0.51	1.20	
	10	0.52	1.18	
9/10/2014	2	0.52	1.18	1.08
	6	0.58	1.04	
	10	0.59	1.03	
9/15/2014	2	0.53	1.15	1.17
	6	0.51	1.21	
	10	0.53	1.16	
9/26/2014	28	0.55	1.12	1.13
	30	0.57	1.07	
	04	0.51	1.20	
10/2/2014	2	0.58	1.06	1.15
	6	0.51	1.20	
	10	0.51	1.19	

2.6.2 Experiment in 2013

During 2013, reflectivity was not adjusted by calibration factor, neither by loss factor due to leaves. At 10 cm depth, reflectivity measurements were found to fit with actual soil moisture content the best using a second order polynomial relationship with R^2 equal to 0.43 (Figure 2.13). Similarly, reflectivity correlated with actual soil moisture content at 20 cm depth, using a second order polynomial relationship with R^2 equal to

0.21 (Figure 2.14). There was no relationship between reflectivity and leaf water potential or stomatal conductance, indicating by low R^2 of 0.04 and 0.02, respectively (Figure 2.15 and 2.16). However, the positive relationship shown in Figure 2.15 was reasonable, since at lower soil moisture contents, it is hard for plant to extract water from soil. Therefore, reflectivity was lower. Also, the relationship of leaf water potential and soil moisture content at 10 cm depth further proved this presumption (Figure 2.17). Meanwhile, there was no relationship between stomatal conductance and soil moisture content (Figure 2.18).

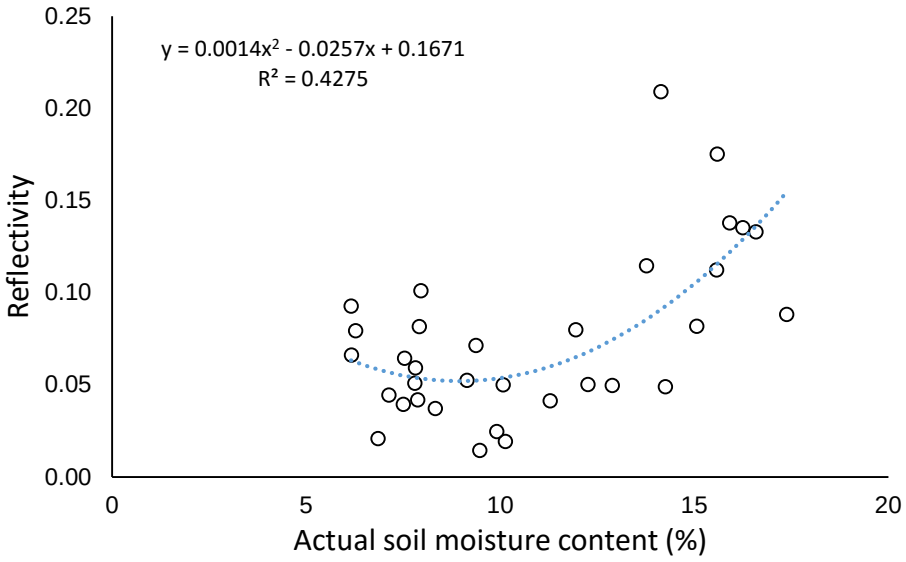

Figure 2.13 Correlation of reflectivity with actual soil moisture content at 10 cm depth during 2013.

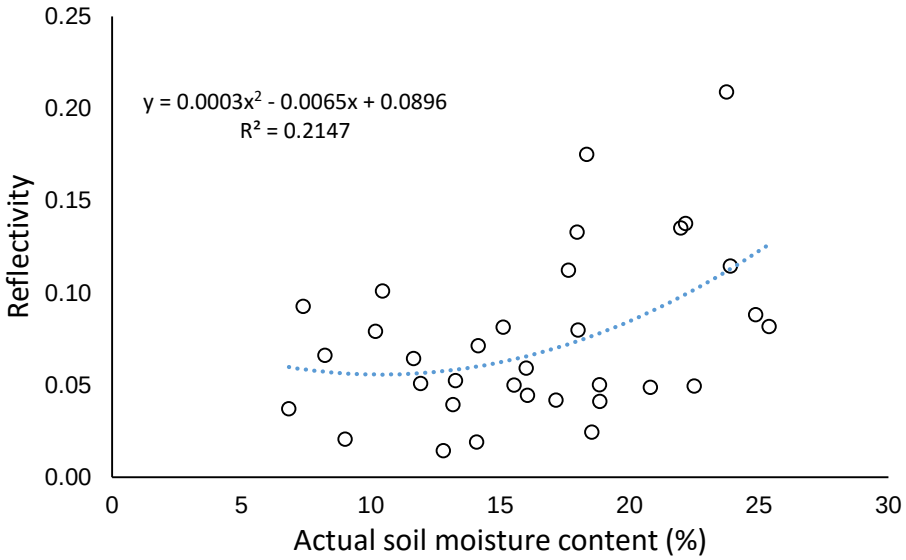

Figure 2.14 Correlation of reflectivity with actual soil moisture content at 20 cm depth during 2013

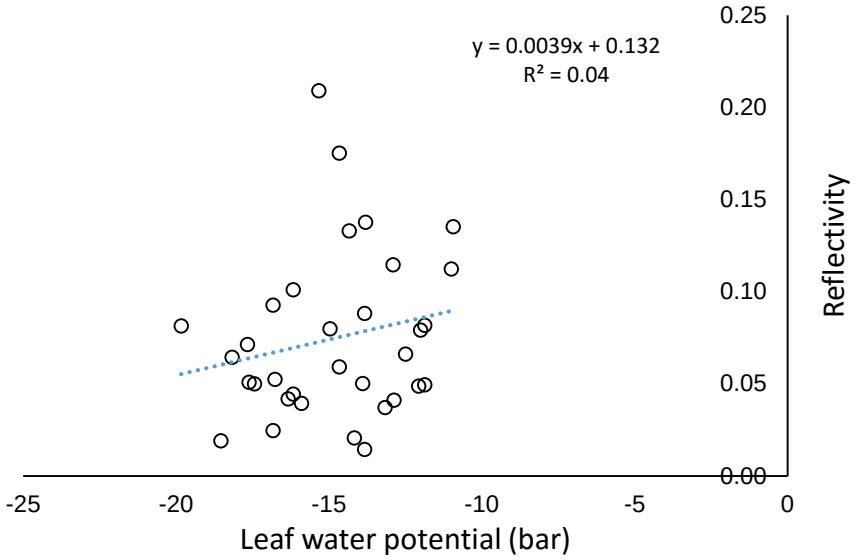

Figure 2.15 Correlation of reflectivity with leaf water potential during 2013.

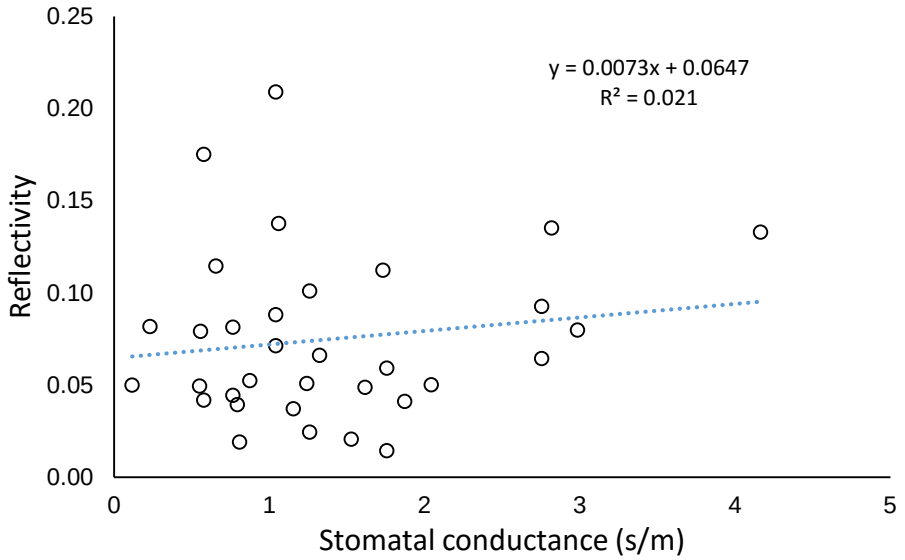

Figure 2.16 Correlation of reflectivity with stomatal conductance during 2013.

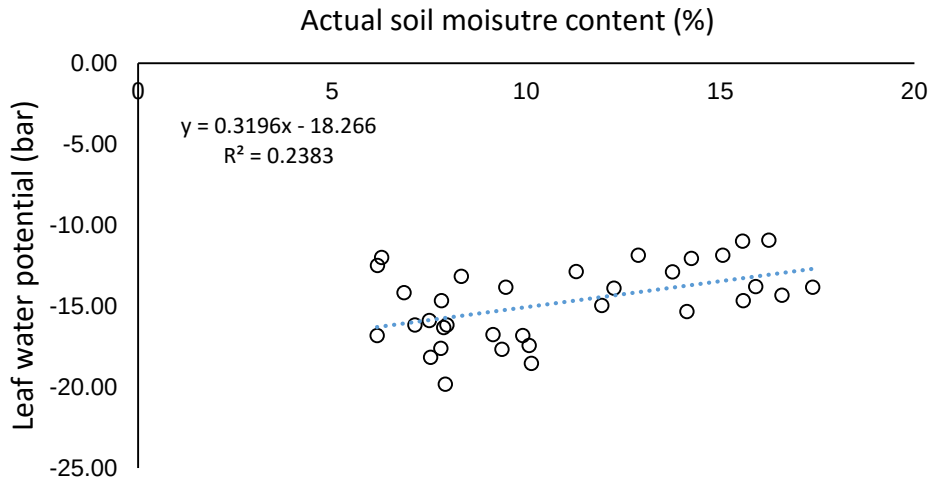

Figure 2.17 Correlation of leaf water potential with actual soil moisture content at 10 cm depth during 2013

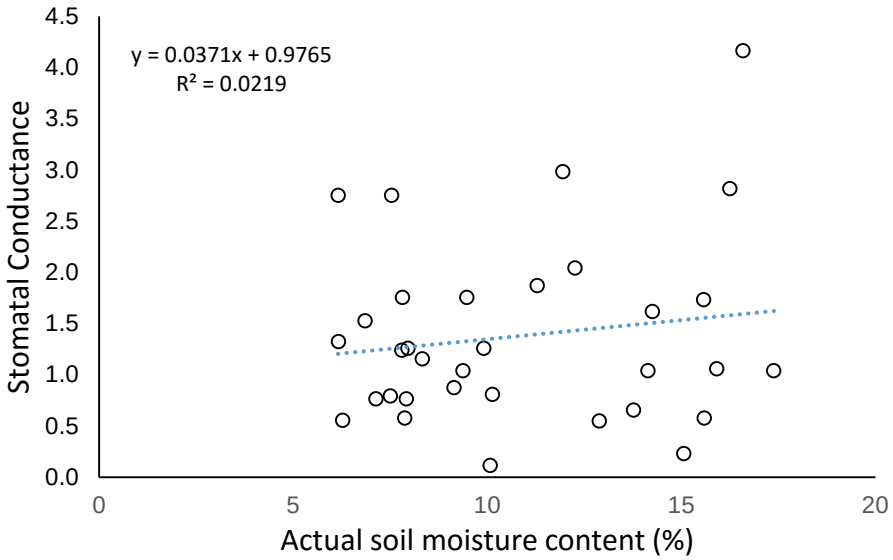

Figure 2.18 Correlation of stomatal conductance with actual soil moisture content at 10 cm depth during 2013

2.6.3 Experiment in 2014

During 2014, reflectivity measurements were scaled by average calibration factor obtained on different dates. Adjusted reflectivity refers to reflectivity that are further corrected by loss factor due to leaves. Average elevation angle was 53° when antennas were mounted at 1.6 m and 2.7 m. Therefore, the footprint of DMR at 1.6 m was smaller, according to equation 2.7 and Figure 2.8. Similar to 2013, the reflectivity measurements were found to correlate with actual soil moisture contents of different depths using second order polynomial relationship. When the antennas were mounted at height of 1.6 m, reflectivity correlated with actual soil moisture content with R^2 equal to 0.55, 0.42, and 0.47, for soil depths of 5, 10 and 15 cm, respectively (Figure 2.19, 2.20, and 2.21 - left). While when the antennas were mounted at height of 2.7 m, reflectivity correlated

with actual soil moisture content with R^2 equal to 0.23, 0.09, and 0.22, for soil depths of 5, 10 and 15 cm, respectively (Figure 2.19, 2.20, and 2.21 - right). The better relationship between reflectivity and actual soil moisture content when antennas were mounted lower (1.6 m) were possibly due to smaller footprint, and thus more accurate soil moisture sampling. There were no relationship between reflectivity and leaf water potential (Figure 2.22).

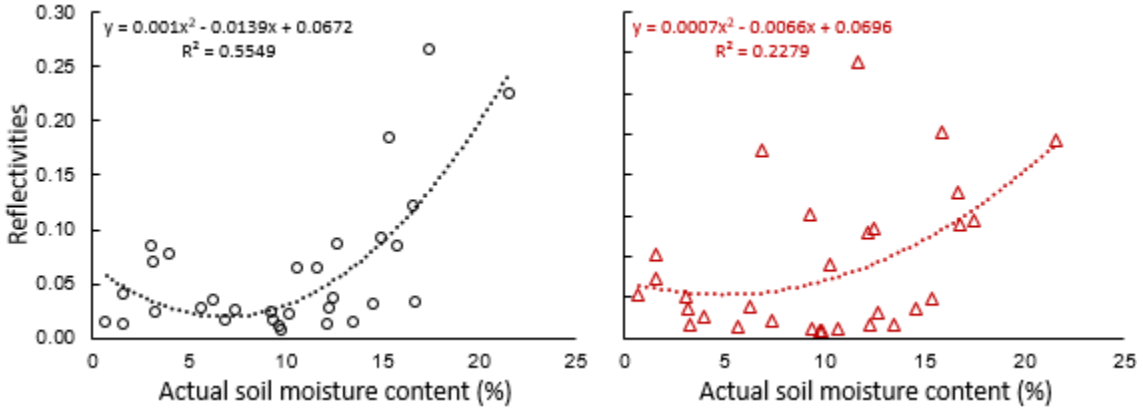

Figure 2.19 Correlation of reflectivity measured at 1.6 m (left) and 2.7 m (right) with actual soil moisture content at 5 cm depth during 2014.

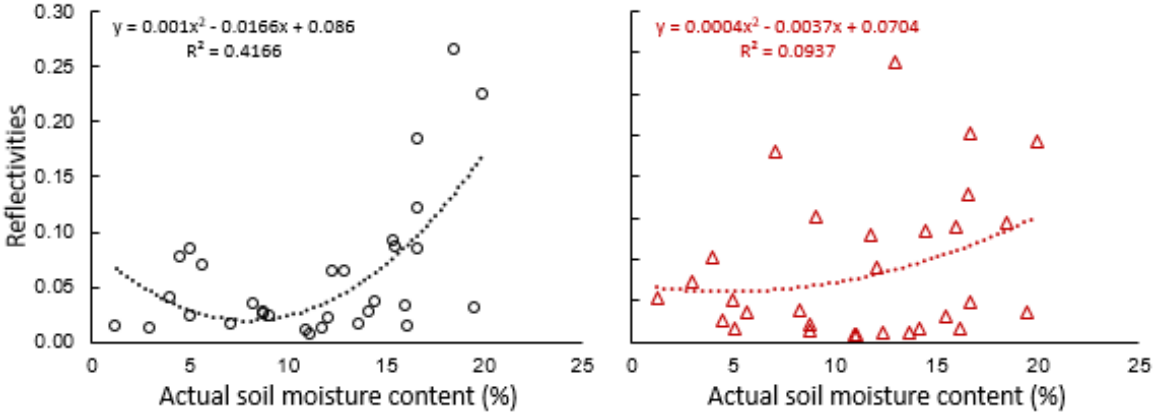

Figure 2.20 Correlation of reflectivity measured at 1.6 m (left) and 2.7 m (right) with actual soil moisture content at 10 cm depth during 2014.

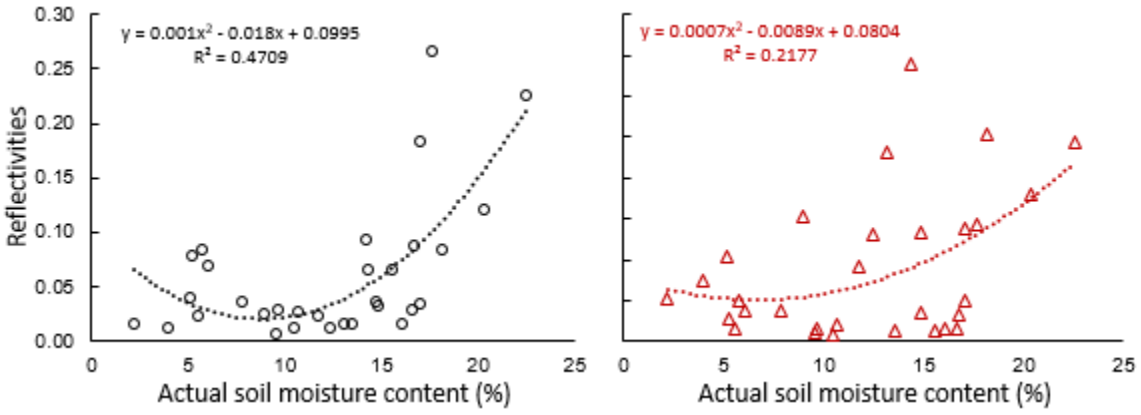

Figure 2.21 Correlation of reflectivity measured at 1.6 m (left) and 2.7 m (right) with actual soil moisture content at 15 cm depth during 2014.

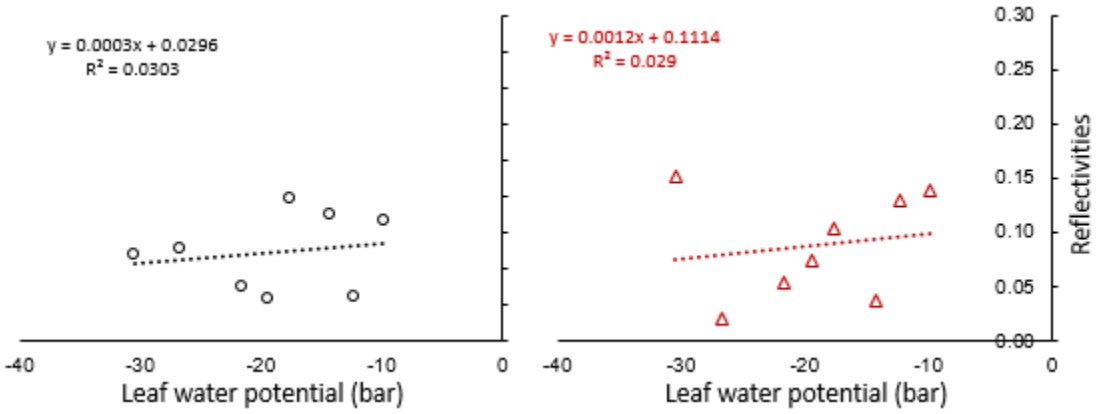

Figure 2.22 Correlation of reflectivity measured at 1.6 m (left) and 2.7 m (right) with leaf water potential during 2014.

Figure 2.23 showed the relationship of dielectric constant of cotton plant, both real and imaginary components, with gravimetric water content of cotton plant. As gravimetric water content of cotton plant increased, the real and imaginary components of dielectric constant of cotton plant increased, which was similar to relationship of dielectric constant with gravimetric water content of corn leaves measured at 1GHz

(Ulaby and Rayes, 1987) (Figure 2.24). In the meantime, loss factor increased as volumetric water content of cotton increased (Figure 2.25),

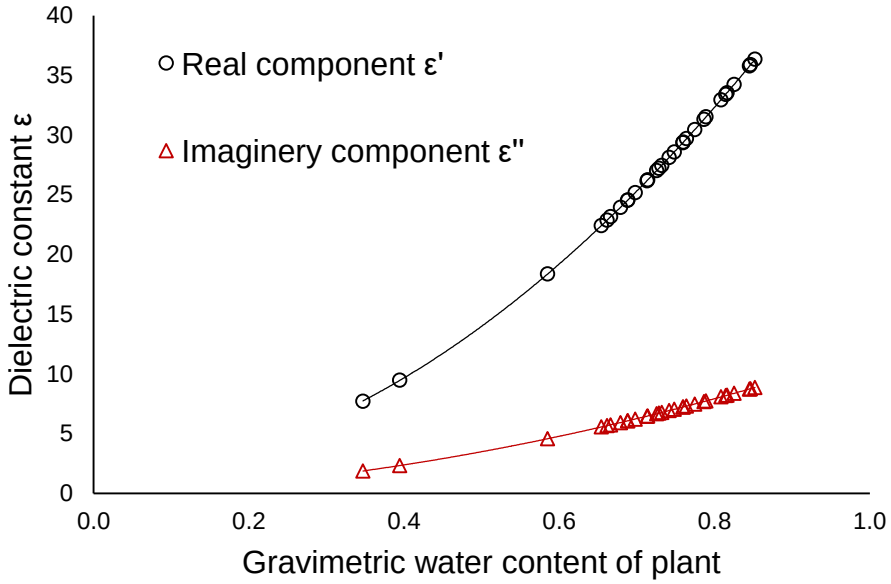

Figure 2.23 Relationship of dielectric constant with gravimetric water content of cotton.

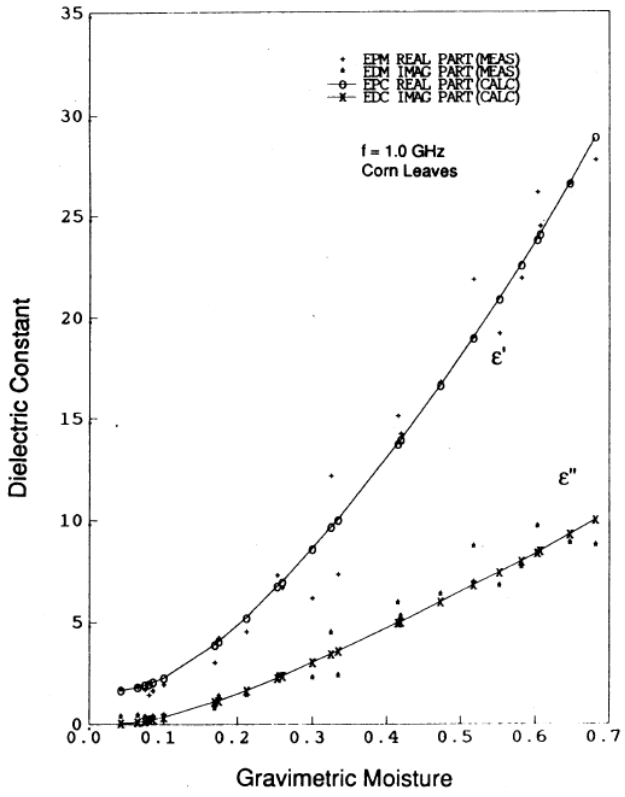

Figure 2.24 Relationship of dielectric constant with gravimetric water content of corn at 1GHz (Ulaby and Rayes, 1987).

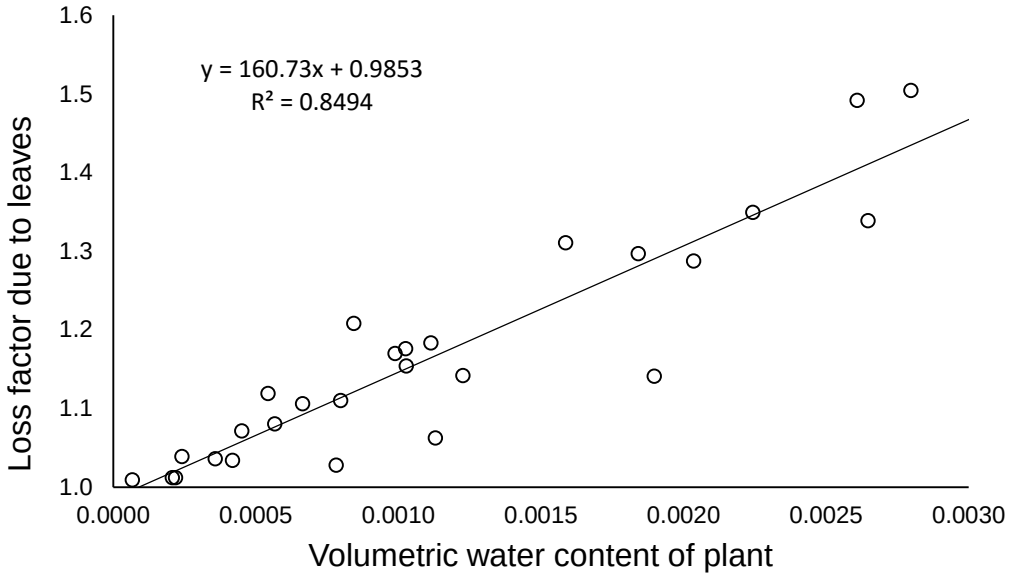

Figure 2.25 Relationship of loss factor with volumetric water content of cotton.

After applying loss factor to reflectivity measured by the DMR, the relationship between reflectivity and actual soil moisture content has been improved, but limited. When the antennas were at 1.6 m, coefficients of correlation of at 5, 10, and 15 cm increased from 0.55, 0.42, and 0.47 to 0.59, 0.43, and 0.50, respectively (Figure 2.26, 2.27, and 2.28). When the antennas were higher, i.e. 2.7 m, coefficients of correlation of at 5, 10, and 15 cm changed from 0.228, 0.094, and 0.218 to 0.235, 0.097, and 0.208, respectively (Figure 2.26, 2.27, and 2.28). There was no relationship between adjusted reflectivity and leaf water potential (Figure 2.29).

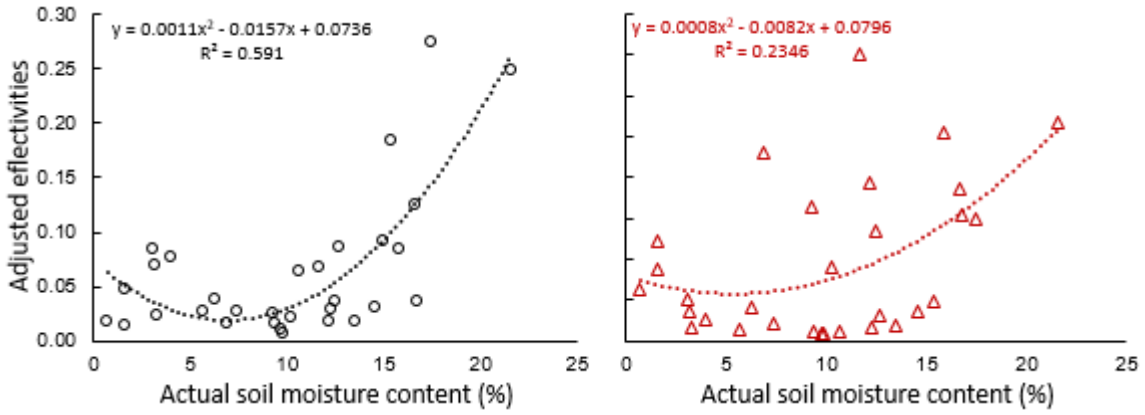

Figure 2.26 Correlation of adjusted reflectivity measured at 1.6 m (left) and 2.7 m (right) with actual soil moisture content at 5 cm depth during 2014.

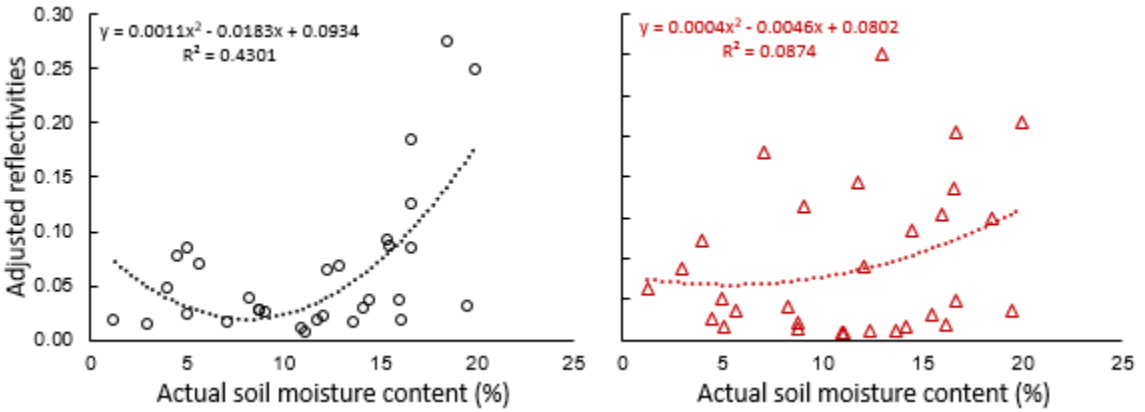

Figure 2.27 Correlation of adjusted reflectivity measured at 1.6 m (left) and 2.7 m (right) with actual soil moisture content at 10 cm depth during 2014.'

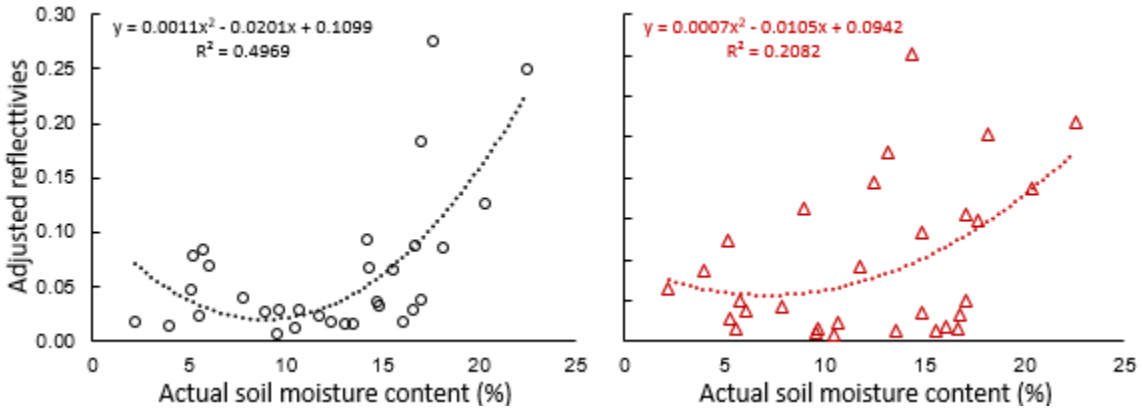

Figure 2.28 Correlation of adjusted reflectivity measured at 1.6 m (left) and 2.7 m (right) with actual soil moisture content at 15 cm depth during 2014.

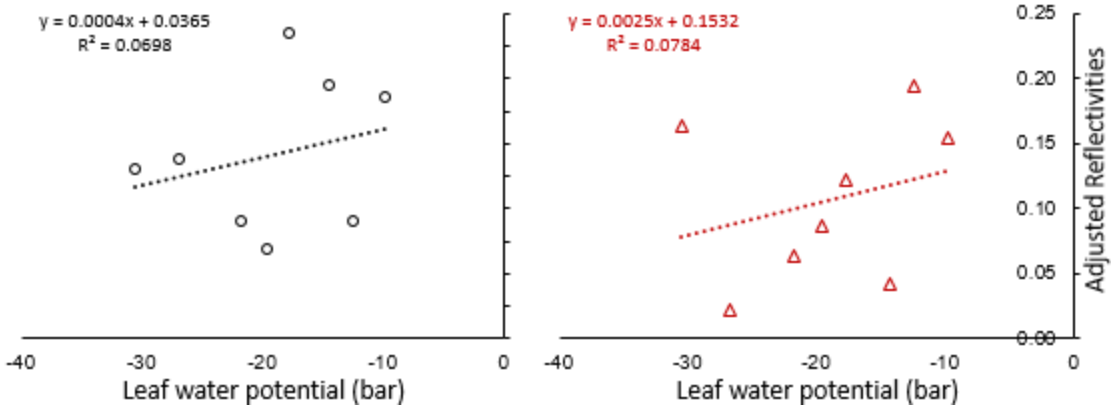

Figure 2.29 Correlation of adjusted reflectivity measured at 1.6 m (left) and 2.7 m (right) with leaf water potential during 2014.

2.7 CONCLUSION

Through the experiments conducted in 2013 and 2014, reflectivity measured by the DMR fitted with actual soil moisture content using a second order polynomial equation. In 2013, when the antennas were mounted on a variable rate irrigation system (4.16 m), it was found that reflectivity measured by DMR correlated with actual soil moisture content at 10 cm and 20 cm depths with R^2 of 0.42 and 0.21, respectively. In 2014, the DMR was evaluated using a RF power divider and result showed that there was no difference between the top and bottom channel. In the meantime, the DMR was calibrated over water, the small variation of calibration factors (1.14 ± 0.06) indicated that noise of the system was stable throughout the experiment. In the same year, when the antennas were mounted on back of a high-boy sprayer (1.6 m), the reflectivity correlated with soil moisture content at various depths with average R^2 of 0.48. However, when the antennas moved to height of 2.7 m on the high-boy sprayer, the correlation became poorer with R^2 of 0.18. This was possibly due to larger footprint when antennas were mounted higher, and thus less accurate soil moisture sampling locations. The dielectric constant of cotton, both real and imaginary components were found to increase with gravimetric water content of cotton. This result was consistent and similar with dielectric constant of corn measured at 1GHz (Ulaby and Rayes, 1987). The loss factor due to leaves increased with volumetric water content of cotton. After applying loss factors to reflectivity, the relationship between reflectivity and actual soil moisture content improved, yet limited. In 2013 and 2014, there were no correlation between reflectivity and leaf water potential, neither between reflectivity and stomatal conductance. The

results indicated that, until effects of vegetation water content and surface roughness on GPS reflected signals are thoroughly studied, utilizing GPS reflected signals for irrigation scheduling of cotton at Southeast Coastal Plain soils is not suitable.

2.8 REFERENCES

Beckmann, P. & Spizzichino, A. (1987). The Scattering of Electromagnetic Waves from Rough Surfaces, Artech House, Inc.

Dobson, M. C., Ulaby, F. T., Hallikainen, M. T., & El-Rayes, M. (1985). Microwave dielectric behavior of wet soil-Part II: Dielectric mixing models.*Geoscience and Remote Sensing, IEEE Transactions on*, (1), 35-46.

Engman, E. T., & Chauhan, N. (1995). Status of microwave soil moisture measurements with remote sensing. Remote Sensing of Environment, 51(1), 189-198.

Entekhabi, D., Njoku, E. G., Neill, P. E., Kellogg, K. H., Crow, W. T., Edelstein, W. N., . . . Johnson, J. (2010). The soil moisture active passive (SMAP) mission. Proceedings of the IEEE, 98(5), 704-716.

Fung, A. K., & Ulaby, F. T. (1978). A scatter model for leafy vegetation. Geoscience Electronics, IEEE Transactions on, 16(4), 281-286.

Garrison, J. L., Komjathy, A., Zavorotny, V. U., & Katzberg, S. J. (2002). Wind speed measurement using forward scattered GPS signals. Geoscience and Remote Sensing, IEEE Transactions on, 40(1), 50-65.

Grant, M. S. (2006). Surface reflected global positioning system signals for terrain classification (Order No. 3225963). Available from ProQuest Dissertations & Theses Global. (304966360). Retrieved from http://search.proquest.com.libproxy.clemson.edu/docview/304966360?accountid=6167

Hallikainen, M. T., Ulaby, F. T., Dobson, M. C., El-Rayes, M., & Wu, L. K. (1985). Microwave dielectric behavior of wet soil-part 1: empirical models and experimental observations. *Geoscience and Remote Sensing, IEEE Transactions on*, (1), 25-34.

Jackson, T. J., Le Vine, D. M., Swift, C. T., Schmugge, T. J., & Schiebe, F. R. (1995). Large area mapping of soil moisture using the ESTAR passive microwave radiometer in washita'92. Remote Sensing of Environment, 54(1), 27-37.

Jackson, T., & Schmugge, T. (1992). Surface soil moisture measurement with microwave radiometry. 43rd Congress of the International Astronautical Federation, IAF 92–0122 (pp. 749–751).

Katzberg, Stephen J., and James L. Garrison Jr. "Utilizing GPS to determine ionospheric delay over the ocean." (1996).

Katzberg, S. J., Torres, O., Grant, M. S., & Masters, D. (2006). Utilizing calibrated GPS reflected signals to estimate soil reflectivity and dielectric constant: results from SMEX02. Remote sensing of environment, 100(1), 17-28.

Kerr, Y. H., Waldteufel, P., Wigneron, J., Martinuzzi, J., Font, J., & Berger, M. (2001). Soil moisture retrieval from space: The soil moisture and ocean salinity (SMOS) mission. Geoscience and Remote Sensing, IEEE Transactions on, 39(8), 1729-1735.

Larson, K. M., Small, E. E., Gutmann, E. D., Bilich, A. L., Braun, J. J., & Zavorotny, V. U. (2008). Use of GPS receivers as a soil moisture network for water cycle studies. Geophysical Research Letters, 35(24)

Masters, D. S. (2004a). Surface remote sensing applications of GNSS bistatic radar: Soil moisture and aircraft altimetry (Order No. 3153856). Available from ProQuest Dissertations & Theses Global. (305203577). Retrieved from http://search.proquest.com.libproxy.clemson.edu/docview/305203577?accountid=6167

Masters, Dallas, Penina Axelrad, and Stephen Katzberg. "Initial results of land-reflected GPS bistatic radar measurements in SMEX02." *Remote Sensing of Environment* 92.4 (2004b): 507-520.

Niyazi, B. (2006). Scheduling site-specific irrigation for cotton in the southeastern coastal plain soils using linear-move irrigation system. PhD diss. Clemson, SC: Clemson University,

Njoku, E. G., & Entekhabi, D. (1996). Passive microwave remote sensing of soil moisture. Journal of Hydrology, 184(1), 101-129.

Parkinson, Bradford W., and Spilker, James J., eds. Global Positioning System Theory and Applications, Volume I. Reston, VA, USA: American Institute of Aeronautics and Astronautics, 1996. ProQuest ebrary. Web. 28 October 2015.

Privette, Charles V., et al. "Utilizing space-based GPS technology to determine hydrological properties of soils." *Remote Sensing of Environment* 115.12 (2011): 3582-3586.

Ulaby, F. T., & El-Rayes, M. (1987). Microwave dielectric spectrum of vegetation-Part II: Dual-dispersion model. Geoscience and Remote Sensing, IEEE Transactions on, (5), 550-557.

Wang, James R., and Thomas J. Schmugge. "An empirical model for the complex dielectric permittivity of soils as a function of water content."*Geoscience and Remote Sensing, IEEE Transactions on* 4 (1980): 288-295.

Schwank, M., Mätzler, C., Guglielmetti, M., & Flühler, H. (2005). L-band radiometer measurements of soil water under growing clover grass. Geoscience and Remote Sensing, IEEE Transactions on, 43(10), 2225-2237.